MACROPOROUS CELLULOSIC SPONGE FOR 3D HEPATOCYTE-BASED APPLICATIONS

BRAMASTA NUGRAHA

(*B.Eng. Hons.*, Nanyang Technological University)

A THESIS SUBMITTED
FOR THE DEGREE OF DOCTOR OF PHILOSOPHY

NUS GRADUATE SCHOOL FOR INTEGRATIVE SCIENCES & ENGINEERING

NATIONAL UNIVERSITY OF SINGAPORE

2013

Declaration

I hereby declare that this thesis is my original work and it has been written by me in its entirety. I have duly acknowledged all the sources of information which have been used in the thesis.

This thesis has also not been submitted for any degree in any university previously

Bramasta Nugraha

1 February 2013

ACKNOWLEDGEMENTS

First of all I would like to thank my PhD advisor, Prof Hanry Yu, for his relentless guidance, inspiration and vigorous mind-shaping throughout 5 years of my PhD study at NUS. Staying at his lab for 4.5 years had really transformed me from an amateur student to be a more professional researcher with the capability of defining the good research direction, brainstorming the ideas as well as be more resourceful in solving technical problems. His passion in guiding students in research in various aspects has nurtured me to be a more passionate in research in my future endeavor. Next, I would like to thank to my mentor Dr. Yue Zhilian for her guidance in the sponge fabrication and synthesis when I just joined the lab in 2007. Her meticulous thinking as well a excellent technical expertise has given me a lot of inspiration to strive and be more advance in doing polymer chemistry stuffs. Her helps and patience have helped me so much in the first two years of my PhD study.

Next, I would also want to thank people at Cell and Tissue Engineering lab both in IBN and NUS labs whom I have interacted during my PhD study. Special thanks to Mr. Abhishek Ananthanarayanan and Ms. Mo Xuejun for the great collaborations for the past few years. We have really made a solid team to strive in different projects we have involved. My work would not be smooth sailing without your feedbacks and helps. I will always remember the days we brainstormed ideas and gave each other inputs. I thank the senior researchers in the lab, Dr.Lou Yan-ru, Dr. Leo Hwa Liang, Dr. Xia Lei, Dr. Toh Yi-chin, Dr. Zhang Wenxia, Dr. Hong Xin, Ms. Qu Ying Hua, Ms. Narmada Balakhrisnan, Ms. Jia Rui Rui, who always helped me whenever I was stuck in the experiments and or having problems in the lab. I also feel grateful to Ms. Lee Shu Ying, Ms. Phoebe Koh and Mr. Zhang Weian for the excellent technical supports as well administrative staffs while I stayed in the lab.

Lastly, I want to thank my parents who have always been supportive in my research career despite my busy time in the study.

CONTENTS

LIST OF PUBLICATIONS

PATENT

1) **B. Nugraha** and H. Yu. Cleavable Macroporous Cellulosic Sponge for 3D Cell Culture and Spheroids Retrieval. ETPL ref: IBN/P/07395/00/SG and IBN/P/07395/01/US IBN Ref: IBN-310 (Filed for Singapore patent on September 20, 2012 Application No. 201207005-8 and US patent on January 9, 2013 Application No. 13/737812)

PEER-REVIEWED JOURNAL PUBLICATIONS

1) **B. Nugraha**, Lay Poh Tan, Modification of drug release profiles of poly (L-lactide) using palmitic acid, **Journal of Biomimetics, Biomaterials and Tissue Engineering** 2008 DOI: 10.4028/www.scientific.net/JBBTE.1.69

2) Haigang Gu, Zhilian Yue, Wen Shing Leong, **B. Nugraha**, Lay Poh Tan, Control of *in vitro* neural differentiation of mesenchymal stem cells in 3D macroporous, cellulosic hydrogels, **Regenerative Medicine** 2010 DOI: 10.2217/RME.09.89

3) Mo, X., Li, Q., Lui, L.W.Y., Zheng, B., Kang, C.H., **B. Nugraha**, et al., Rapid construction of mechanically-confined multi-cellular structures using dendrimeric intercellular linker. **Biomaterials** 2010 DOI: 10.1016/j.biomaterials.2010.06.020

4) **B. Nugraha**, Xin Hong, Xuejun Mo, Looling Tan, Wenxia Zhang, Yan Wang, et al., Galactosylated cellulosic sponge for multi-well drug safety testing. **Biomaterials** 2011 DOI: 10.1016/j.biomaterials.2011.05.087

5) Magalhães, R., **B. Nugraha**, Pervaiz, S., Yu, H., Kuleshova, L.L. Influence of cell culture configuration on the post-cryopreservation viability of primary rat hepatocytes. **Biomaterials** 2012 DOI: 10.1016/j.biomaterials.2011.10.015

6) Lei Xia, Yinghua Qu, Xin Hong, Rashidah bte Sakhban, Wenxia Zhang, **B. Nugraha** et al. Tethered spheroids as an in vitro hepatocyte model for drug safety screening. **Biomaterials** 2012 DOI: 10.1016/j.biomaterials.2011.12.006

7) Yan Wang*, Yi-Chin Toh*, Qiushi Li, **B. Nugraha**, Baixue Zheng, Thong Beng Lu, et al., Mechanical compaction directly modulates the dynamics of bile canaliculi formation. **Integrative Biology** 2013 DOI: 10.1039/c2ib20229h (*equal contribution)

8) BC. Narmada*, Y. Kang*, L. Venkatraman, Q. Peng, RB. Sakban, **B. Nugraha**, et al., HSC-targeted delivery of HGF transgene via bile duct infusion enhances its expression at fibrotic foci to regress DMN-induced liver fibrosis. **Human Gene Therapy**. August 2012 (Submitted) (*equal contribution)

9) Zhang W., Rashidah bte Sakhan, **B. Nugraha**, Xin Hong, Yu. H. Modulation of Cyp function and expression by spices in rat hepatocytes in 2D monolayer, collagen sandwich, and cellulosic sponge systems. Manuscript in preparation

10) **B. Nugraha**, A. Ananthanarayanan, H. Yu. HepaRG accelerated differentiation and retrieval in cleavable cellulosic sponge. Manuscript in preparation

11) A. Ananthanarayanan, **B. Nugraha**, M. Triyatni, S. Sankuratri and H. Yu. Scalable 3D model of human liver cells for screening anti-HCV therapeutics. Manuscript in preparation

CONFERENCE PROCEEDINGS

1) **Bramasta Nugraha**, Yue Zhilian, and Hanry Yu. Mitochondrial Drug Delivery System for Cancer Treatment: A Preliminary Study. Tohoku-NUS Student Joint Symposium. Tokyo & Sendai, Japan 10-12 May 2008 (Oral Presentation)
2) **Bramasta Nugraha**, Yue Zhilian, and Hanry Yu. Cellulosic Scaffold for 3D Hepatocyte Culture. NUS-Tohoku Graduate Student Conference in Bioengineering. Singapore 9-10 December 2008 (Oral Presentation)
3) **Bramasta Nugraha**, Yue Zhilian, and Hanry Yu, 3D Cellulosic Gel for Hepatotoxicity Screening, 31st Annual Meeting of the Japanese Society for Biomaterials (JSB). 16-17 November 2009, Kyoto, Japan (Poster Presentation)
4) **Bramasta Nugraha**, Yue Zhilian, and Hanry Yu, Novel Cellulosic Hydrogel Scaffold for Liver Tissue Engineering, 3rd East Asian Pacific Student Workshop on Nano-Biomedical Engineering. 21-22 December 2009, Singapore (Oral Presentation, Awarded as 2nd Best Oral Presenter)
5) **Bramasta Nugraha**, Yue Zhilian, and Hanry Yu, Novel Cellulosic Hydrogel Scaffold for Liver Tissue Engineering, 2nd NGS Student Symposium. 5 February 2010, Singapore (Oral Presentation)
6) **Bramasta Nugraha** and Hanry Yu, Cellulosic Hydrogel Scaffold for Liver Tissue Engineering Application. The 5th Society of Biological Engineering International Conference on Bioengineering and Nanotechnology (ICBN). 1-4 August 2010, Biopolis Singapore (Poster Presentation)
7) **Bramasta Nugraha** and Hanry Yu, Cellulosic Hydrogel Scaffold for Liver Tissue Engineering Application. 14th International Conference on Biomedical Engineering (ICBME). 1-6 August 2010, Singapore (Poster Presentation)

8) **Bramasta Nugraha** and Hanry Yu. Macroporous Cellulosic Hydrogel Scaffold as 3D Hepatocyte Culture Platform. 2010 International Symposium of Materials on Regenerative Medicine (2010 ISOMRM), 3-6 November 2010, Zhunan, Taiwan (Oral Presentation)

9) **Bramasta Nugraha** and Hanry Yu. Macroporous Cellulose Hydrogel Scaffold as Template for in vitro Liver Tissue Engineering. 32nd Japanese Society for Biomaterials Meeting, 29-30 November 2010, Hiroshima, Japan (Oral Presentation)

10) **Bramasta Nugraha** and Hanry Yu. Macroporous Cellulosic Hydrogel Scaffold as 3D Hepatocyte Culture Platform. TERMIS North America Meeting 2010, 5-8 December 2010, Orlando, Florida, USA (Poster Presentation)

11) **Bramasta Nugraha** and Hanry Yu. Macroporous Cellulosic Hydrogel Scaffold as 3D Hepatocyte Culture Platform. 4th East Asian Pacific Student Workshop on Nano-Biomedical Engineering, 15-16 December 2010, Singapore (Oral Presentation)

12) **Bramasta Nugraha** and Hanry Yu. Galactosylated Cellulosic Sponge Accelerates Hepatocyte Repolarization. 29th Canadian Biomaterials Society Meeting, 1-4 June 2011, Vancouver Canada (Oral Presentation, Awarded Best Abstract/Travel Award)

13) **Bramasta Nugraha** and Hanry Yu. Cellulosic Sponge for Multi-well Drug Safety Testing. TERMIS Asia Pacific Meeting, 3-5 August 2011, Singapore (Oral Presentation)

14) **Bramasta Nugraha** and Hanry Yu. Cellulosic hydrogel sponge for cell-dense 3D culture platform. World Biomaterials Congress, 1-5 June 2012, Chengdu, China (Poster Presentation)

15) **Bramasta Nugraha,** Chukwuemeka Anene-Nzelu, Yi-Chin Toh and Hanry Yu. *In vitro* Toxicology Models Based on Tissue-Engineered Constructs. A*STAR Scientific Conference, 18–19 October 2012, Singapore (Poster Presentation)

Abstract

A new class of soft hydrogel-based macroporous sponge made of cellulose derivative has been synthesized and investigated for several hepatocyte-based applications. Firstly, we have synthesized and fabricated a galactosylated macroporous cellulosic hydrogel sponge as a platform to culture primary rat hepatocytes as 3D spheroids for *in vitro* drug safety testing applications. The soft macroporous cellulosic sponge with conjugated galactose facilitates the formation of hepatocyte spheroids by presenting both the mechanical cues (via matrix rigidity) and chemical cues for the hepatocytes to reorganize into 3D spheroids within 7 hours post-seeding. The constrained hepatocyte spheroids maintain cell viability, cell polarity markers, and 3D cell morphology. These translate into maintained hepatocyte-specific functions and expression of drug metabolic enzymes and drug transporters. Furthermore, hepatocyte spheroids grown in the sponge show inducibility of various drug metabolizing enzymes including CYP1A2, CYP2B2 and CYP3A1, with higher mean basal drug metabolizing expression. The sponge also has comparable or lower drug absorbency compared to other cell culture scaffolds.

Secondly, we have elucidated the usefulness of our galactosylated cellulosic sponge for primary human hepatocyte and Huh 7.5 cell 3D culture as spheroids for multi-well HCV entry and inhibition study. Human hepatocyte and Huh 7.5 spheroids are formed in the sponge within 24 hours post-seeding and constrained in the sponge macroporosity for prolonged culture. The size of the spheroids lies within mass transfer barrier-free range. Spheroids viability is well maintained up to 5 and 2 weeks for human hepatocyte and Huh 7.5, respectively. The compact spheroids morphology is observed at least up to 2 weeks of culture. Compact spheroids morphology

correlates well with gene expression showing minimal dedifferentiation of human hepatocyte spheroids and upregulation of mature hepatocyte genes in Huh 7.5 spheroids. Both types of spheroids express liver polarity markers and HCV entry markers. When these spheroids are inoculated with HCVpp, an available in vitro model to study HCV entry, ~80% of the spheroids are infected with HCVpp distributed throughout whole spheroids region. Human hepatocyte spheroids have shown the ability to be infected at prolonged culture indicating the maintenance of HCV entry markers. By co-incubating both types of spheroids with HCVpp and CD81 antibody, HCVpp entry is inhibited at dose-dependent manner.

And lastly, we have tuned the property of the cellulosic sponge into a cleavable hydrogel sponge, with conjugated galactose as a platform to culture primary rat hepatocytes as 3D spheroids with the ability to retrieve the spheroids at physiological condition. Hepatocyte spheroids retrieval is performed through rapid non-cytotoxic sponge cleavage. The soft macroporous structure of cleavable cellulosic sponge conjugated with galactose facilitates the formation of hepatocyte spheroids by presenting both the mechanical cues (via matrix rigidity) and chemical cues for the hepatocytes to reorganize into 3D spheroids within 24 hours post-seeding. The constrained hepatocyte spheroids maintain cell viability for at least a week of culture. Upon spheroids retrieval through sponge cleavage, polarized hepatocyte phenotypes are well maintained; drug metabolizing enzymes (CYP1A2, CYP2B2 and CYP3A2), polarity marker (cortical F-actin), tight cell-cell adhesion, apical hepatocyte domain marker (MRP2), biliary excretory function, spheroid compact morphology and cell viability. The living retrieved spheroids are replatable on both collagen coated and poly-L-lysine coated dishes for further use.

LIST OF FIGURES

LIST OF TABLES

LIST OF SYMBOLS AND ABBREVIATIONS

2D	Two-dimensions/ two-dimensional
3D	Three-dimensions/ three-dimensional
AAT	α-1-antitrypsin
ADME Tox	Absorption, distribution, metabolism, excretion and toxicity
AFM	Atomic Force Microscopy
AHG	1-O-(6-aminohexyl)-D-galactopyranoside
APAP	Acetaminophen
ASGPR	Asialoglycoprotein receptor
BLAD	Bioartificial Liver Assisted Devices
BSA	Bovine Serum Albumin
Bsep	Bile Salt Export Pump,
$CaCl_2$	Calcium chloride
CD147	Hepatocyte basolateral domain marker
CD81	Cluster of differentiation 81
CDI	1,1'-carbonyldiimidazole

cDNA	Complementary DNA
CTG	Cell Tracker Green
CYP450	Cytochome P450
Cys	Cysteine
DAPI	4',6-diamidino-2-phenylindole
DI H_2O	Deionized water
DMAP	Dimethylaminopyridine
DMEM	Dulbecco's Modified Eagle Medium
DMF	Dimethyl formamide
DMSO	Dimethyl sulfoxide
DPBS	Dulbecco`s Phosphate Buffered Saline
dsDNA	Doube stranded Deoxyribonucleic acid
DTDP	3,3’-dithiodipropionic acid
DTNB	5,5′-dithio-bis(2-nitrobenzoic acid)
DTT	Dithiothreitol
ECM	Extracellular matrix
EDC	1-ethyl-3-(3-dimethylaminopropyl) carbodiimide
EGF	Epidermal Growth Factor

FBS	Fetal Bovine Serum
FDA	Food and Drug Administration
FDA (dye)	Fluorescein diacetate
FITC	Fluorescein isothiocyanate
FTIR	Fourier transform infrared spectroscopy
GSH	Glutathione
HA	Hydroxypropyl cellulose allyl
HA Gal	Galactosylated hydroxypropyl cellulose allyl
HCl	Hydrochloric acid
HCV	Hepatitis C virus
HCVpp	HCV pseudoparticles
HEPES	4-(2-hydroxyethyl)-1-piperazineethanesulfonic acid
HGF	Hepatocyte Growth Factor
HNF4α	Hepatocyte Nuclear Factor 4α
HPC	Hydroxypropyl cellulose (HPC)
HPCSS	Disulfide-containing hydroxypropyl cellulose
HPLC	High Performance Liquid Chromatography
IACUC	Institutional Animal Care and Use Committee

KCl	Potassium chloride
KH_2PO_4	Monopotassium phosphate
KHB	Krebs-Henseleit- bicarbonate
LC-MS	Liquid Chromatography-Mass Spectrometry
Mdr1a	Multi-Drug Resistance 1a
$MgSO_4$	Magnesium sulfate
MRP2	Multidrug Resistance Protein 2, hepatocyte pical domain marker
MTT	3-(4,5-dimethylthiazol-2-yl)-2,5-diphenyltetrazolium bromide
NaCl	Sodium chloride
$NaHCO_3$	Sodium bicarbonate
NH_4Cl	Ammonium chloride
NHS	N-hydroxy succinimide
NMR	Nuclear Magnetic Resonance
Ntcp	Na/taurocholate Co-transporting Polypeptide
Oatp1	Organic Anion Transporting Polypeptide 1
OsO_4	Osmium tetraoxide
PEG	Polyethylene glycol

PEO	Polyethylene oxide
PET	Polyethylene terephthalate
PGA	Polyglycolic acid (PGA),
PHA	Poly (hydroxyl alkanoate)
PI	Propidium Iodide
PLA	Polylactic acid
PLGA	Poly(lactic-co-glycolic acid)
PS	Polystyrene
PVLA	Poly-N-p-vinylbenzyl-D- lactonamide
RGD	Arginine-Glycine-Aspartate
RNA	Ribonucleic acid
RT PCR	Reverse transcriptase polymerase chain reaction
SEM	Secondary Electron Microscope
SR-B1/SCARB1	Scavenger receptor type B class 1
sulfo-NHS	N-hydroxysulfosuccinimide
TCEP	Tris(2-carboxyethyl) phosphine
TEM	Transmission Electron Microscope
TFA	Trifluoroacetic acid

TRITC	Rhodamine-labeled antibodies
UV	Ultraviolet
XPS	X-Ray Photoelectron Spectroscopy

CHAPTER 1

INTRODUCTION

The recent increasingly explored 3D cell culture technology has made various efforts towards presenting complexity to the cultured cells *in vitro* for various biomedical and pharmaceutical applications ranging from bio-artificial assisted devices to drug and antiviral screening platforms [1-4]. This new concept of culturing cells in 3 dimensions was initiated by various revealed facts that cells behaved differently compared to their native niche when they were cultured on conventional flat tissue culture flasks, known as 2D culture [5]. 2D culture is also unable to present the complexity of *in vivo* tissue modality *in vitro* thus could not correlate between the real tissue physiological microenvironment and cultured cells [5]. The possibility of culturing cells in 3D microenvironment mimicking the microenvironments in the native organ could enhance various biological investigation responses which possibly cannot be performed in the organ directly due to ethical issues and source scarcity. Culturing cells in the 3D culture and having close correlation with the studied organ could then minimize the use of expensive and labor extensive animal studies.

The design of the existing 3D cell culture technology was inspired by the architecture of the cells orchestration *in vivo* in the organ and their replica was built using bottom top approach towards tissue miniature. By combining various scientific backgrounds such as cell biology, materials science and bio-imaging technique, various kinds of 3D cell culture technology can replicate the tissue complexities *in vitro*, known as engineered tissue. This technology also ranges from microscale into macroscales for different applications in the current bioengineering demands.

During development of 3D cell culture technology, thing to consider is a way to mimic how cells *in vivo* interact with neighboring cells and with their own native matrices, known as cell-cell and cell-matrix interaction, respectively. Efforts to create 3D culture by looking at these factors hopefully can restore cell functionalities *in vitro* better than what people conventionally have done for decades, by just simply plating the cells on a flat tissue culture flask.

A different way to culture cells in 3D is by using a scaffold. The classical principle of synthetic polymeric scaffold usefulness in 3D cell culture technology and tissue engineering is to serve as temporary conducive template for cells to attach and maintain the functions prior to implantation [6, 7]. Therefore scaffold properties play important role in controlling 3D cellular microenvironments. By closely mimicking *in vivo* 3D cellular microenvironment cellular functions can be preserved prior to implantation [8]. Many factors in the scaffold are regulating cell survival, proliferation, differentiation and functions such as spatially and temporally controlled milieu of biochemical and topographical cues which includes interconnectivity of sponge porosity, mechanical stiffness and required cell ligand presentation [9]. Examples of classically studied scaffolds in the past are polylactic acid (PLA), polyglycolic acid (PGA), polycaprolactone or their blends [10]. However, these examples limit the application for soft tissue cultures due to relatively hydrophobic scaffold surface property, stiff mechanical stiffness, and even fabrication step which involves toxic organic solvents [11].

In this project, we would like to propose a novel hydrogel scaffold sponge made of cellulose derivative as the basic material for multi-well format 3D culture. The porous structure of the sponge was created by cellulose colloidal nanoparticles, which

are temperature responsive substances [12, 13]. The primary concept of making porous cellulose hydrogel from cellulose nanoparticle networks was introduced in year 2000 by Zhibing et al. and the early development of our cellulosic sponge for 3D cell culture has been elucidated by Yue et al. in 2010 [14, 15]. The advantages of making hydrogel from nanoparticles networks are it has two levels structural hierarchies' e.g. primary network of polymer chain and secondary network of cellulose nanoparticles. In comparison with other porous gels, the nanoparticle network hydrogel has the advantages of high uniformity and easily tunable mesh sizes. For example, pore size in a nanoparticle network can be well controlled by varying either nanoparticle size (molecular weight of the cellulose used) or the average number of nearest neighbors (polymer concentration in solvent) [14].

We propose by combining the advantages of hydrogel as soft tissue matrix and sponge macroporosity, we can present proper spatiotemporal cues for soft-tissue cultures. Found to be abundant in bacteria and plant fibers, cellulose has been studied extensively as drug carrier in drug delivery research [16-19], bioadhesive cellulose gels as vascosurgical devices, investigations in bone tissue engineering, cartilage tissue engineering and tissue engineering in post-injury brain and for connective tissue formation [20]. Cellulose derivative we used in the sponge synthesis and fabrication is hydroxypropyl cellulose (HPC) which is more water soluble as compared to the original native cellulose material. In addition to its high water solubility, HPC has also been proven to be biocompatible with an example of HPC-based FDA-approved commercial artificial tears material (Lacrisert) [21-23]. Thus the sponge materials construction is based on water environment hence named hydrogel sponge.

Three-dimensional construct formed in the porous sponge we are interested to observe is multi cellular aggregates, or called hepatocyte spheroids. Hepatocyte spheroids are three-dimensional, multi-cellular aggregates that exhibit high degree of cell-cell contacts. These spheroids sustain viability for extended culture periods and maintain higher level of liver-specific functions including albumin secretion, ureagenesis and cytochrome P450 activity, as compared to hepatocytes cultured as 2D monolayer [24]. Proven to be able to maintain polarity gradually and functionally resemble bile canaliculi, hepatocyte spheroids also possess tubular structure encircled with actin, similar to bile canaliculi observed *in vivo* [25].

3D spheroid culture has been extensively used *in vitro* for various cell types e.g. cancer, primary cells and stem cells [5, 25-28]. The extensive cell-cell interaction in the spheroid is analog to *in vivo* environment in promoting partial function maintenance of original tissue. These spheroids can be maintained without vascularization when the size of spheroid diameter is within diffusible dimension (less than 200 μm) to allow sufficient nutrients and oxygen penetration [29]. And most importantly, the hepatocyte spheroid can be a good and simple model in drug metabolism and hepatitis viral infection study.

Thesis hypothesis, project objectives and specific aims of the thesis

The general thesis hypothesis is macroporous cellulosic sponge can provide optimum physical and chemical cues for formation of functional and constraint hepatocyte spheroids for drug testing and antiviral screening applications. Final aim of this study is to have a robust hydrogel sponge scaffold with improved properties in terms of materials properties and cellular spatiotemporal cues as *in vitro*

drug safety testing and anti-viral screening platform. The basic material we are using is hydroxypropyl cellulose with interesting hydrogel properties. Being hydrogel-based cellulosic sponge, the hydrophilicity and stiffness properties is tunable for soft tissue cultures [30]. Not forget to mention, our cellulose sponge is also easily functionalized with ligands or other chemical modifiers thus provides versatility for further applications i.e for synthesizing a cleavable sponge.

This project focused on the development of multi-well cellulosic sponge for 3D hepatocyte culture and utilization of the sponge as *in vitro* cell drug safety testing platform and anti-viral screening using primary and human liver tumor-derived cells e.g. primary rat and human hepatocyte as well as human liver cell line (Huh 7.5 cell).

There are several methods researchers have performed in the past to form 3D cellular spheroids such as hanging drop technique, rotary culture of cell suspension on positive substrate (Primaria dish), cells entrapment in 3D hydrogel matrices, polymeric nanofibers scaffolds and cellular linker [24, 26, 31-33]. However, the process for Primaria dish culture can be tedious, after spheroids are formed they still need to be embedded in matrigel to serve as supporting substrate thus spheroid can be manipulated for further assay. Whereas nanofiber scaffolds have limitation for fabrication in larger scale due to its complex fabrication. In addition, higher surface per volume ratio of nanofiber may increase drug absorption.

Hence we have been thinking to propose a novel thin hydrogel sponge which would be able to form hepatocyte spheroids rapidly in response to the sponge mechanical stiffness, porosity and proper ligand presentation (galactose for hepatocyte), easy cell seeding procedure, low drug absorption as well as versatile manipulation of spheroids cultured in the sponge. Hepatocyte spheroids we refer here

are constrained and tethered hepatocyte spheroids in the macroporous network of the cellulosic sponge, rather than encapsulated in the sponge. Developing this constrained hepatocyte spheroid in the macroporous sponge is an improvement of previous work on galactose-conjugated polyethylene terephthalate membrane [34]. This membrane could form hepatocyte spheroids but at slow speed i.e. 3 days post-seeding and showed drawback in prolonged culture i.e. the inability of the membrane to anchor compact spheroids on the surface more than one week. In addition, this membrane could not guarantee to form a stable constrained cryopreserved primary human hepatocyte spheroids for prolonged culture, due to 5 folds less ASGPR receptors in human hepatocyte compared to rat hepatocytes [35].

Towards realization use of our in house cellulosic sponge 3D culture platform, which is inspired by the hepatocyte orchestration in liver lobe, three specific aims of this thesis are divided as follows.

Specific Aim 1

To develop galactosylated cellulosic sponge for 3D hepatocyte culture and drug safety testing

Hypothesis

Presentation of galactose ligands in macroporous cellulosic sponge can help inducing rapid and functional hepatocyte spheroids and subsequently constrain them in the macroporous networks

Experimental designs

1) Optimize the synthesis and fabrication of galactosylated cellulosic sponge with the soft hydrogel characteristics

2) Prove that cultured primary rat hepatocyte could rapidly reorganize to form hepatocyte spheroids and maintain the function for one week culture period

3) Move towards the application of the hepatocyte spheroid cultured in galactosylated cellulosic sponge for drug induction study

Specific Aim 2

To use the galactosylated cellulosic sponge as multi-well platform to study hepatitis C virus infection

Hypothesis

Constraint hepatocyte spheroids in the well-plate based macroporous cellulosic sponge have enhanced hepatocyte polarity and localization of hepatitis C virus entry receptors thus useful for antiviral screening

Experimental designs

1) Observe, assess and prove the rapid formation of primary human hepatocyte and Huh 7.5 spheroids in the galactosylated cellulosic sponge,

2) Characterize the hepatocyte polarity markers, requirements for hepatitis C virus infection study, over prolonged culture

3) Investigate the hepatitis C virus entry markers in the spheroids and prove their existence

4) Study and show the hepatitis C viral entry and inhibition in the cultured hepatocyte spheroids

Specific Aim 3

To synthesize and fabricate the cleavable cellulosic sponge for 3D hepatocyte culture and spheroids retrieval

Hypothesis

Reducible disulfide bonds insertion into the side chain groups of hydroxypropyl cellulose makes cellulosic sponge rapidly cleavable in physiological reduction environment

Experimental designs

1) Optimize the synthesis and fabrication steps of cleavable cellulosic sponge and investigate the cleavage rate of this new generation of the sponge in physiological and non-toxic reduction environment

2) Establish the platform to culture primary rat hepatocyte as spheroids and show rapid formation of these spheroids

3) Study and prove the ability to retrieve the cultured hepatocyte spheroids physiologically by cleaving the sponge

4) Elucidate the effect of cleaving process in the retrieved hepatocyte spheroids and prove the harmless effect of the reductant addition

This thesis elucidates the general introduction of the study as well as thesis specific aims in chapter 1. Chapter 2 covers the background theory and significance of the project we have been working. Chapter 3 explains the development of galactosylated cellulosic sponge to culture primary rat hepatocyte as spheroids for multi-well drug safety testing platform. Chapter 4 discusses the application of galactosylated cellulosic sponge to culture primary human hepatocyte and Huh 7.5 spheroids as a platform to study hepatitis C infection. Chapter 5 includes the further development of new generation of cellulosic sponge towards cleavable sponge for easy and rapid retrieval of hepatocyte spheroids cultured in the sponge. And to summarize this thesis, conclusion and recommendations for future works are covered in chapter 6.

CHAPTER 2

BACKGROUND AND SIGNIFICANCE

2.1 Liver physiology

Liver is a known organ that can rejuvenate by itself up to 80% mass loss in case of any injury [36]. It is body largest internal organ, which has four lobes, weighing about 1.4-1.6 kilogram and possesses complex functions in regulating body homeostasis [37]. In the body, liver serves numerous functions such as: a) synthesize proteins such as albumin, low density lipoprotein and coagulation factor, b) glycogen storage from glucose and converts it back for the needed energy, c) metabolize fatty acids, amino acids and cholesterol, d) produce biles to break down fats into smaller components and the most important function that is covered in this thesis is e) detoxification and elimination of toxic substances i.e. drugs by its cytochrome P450 enzymes to be more easily excreted substances [38] .

There are 4 major different cell types present in the liver such as hepatocytes, sinusoidal endothelial cells, Kupffer cells, and stellate cells [39] . Hepatocytes which count of ~80% liver cell mass play the most significant role in doing the job in liver metabolic, secretory and detoxifying capability [40]. Therefore in most liver tissue engineering platforms, primary hepatocyte is considered to be the main cell used in the model [41].

As shown in **figure 1**, hepatocytes are orchestrated in the liver lobe in a complex manner; the cells are aligned in a regular manner where cell-cell and cell-matrix play important roles in regulating cellular functions. The channels formed between adjacent hepatocytes called bile canaliculi, a thin tube-like structure which

collects bile secreted by hepatocytes. In the extended area, bile canaliculi merge and form bile ductules, which finally perpetuate as bile duct. In between each row of hepatocytes, there exist small cavities, called sinusoids which are constituted of liver sinusoidal endothelial cells.

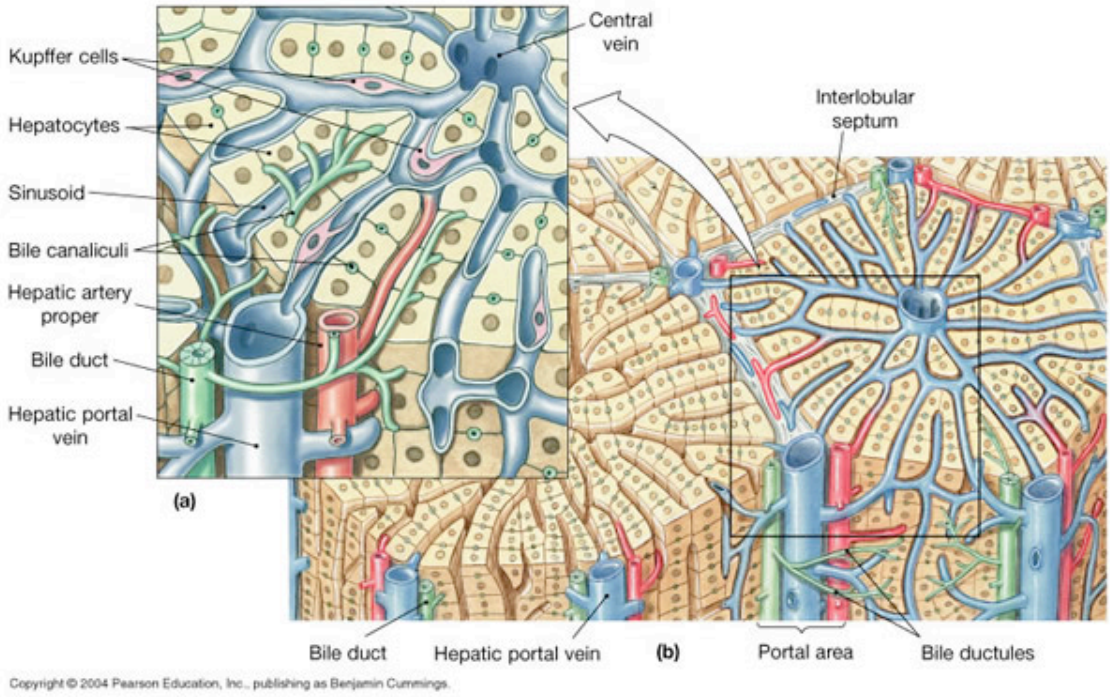

Figure 1. Anatomy of human liver and its biliary tracts (adapted from [37])

In this sinusoid, there are Kupffer cells which have similar functions like macrophages: to get rid of amino acids, nutrients, sugar, old red blood cells, bacteria and other debris from the blood. The functions of sinusoid are to destroy old red blood cells, bacteria and other foreign particles from the blood and to detoxify toxins and harmful substances. Other cells beside these cells are also present such as biliary epithelial cells, hepatocyte precursor cells (or called small hepatocyte) and fibroblasts which also perform metabolic capability. In estimation, liver is flown with 1.5 L of blood per minute, 75% of this blood comes through portal vein and the rest is oxygen-

rich blood carried by hepatic artery. This thus indicates liver as one of the most vascularised organ in the body [42].

The hepatocytes arrangement in the liver lobe also depicts the importance of this structure for liver functions. The cell substratum, cell-cell interaction as well as other cues like shear stress and or chemical cues have significant effects into how well the cells function and do their duty [43]. Various efforts to regenerate healthy and well function hepatocyte *in vitro* are inspired by these phenomena.

2.2 *In vitro* liver regeneration

Liver transplantation is a known treatment in resolving end-stage liver disease, however donor organ shortage remains a serious problem [44]. Bunch of patients are dying while seeking for a transplant and those with chronic disease often deteriorate resulting in lower chance of survival after transplantation. Thus a device that can support liver function until liver from a donor became available or the patient's own liver recovered is an aim. Extensive researches to regenerate artificial liver microtissues have been fostered since few decades back, known as Extracorporeal Bioartificial Liver Devices or Bioartificial Liver Assisted Devices (BLAD) [45]. This bioartificial liver is an extracorporeal device filled with living primary hepatocytes for temporary support of liver functions. Most of the other available liver assisted support systems could get rid of toxins normally metabolized by liver through dialysis, charcoal hemoperfusion or exchange transfusion [46-48]. However still none of these systems can have complete complex functions performed by a normal and healthy liver.

It is known to be a major challenge to maintain the differentiated phenotypic characteristics and functions of hepatocytes in the culture more than a week since it is

difficult to mimic the proper microenvironment for hepatocytes to proliferate and function [49]. These adhesion-specific cells require intricate interplay of various important factors to maintain proper biological functions failing which hepatocyte will trans-differentiate into fibroblast-like cells. Hepatocytes as the functional cell source in BLAD must be maintained by cultivating the cells in 3D structure, such as sandwiching them between two collagen gel layers [50]. In this configuration, hepatocytes can secrete functional markers at physiological levels. Hepatocytes must also be attached to polymer substrata to maintain their differentiated functions and viability. Hepatocytes cultured on appropriate polymers can form tissue resembling those observed in organ and shown evidence of bile ducts formation and bilirubin removal [51]. By culturing hepatocytes within artificial scaffolds, they can be cultured *in vitro* then transplanted *in vivo* which can be performed in the diseased liver, but still the trans-differentiation of these cells remains a major challenge [52]. From this observation, plating hepatocytes on a carefully designed and appropriate substratum points out a very important factor in maintaining differentiated functions correlated with cell-matrix interaction.

2.3 Scaffolds for liver tissue engineering

Tissue engineering scientists have made extensive efforts to develop variety of scaffolding materials to regenerate scalable tissues such as nerve, skins, bone and blood vessels [53]. Scaffold is a temporary construct that mimics the native extracellular matrix (ECM) of the tissues to provide structural integrity of tissues and facilitate cells to adhere, proliferate and migrate [54]. It provides suitable microenvironments to the cells for maintaining proper functions [55]. Therefore it is important to create scaffolds that mimic the ECM properties of the native tissues. The

successfulness of these ECM-mimicry scaffolds developments lies in the matrix design to support cell adhesion, proliferation, maturation and differentiation. In specific for liver tissue engineering, the scaffolds need to be accommodating cell adhesion with permissive microenvironment and surface chemistry, three dimensional features to promote cell-cell contact and desirable porosity to maintain diffusion of nutrients and gas exchange. Mechanically soft scaffolds are desirable to prevent cells spreading which could induce dedifferentiation.

Approaches to establish proper cell-matrix interaction in anchorage-dependent cells i.e. hepatocyte cultures have been developed to regenerate tissues by attaching isolated cells to scaffolding biomaterials that serve as guiding structures for initial tissue development. Other approaches such as culturing hepatocyte in suspension, liver microsomes or culturing precision liver slices could not exhibit long term stability since they are unable to mimic the *in vivo* liver microenvironment completely [32, 56, 57]. Ideal scaffolds should be biocompatible, non-toxic and manufacturable [58]. Different forms of scaffolds such as nanofibers, membranes and hydrogels that attempted to mimic liver extracellular matrices have been developed to sustain liver metabolic functions for successful liver tissue regeneration [24, 59, 60]. Many methods involved in the fabrication steps of the scaffold with desirable properties for regenerating liver tissues such as phase separation, particular leaching, freeze-thaw and electrospinning [24, 61-63].

Important factors in the scaffold design and fabrication that have to be strictly controlled are a) pore size and porosity to maintain proper diffusion of nutrients and gas exchange for cellular growth and b) scaffold surface chemistry to present proper cues to the cells grown in the region. When the pore size of the scaffolds is larger than 500 μm, cells cannot migrate anymore to reorganize as they do not recognize the

surface anymore. Pore size with high interconnectivity should ideally be in the range of 50 to 150 μm for hepatocyte culture [64]. Within this dimension, hepatocytes cell-cell contact would be enhanced to maintain their differentiated phenotypes when compared to two dimensional systems. Hepatocytes when cultured on 2D collagen monolayer tend to dedifferentiate rapidly and lost their liver specific functions [65]. The surface chemisty of the scaffold material will also influence cell adhesion, proliferation and functions. When hepatocytes were cultured on an Arginine-Glycine-Aspartate (RGD) modified polyethylene glycol gel and type 1 collagen modified polysulfonate sponges, long term enhancement of liver differentiated functions have been observed but not on the unmodified respective substrates [61, 66]. Therefore, incorporation of cell-adhesion specific ligands on the scaffold surface is important to promote cell-matrix interaction.

Scaffold raw materials can be natural materials such as extracellular components (collagen, fibronectin, fibrin, laminin, matrigel) or decellularized liver matrices [67]. However, these natural materials scaffold are not cost-effective, impose batch-to-batch variation, may induce immunogenic reactions as well as in particular for matrigel, the exact composition of its constituent is still unknown thus rendering its irreproducibility [68, 69]. On the other hand synthetic materials are advantageous in their chemistry and materials properties to be well controlled and tunable [70]. Scaffold-based tissue engineering in majority has utilized synthetic polymers e.g. poly (glycolic acid) (PGA), poly (lactic acid) (PLA), or poly (hydroxyl alkanoate) (PHA) [71]. These polymer scaffolds are designed to guide cell organization and growth allowing proper diffusion of nutrient to the cells. However, the use of these polymers for liver tissue engineering applications is limited with the lack of cell recognition motif and mechanical stiffness mismatch [72]. When synthetic galactose-conjugated

hydrogels are used to culture hepatocytes, the cells reorganize to spheroids, which is important in establishing maintenance of hepatocyte differentiated functions [67].

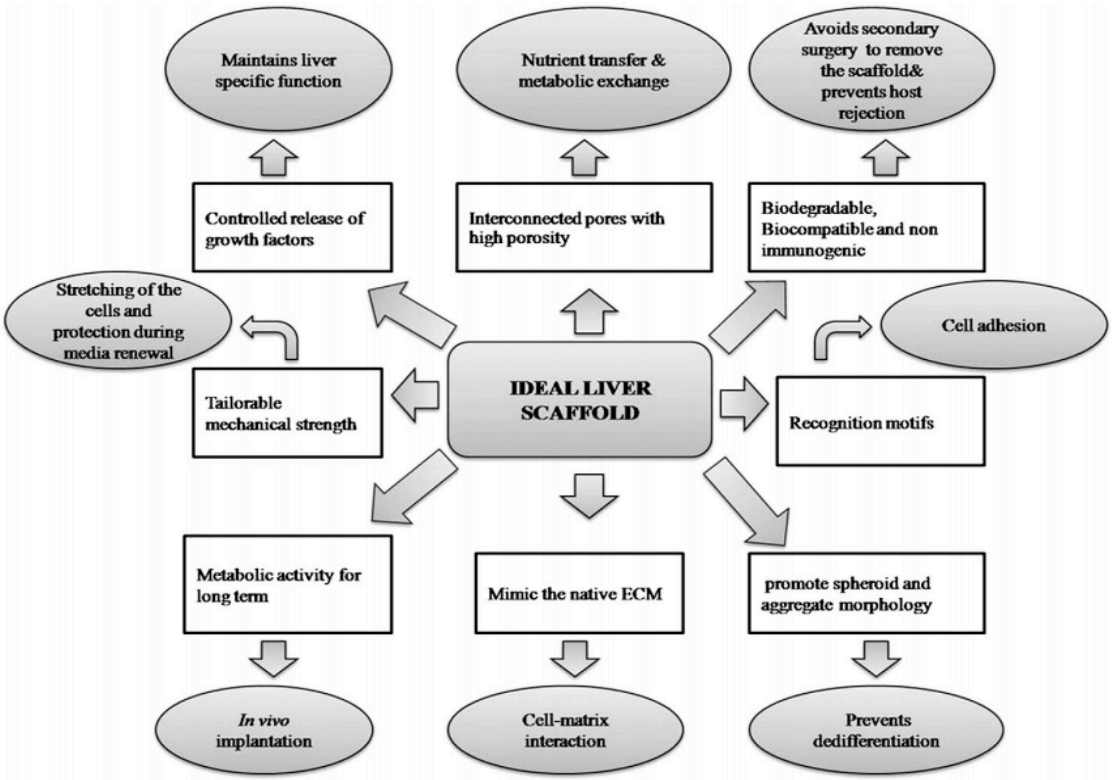

Figure 2. Ideal requirements for liver tissue engineering scaffolds (adapted from [67])

Figure 2 depicts the ideal requirements to have good and reliable liver tissue engineering scaffolds. Basically scaffold mechanical property, cell ligand motif presentation, biocompatibility, interconnected porosity and the ability to promote spheroids formation are the main requirements. The presentation of galactose on the scaffold surface acts to interact with asialoglycoprotein receptor (ASGPR) on the hepatocyte membrane to enhance cells retention in the porous scaffold and eventually to induce formation of cell aggregates or spheroids. The formed spheroids have been reported to enhance hepatocyte functions [60].

Table 1. Different scaffolds materials for liver tissue engineering (adapted from [67])

Material	Hepatocyte morphology/ function	Time points	Remarks	Refs
PLGA and PLA blend sponge	Decreased in cell number in 7 days	14 days	Limited nutrient transfer across the scaffold	[73]
Polyester scaffold	Small aggregates formation	3 days	Poor oxygen supply caused cell death	[74]
Polyacrylamide-linked galactosidase	Cells attachment in 30 min	1 day	The presence of ASGPR helped in cell attachment	[75]
3D gelatin sponge with galactose	Spheroids aggregated which maintained liver specific function	7 days	Liver specific functions maintained compared with unmodified sponge	[33]
Galactose-derivatives PS, PVLA	Cells adhered due to ASGPR motifs	1 day	Lack of functionality due to the absence of signals	[76]
PEO hydrogel with galactose	Cells attachment and spreading in 4 hours	7 days	Presence of ASGPR promoted cell attachment	[77]
PVLA on PS	Spheroids formation	7 days	Cells adhered and maintained function	[78]
Copolymer of poly(ε-caprolactone-co-ethylene)	Cells attachment and spheroids formation	7 days	Decreased liver specific function after 5 days	[72]
Galactosylated PET membrane	Spheroidal aggregates formed that helped in increased metabolic activity	6 days	Increased cell attachment as the galactose concentration increased	[59]
Micropatterned agarose with collagen	Rapid growth of cells similar to cells cultured in collagen	7 days	Proper and distinct growth of hepatocytes	[79]
Galactosylated cellulosic	Spheroids formation in	7 days	Physical and chemical cues in the sponge along with	[80]

sponge	7 hours of culture and two folds increase in metabolic activity when compared to other galactose conjugated scaffolds		ASGPR interaction promoted better cell activity	
Heparin-PEG hydrogel with HGF	Hepatic spheroids were formed in the presence of HGF	20 days	Metabolic activity was well maintained in spheroidal culture	[33]

Table 1 summarizes various available galactose containing scaffolds that have been investigated as platform to culture hepatocyte as spheroids. One of the examples denoted in **table 1** is our own in house galactosylated cellulosic sponge which has salient feature in quickly aggregating hepatocytes to form spheroids as fast as 7 hours post-seeding and higher fold of increase in metabolic activity when compared to other galactose conjugate scaffolds. In addition, we have found that primary human hepatocyte spheroids cultured in our galactosylated cellulosic sponge are still functional and viable up to 40 days post-seeding.

The fundamental development of our in house cellulosic sponge was initiated by the absence of a platform which combines the advantages of having macroporous diffusible networks for good mass transfer, soft mechanical stiffness needed to culture soft tissues i.e. hepatocytes and the ease of functionalization with cellular ligand/modifier. Hydroxypropyl cellulose, a cellulose derivative, is a FDA-approved material which has been used as commercial artificial tears material (Lacrisert) [22, 23]. Hydroxypropyl cellulose and water mixture show interesting temperature

sensitive behavior and form biphasic stable state beyond its liquid crystal solution temperature (LCST) [81]. This temperature sensitivity is due to hydoxypropyl cellulose colloidal nanoparticles response to increasing temperature. The primary concept of making porous cellulose hydrogel from cellulose nanoparticle networks was introduced in 2000 by Zhibing et al. [14]. The advantages of making hydrogel from nanoparticles networks are it has two levels structural hieararchy e.g. primary network of polymer chain and secondary network of cellulose nanoparticles. In comparison with other porous gel, the nanoparticle network hydrogel has the advantages of highly uniformity and easily tunable mesh sizes. For example, pore size in a nanoparticle netwoek can be well controlled by varying either nanoparticle size (molecular weight of cellulose used) or the average number of nearest neighbours (polymer concentration in solvent) [14]. We hypothesized by combining the advantages of hydrogel as soft tissue matrix and porous sponge, we can present proper spatiotemporal cues for soft tissue cultures.

2.4 3D hepatocyte culture platforms for drug safety testing

In the pharmaceutical industry pipeline, new drugs are developed through rigorous processes involving compound target validation governing its absorption, distribution, metabolism, excretion and toxicity (ADME Tox) (**figure 3**). ADME Tox is a critical step to screen whether a compound target is safe enough to enter clinical stage, yet it remains the major challenge for the pharmaceutical industry as evidenced by the annual drug withdrawal or severe use limitation of marketed drugs due to unexpected adverse effects (lack of efficacy, toxicity, and unfavorable pharmacological properties) [82]. Advancements in system biology, genomics, epigenetics, bioinformatics and proteomics lead to the fast increase in lead

compounds production. This has shifted the importance of ADME Tox prediction to before pre-clinical stage, unlike what it usually happened in the past to be done at the end stage of pre-clinical stage. Screening lead compounds before pre-clinical stage will tremendously save the cost of expensive pre-clinical stages and predict the toxicity of the compounds more accurately. Moreover, most of the tested compounds are still not massively produced thus still in minute amounts. High throughput *in vitro* platform which only needs minute amount of compound with good ADME Tox prediction is highly desired. Hepatocytes as the cells in the body that primarily metabolize and detoxify uptake drugs have been used as the major cell model. The importance of using hepatocytes as the cell model is their ability to retain species specific drug metabolizing enzymes (cytochrome P450).

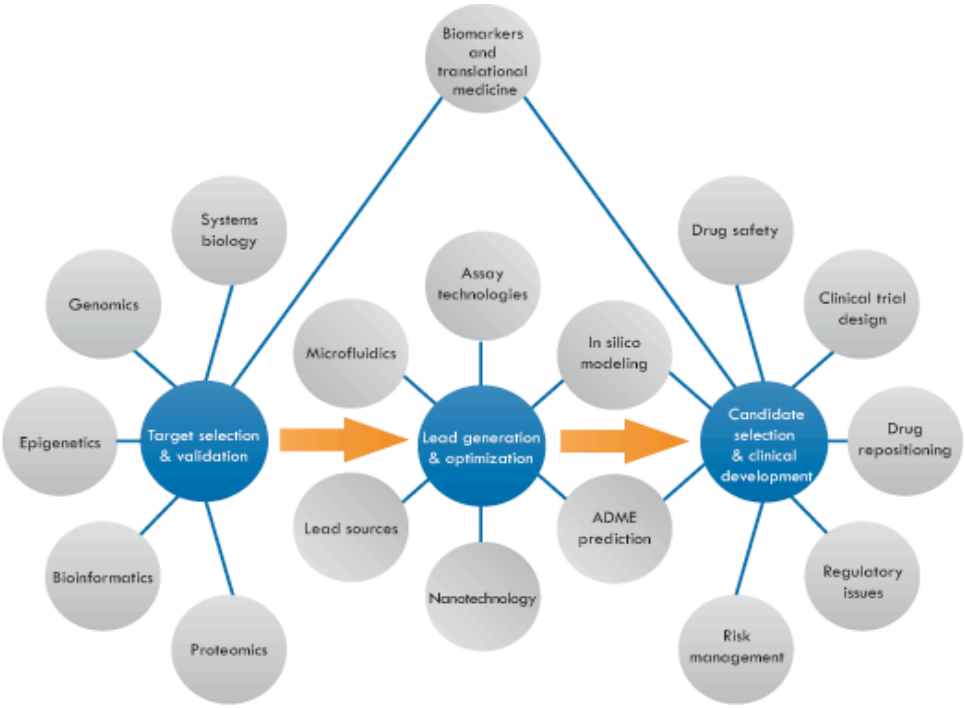

Figure 3. Drug-discovery pipeline: the ADME Tox strategies are important screening step before clinical trials of new drug candidates (adapted from [83])

By observing the compound target metabolic profile predicted by hepatocytes culture models, one can predict whether the oral administered drugs will be metabolized by cytochrome P450 enzymes in the liver before moving to the systemic circulation. If the liver-metabolized compound target found to result in toxic by-product metabolized compounds, one can find an alternative to administer the drugs by other route with comparable pharmacological activity. In addition, one can also investigate which cytochrome 450 is important in metabolizing certain compound [84].

Various available hepatocyte-based platforms (see **table 2**) can predict the toxicological phenomena of various compound targets. These platforms in general can characterize whether the effect of liver metabolism is toxic or not. Thus they are very useful tool in evaluating the compound target toxicity. By elucidating the metabolic mechanism, one can extend the analysis of the target toxicity from various dose concentration, or inter-specific toxicity responses, and from acute to chronic exposure [84]. The importance of these hepatocyte-based *in vitro* platforms is also to bridge the gap between animals and humans as well as close prediction the compound toxicity to the desired species [84]. In addition, *in vitro* cell models can replace the animals use in safety testing for cosmetics and pharmaceuticals [84]. In Europe, there has been a recent push to develop better *in vitro* models in response to new laws to limit animal use [85].

Table 2. Various engineered-liver cell models for *in vitro* testing of xenobiotics (adapted from[84])

Models	**Features**	**Refs.**
Sandwich cultures system, collagen with collagen, collagen with matrigel or RGD-galactose	Polarized cells for studying drug metabolism, cytochrome induction, transporter activity, acute toxicity and idiosyncratic toxicity	[86, 87]
3D liver surrogate (Regenemed)	3D Co-cultures of hepatocytes and liver stromal cells in nylon scaffolds for chronic toxicity and chronic enzyme inductions	[88]
Spheroid cultures	Hepatocyte aggregates formation to facilitates bile canaliculi formation and study of acute toxicity	[89]
Flat-plate bioreactor	Perfusion-based system with varying oxygen concentration to test zonation-mediated toxicity and acute toxicity	[90]
Microscale perfusion bioreactors	Shear-mediated signaling by mimicking blood flow through the liver with high surface to volume ratio, which facilitates improved study of cytochrome induction, drug clearance and acute toxicity with little reagents	[91-93]
Microscale patterned co-cultures	Micro-patterned co-cultures (hepatocytes and NIH3T3 fibroblasts) with optimal homotypic and heterotypic interactions to study chronic toxicity, drug-drug interactions, acute toxicity responses and hepatitis viral replication	[94]

Specifically for drug safety testing application, there are some scaffolds which are currently available in the market or still being developed by several research groups. Those scaffolds are helping the cell function to be maintained by enhancing cell to cell contact i.e. 3D spheroid formation. Taking PuraMatrix™ as the first interesting example to elucidate, this peptide hydrogel contains nanofibers inspired by the fragment of yeast protein design, zuotin, consisting of 16 peptides sequence [95-

98]. Developed in 1992 by Prof Shuguang Zhang lab in MIT, it has been commercialized under company flag 3DM Incorporation since 2003. And now PuraMatrix™ gel has been used in several research fields such as stem cells differentiation, wound healing assays, angiogenesis assay, and lastly 3D hepatocyte spheroid culture with distinctive channels formed in the spheroid [99-102]. However, till today there is still no concrete evidence of direct application as multiwell *in vitro* drug testing platform. Essential drawbacks we find to be critical and needs to be eliminated are the acidic pH of peptide solution prior to gelation (pH 3.0). The requirement for component mixing during gelation can be detrimental to sensitive and anchorage dependent cells like hepatocytes.

Next example of commercially available hydrogel scaffold for 3D cell culture is Algimatrix™. Developed by Invitrogen in 2007, this animal-free macroporous scaffold is sold in dry state in the well-plate format. Algimatrix™ is synthesized by physical crosslinking of alginate matrix. Physical crosslinking is done by mixing divalent cation (Ca^{2+}) with the native alginate solution which then creates stiffer matrix [103-105]. We realize since the crosslinking is done only by physical ionic crosslinking, the scaffold stability over time in culture medium is an issue. Ionically-crosslinked alginate matrix may undergo ion exchange process during cell culture involving loss of divalent cation. This process is generally uncontrollable and unpredictable. Therefore Algimatrix™ in this case may not be suitable for hepatocyte spheroid culture over prolonged culture. In addition, the divalent cation may diffuse into the medium and interfere if used for kidney-tissue cell culture.

Another polystyrene scaffold which was proposed as *in vitro* drug testing platform, developed by Prof Przyborski in 2004, has also been commercialized under company Reinnervate Durham UK (trade name Alvatext scaffold). His research group

has gone into simple drug testing trial of cultured HepG2 cells and methotrexate (MTX) [106, 107]. HepG2 cells could form cellular aggregates with excellent microvili and bile canaliculi formation confirmed by TEM imaging. However, there is no special feature in the mechanical stiffness issue and ligands needed for specific soft tissue/cell culture and long term culture function maintenance. In addition, we are not convinced by how the cells behave in the nanoscale of the polystyrene scaffold since there is no significant difference with conventional polystyrene tissue culture flask in that scale.

Latest group to date which is developing inverted colloidal crystal polyacryl amine hydrogel scaffold is Kotov's lab from University of Michigan [108]. They are developing uniform macroporous hydrogel polyacryl amine scaffold using polymethyl metacrylate spheres as pores template, known as 3D Biomatrix scaffold in the market. Hepatocyte spheroid will be uniformly formed and distributed in the pores.

All the above examples of market available and ongoing research scaffolds for 3D cell culture platforms mainly function to maintain cell-cell contact and finally have 3D spheroid as cell culture model.

2.5 Hepatocyte culture models for hepatitis C antiviral screening

Hepatitis C virus (HCV) is a major cause of acute and chronic hepatitis in the world. Infected HCV patients almost result in chronic hepatitis infection, with 60-70% of all cases develop active liver diseases and the rests include cirrhosis, end-stage liver disease and liver cancer. In estimation, 3% of world's population is chronically infected with HCV [109, 110]. Within 20 years of infection, chronic HCV patients have developed cirrhosis, which in turn elevate the risk of hepatocellular carcinoma and liver failure. This complication of HCV infection has significantly

increased the needs of liver transplantation and related mortality [111]. There are 6 major HCV genotypes exist in the world with approximately three quarters of patients with chronic HCV have genotype 1 infection [112]. This majorly affecting genotype 1 HCV is more resistant to the current available treatments, PEG interferon 2 α and ribavirin [110]. There are still no available effective preventive vaccines. Therefore there is a strong need to develop new therapies against HCV genotype 1 infection.

The available standard therapy for chronic HCV infection, the combination of PEG interferon 2 α and ribavirin, still leads to side effect upon 48-week administration; the virus sustain its virological responses [113]. In addition to this, this combination treatments are often poorly tolerated thus causes other side effects such as influenza, cytopenias and neurophyschiatric symptoms [113]. These problems had led efforts to combat HCV with different strategies. Instead of combating the virus itself, efforts needs to be attempted to disrupt the pathways that the virus undertakes to infect the host.

As shown in **figure 4**, HCV infects the host cell through some host cell glycoprotein receptors. It has been known that HCV exploits human host proteins for its own purposes. With these host factors identification for the HCV life cycle, the development of new anti HCV vaccine can be greatly sophisticated. This strategy in targeting the host cell proteins enables the broader treatments to combat HCV more effectively [110].

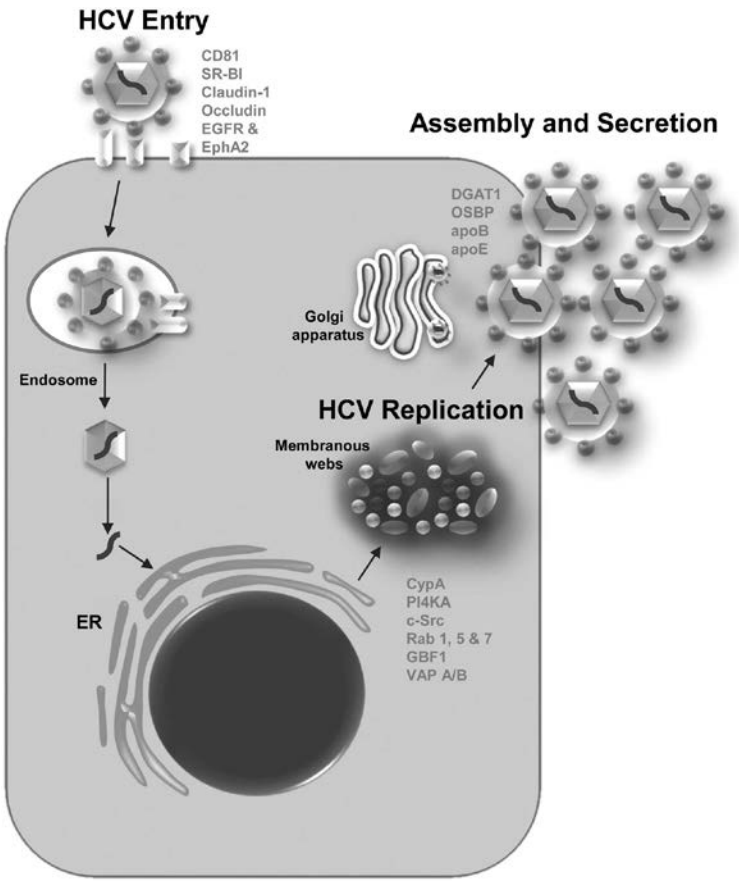

Figure 4. Many host factors are involved at each step of the HCV life cycle, which starts with virus binding to its specific receptors (CD81, Claudin1, Occludin, and SR-BI/SCARB1). After viral uncoating, the positive-sense HCV RNA is translated and also serves as a template for RNA replication and polyprotein translation. Viral RNA replication occurs on an altered host membrane compartment known as the membranous web; a short list of host factors believed to support web formation and/or RNA replication is shown. (adapted from [110])

HCV is one of the viruses in *Flaviviridae* family with single-stranded RNA virus approximately 9600 nucleotides in length [114]. As depicted in **figure 4**, HCV infection into the host cell is initiated by the attachment of viral E1/E2 heterodimers to the hepatocyte cell membrane. The hepatocyte cellular receptors and co-receptors to this infection include glycosaminoglycan, cluster of differentiation 81 (CD81), scavenger receptor type B class 1 (SR-B1/SCARB1), Claudin1 and Occludin [115-119]. The first interaction during HCV infection occurs between glycosaminoglycan on the hepatocyte cell surface with HCV virions. This then continued with binding of

CD81 and SCARB1 with HCV E2 envelope protein, at the same time point in viral entry [120]. Claudin1 and Occludin, both are tight junctions proteins of polarized hepatocytes, act only at the late HCV post-binding step [119]. By understanding these host factors involved in the early stage of HCV live cycle, the development of novel antiviral leads to the increases in the number of options for combining drug therapy.

The host specificity of HCV only in chimpanzee and human liver has made the study to be greatly challenged over the past decades [121]. It has been hampered by the lack of adequate human hepatocyte culture and small animal models [122]. Since the use of chimpanzee as HCV infection model is not cost effective and not in tally with the efforts to reduce the animal use in research, most efforts are paid towards the culture of human liver cells [84]. Huh 7 as cell source in HCV infection model has been investigated but found to be lack in effective RIG-I-mediated interferon production thus unsuitable for innate immunity studies in HCV infection [123]. Previously reported cell lines outside the Huh 7 family that are able to support HCV infection, are either derived from tumor tissues or immortalized, making them incompatible with research intended to determine potential oncogenic effects of HCV infection [124]. Therefore, primary human hepatocytes are still regarded as the gold standard in HCV infection elucidation. Primary human hepatocytes in this case need to be cultured in a proper system to be polarized over extended culture period, because viral entry into the cells is controlled by cell polarization and cellular localization of different markers such as cluster of differentiation 81 (CD81), SCARB1 and Claudin1 [125, 126]. This presents a challenge to create a robust 3D cell culture platform to maintain primary human hepatocyte polarity. There is a need to properly recapitulate hepatocyte polarity in the form of cell-dense construct such as spheroids which act like artificial human liver tissue. By achieving properly polarized

human hepatocyte models *in vitro,* one can study the HCV infection as well as replication over some period of time and thus one can screen new candidate compounds for anti viral drugs. The *in vitro* human hepatocyte model is considered to be more economic compared to one other methods of repopulating mouse liver ectopically with human hepatocytes, which show its ability to replicate HCV [127]. It is described in **table 3** various reported 3D cell culture models with different cell sources and platforms to show HCV infections.

Table 3. Various engineered-liver cell models for *in vitro* testing of HCV infection study

Models	**Features**	**Refs.**
Micropatterned co-culture models of primary human hepatocyte and stromal cells	Model showed persistent HCV replication up to two weeks of culture but number of infected cells were low (~1%)	[118]
Matrigel-embedded 3D culture of Huh 7 cells as spheroids	Cell lines used as cell model. Localization of several HCV receptors e.g. Occludin, Claudin1 and SCARB1 are still not comparable to those observed in primary human hepatocyte	[4]
Primary human hepatocytes spheroid suspension culture	Orbital shaker used to form spheroids which might not be high throughput. Single patient's HCV derived serum used for viral inoculation.	[128]
Human hepatocellular carcinoma-derived cell line, FLC4 (Functional Liver Cell 4) cultured in the three-dimensional radial-flow bioreactor	Carcinoma cells used as cell model. HCV receptors were not investigated. Single patient's HCV derived serum used for viral inoculation.	[129]
3D culture of cell lines bearing dicistronic HCV RNAs in thermoreversible hydrogel	Carcinoma cells used as cell model. HCV core and NS5A proteins expressions were lower compared to monolayer culture.	[130]

2.6 Cell source issue in organotypic liver culture models

2.6.1 Primary cells

Cell source used in the development of *in vitro* hepatocyte models for both drug safety testing and disease models needs to be carefully examined. In this thesis, primary hepatocytes, readily available in our lab, were used as the main cell source. Freshly isolated primary hepatocytes are the preferred cell model for recapitulating the functional responses of the liver, especially for *in vitro* studies to predict *in vivo* drug metabolism and clearance [87, 131-133]. Although primary hepatocytes could offer significant functional benefits, their routine use in cell culture systems also imposes challenges. The most significant challenge is the scarcity in obtaining primary cells and the tissues from which they are isolated. The quality variability of primary human hepatocytes isolated from different patients is another challenge; differences in patients' medical history, genetics and method of isolation can contribute to the difficulty in getting reproducible results and comparing results from different labs [124}]. Moreover, not all labs have the facility to isolate primary cells in routine basis. Hence, currently many commercial vendors have become important sources for obtaining primary cells, particularly those of human origin. The advances in the cryopreservation technique to store human hepatocytes for long term has improved the conveniency and capabilities associated with the use of primary cells, removing limitations of the urgency to culture hepatocytes within couple of hours post-isolation and enabling repeat experiments using the same batch of cells. When properly stored and handled, cryopreserved hepatocytes exhibit similar viability and functions after thawing compared to freshly isolated hepatocytes [134-136]. However,

finding a reliable commercial source of fresh and or cryopreserved hepatocytes from other important toxicology species, such as dog, monkey and mouse, can be problematic. Therefore to be widely applicable for others' routine use, we also have to consider other different liver cells such as immortalized cell lines and stem cell derived hepatocytes.

2.6.2 Immortalized liver cell lines

A cell line is a permanently established clonal lineage, sometimes derived from hepatoma, where the daughter cells will proliferate unlimitedly in proper medium and growth conditions. In contrast to primary cells, cell lines are not confined to a limited number of cell divisions due to mutations in one or more growth control pathways thus have become immortalized [137, 138]. Liver cell lines are very popular *in vitro* model to study liver function and general mechanisms of toxicity. However, cell lines do not contain all the metabolic enzymes, and the enzymes that are present are not at their physiological levels thus they are typically unsuitable for drug metabolism and toxicity prediction studies [139]. Other drawbacks when using cell lines as the cell source in organotypic culture models are the dependence of gene expression on several factors such as passage number and genomic instability, hence leading to dedifferentiated cells whose phenotype no longer resemble the native cells *in vivo* [139].

One of the most commonly used human liver cell line is HepG2 cell, which was derived from liver tissue with a well differentiated hepatocellular carcinoma. This cell exhibits epithelial-like morphology when cultured as monolayer and cellular aggregates. HepG2 cell could secrete typical hepatic plasma proteins like albumin and transferrin and is able to perform biotransformation of many, but not all, xenobiotic

compounds. The versatility of culturing HepG2 cell compared to primary human hepatocytes makes this cell attractive in various toxicogenomic studies. However, comparisons between HepG2 and primary hepatocytes show substantial differences in basal gene expression [140-142]. HepG2 show higher expression of genes involved in cell cycle regulation, DNA, RNA, and nucleotide metabolism, transcription, transport, and signal transduction, and lower transcription levels are associated with cell death, lipid metabolism, and xenobiotic metabolism [142]. Basal gene expression levels of xenobiotics biotransformation enzymes (CYP1A1, CYP1A2, CYP2C9, CYP2E1, and CYP3A4) are substantially lower in HepG2 cell compared to primary hepatocytes [142]. The inherent lack of bioactivation potential leads to an underestimation of metabolic-dependent toxicity for particular compounds, such as aflatoxin B1, making HepG2 cells a less predictive *in vitro* model system [41, 142, 143]. Some researchers have created variants or subclones of HepG2 to address some of these shortcomings by transfecting HepG2 cell with constructs which express increased levels of phase 1 enzymes (such as CYP1A1, CYP1A2, CYP2E1 and CYP3A4) or glutathione-S-transferases [144, 145]. Therefore, HepG2 and its various subclones that have been identified (including C3A) provide a biological model that enables some rudimentary approximation of hepatic function that offers some value in certain applications, but these cells still could not recapitulate many important aspects of primary hepatocyte function and phenotype. In liver disease model, studies of HCV infection in hepatocyte cell line HepG2 gave poor result due to inadequate expression of proper HCV entry receptors [146] .

Another popular cell line in organotypic liver culture model is HepaRG, which is a cell line derived from adult hepatocellular carcinoma [147]. When cultured in monolayer, HepaRG cells consist of two cell types i.e. flattened cell with clear

cytoplasm, biliary epithelial cell and primary human hepatocyte-like cell. In order to be fully differentiated into hepatocyte-like cell, HepaRG cells must be treated with addition of dimethyl sulfoxide (DMSO) at rather high concentration (1%). Fully differentiated HepaRG cells exhibit various cytochrome P450 enzymes such as CYP1A2, CYP2B6, CYP2C9, CYP2E1 and CYP3A4 significantly higher than HepG2 and its subclones. They also exhibit phase 2 enzymes and liver transporters normally found in primary human hepatocytes [147-149]. HepaRG cells also express receptor pathways involved in xenobiotic metabolism and clearance, including constitutive androstane receptor (CAR), pregnane X receptor (PXR), and aryl hydrocarbon receptor (AhR). This improved nuclear receptors results in more *in vivo*-like expression of CYP1A1, CYP1A2, CYP2B6, CYP2C8, CYP2C9, CYP2C19 and CYP3A4 enzymes in HepaRG compared to most other hepatic cell lines [148-150]. However, the use of high concentration of DMSO (1%) in order to maintain cell differentiated state and optimal expression of metabolic enzymes, otherwise the CYPs activities decrease, has resulted in the activation of receptor pathways involved in the regulation of phase 1 and 2 biotransformation enzymes (e.g. CAR and PXR) [151, 152]. In these conditions, CYP3A4 enzyme in HepaRG cells is unable to respond to drug inducers, such as phenobarbital (PB) and rifampicin (RIF). On the other hand, HepaRG cells have shown the promise to be used in HCV infection study; their progenitor cells permit HCVpp entry while differentiated cells support long term production of infectious HCV particles [153]. Nevertheless, HepaRG still represents the most promising surrogate to primary human hepatocytes and has served as a valuable tool for conducting some preclinical development studies [148, 150].

2.6.3 Stem cells derived hepatocytes

The challenges associated with primary hepatocytes and their surrogates have sparked interest to use stem cells derived hepatocytes as the cell source in organotypic culture. Both embryonic stem cells (ESCs) and induced pluripotent cells (iPSCs) are capable to perform self renewal and retain the ability to differentiate into each of the three germ layers (endoderm, mesoderm and ectoderm). Thus these cells theoretically can differentiate into any cell lineages [154]. Some researchers have established the protocols to differentiate these pluripotent cells towards hepatocytes [154-158]. The protocols have a common procedure to initiate the endodermal differentiation process that is by adding activin A followed by fibroblast growth factor and Wnt3a to facilitate differentiation towards hepatic lineages. Subsequently, hepatic differentiation is facilitated by treatment with cocktails mixture of hepatocyte growth factor, epithelial growth factor, oncostatin M and fibroblast growth factor [159], and by increasing cellular confluency [160, 161]. The advantage of using cells that are derived from adult source i.e. iPSCs is their ability to create donor pool that is pre-selected thus represent polymorphic variants within a target population. This advantage is difficult to achieve with primary cells.

Despite the advantages in sourcing and expansion of these stem cell derived hepatocytes, limitations still exist such as the persistent fetal phenotype exhibited by these cells [159, 162], although the current iPSCs based approaches managed to minimize this effect [157, 163]. From the perspective of drug safety testing, it is important that the cells used as hepatocyte source to have expression of phase 1 and 2 enzymatic activities, as well as uptake and efflux transporter activity. To date, all stem cell based approaches still exhibit suboptimal phase 1 activity, with no clear

information on phase 2 or transporter activity [162]. Reported deficiencies in phase 1 enzyme activity in stem cell populations could be triggered by the heterogeneity of the differentiated cell lineages population, as purified populations actually exhibit CYP3A4 activity at levels similar to those in primary human cells [164]. Human hepatocyte-like cells derived from iPSCs have been reported to support the complete HCV life cycle including inflammatory response of infection, thus enabling study of viral pathogenesis correlation with host genetics [165].

CHAPTER 3

DEVELOPMENT OF GALACTOSYLATED CELLULOSIC SPONGE FOR 3D HEPATOCYTE CULTURE AND DRUG SAFETY TESTING

3.1 Introduction

The content of this part of the thesis is slightly modified from author own published paper [80] and permission to reproduce full article had been obtained (see appendix). The early development of cellulosic sponge as cell culture platform has shown the salient features of this sponge in creating 3D cell microenvironments within its macroporous hydrogel networks [15, 166]. The chemical property of the cellulosic sponge raw material, FDA-approved hydroxypropyl cellulose (HPC), has offered the ease of functionalization of its side chain group with different cell ligands. The needs to have a proper surface chemistry in the 3D cell culture scaffold have been facilitated by this chemical versatility. In liver tissue engineering, one of the widely studied cell construct is spheroids which are formed by the interaction of conjugated galactose on a cell culture substrate with hepatocyte membrane asialoglycoprotein receptor (ASGPR).

Spheroids are three-dimensional multi-cellular aggregates that exhibit a high degree of cell-to-cell contact. Compactness of cells contained in 3D spheroids *in vitro* preserve complex *in vivo* cell phenotypes which are otherwise absent in conventional 2D cultures [167, 168]. 3D multi-cellular spheroids have been useful in multiple applications including stem cell, cancer biology and tissue engineering research [95, 169-171]. In 3D hepatocyte spheroids, tight cell-cell junctions help sustain cell

viability for extended culture periods and maintain high level liver-specific functions e.g. albumin secretion, urea synthesis and cytochrome P450 activity [25, 172]. These attributes make 3D hepatocyte spheroids potentially attractive for in vitro drug safety testing.

Growing spheroids using previously described methods such as by hanging drop, centrifugation, on 2D substrates, or in suspension culture are limited since these methods provide no means of physical spheroid constraint during extended culture. Consequently there is difficulty in controlling spheroid size and in manipulating floating spheroids for cell-based drug safety testing applications [173-176]. When smaller spheroids collide to form larger spheroids in culture, mass transfer of oxygen, nutrients, metabolites and drugs can be impeded in the inner core yielding high variability during drug safety testing [175]. Attempts to constrain 3D spheroids in a diffusible dimension have been achieved by growing spheroids on microfabricated platforms [177, 178], polyurethane foams [179, 180], and polymeric scaffolds [108], but these methods do not provide the optimal chemical and mechanical microenvironments needed to maintain high-level cellular functions. Furthermore, scalability in manufacturing and simplicity in operation for high-throughput, large-scale drug safety testing applications is also problematic.

To address these concerns we have constrained hepatocyte spheroids in a macroporous network of a soft galactosylated cellulosic sponge. The macroporosity of the sponge provides control over spheroid size while the conjugated galactose ligands present chemical cues to the cells to form spheroids. The soft hydrogel-based sponge would be proper to maintain mature hepatocyte differentiated functions via control of the matrix rigidity [181]. The configuration of the sponges supports high-

throughput applications and ease of use, similar to readily available 2D culture platforms. Sponges are fabricated in bulk and sliced thin to minimize drug absorption. Hepatocyte spheroids grown in the sponge can maintain 3D cell morphology, cell-cell interactions, polarity, transporter expression, excretion and metabolic functions; and exhibit in some cases improved CYP450s enzyme activities.

3.2 Materials and Methods

3.2.1. Materials

All chemicals and reagents were purchased from Sigma Aldrich (Singapore), unless otherwise stated.

3.2.2 Chemical synthesis of galactosylated hydroxypropyl cellulose allyl (HA Gal)

Hydroxypropyl cellulose (HPC), Mw = 80,000 g/mol and ~3.4 degree of etherification was dehydrated by azeotropic distillation in toluene. 4 grams of dried HPC was dissolved in anhydrous chloroform (100 mL), to which 2.095 mL allyl isocyanate 98% and 1 mL dibutyltin dilaurate 95% were added dropwise. The mixture was stirred vigorously for 48 hours at room temperature, after which it was precipitated in an excess amount of anhydrous diethyl ether. Following vacuum drying, the product was dissolved in deionized water (DI H_2O), purified by dialysis for 3 days, and finally lyophilized to the intermediate product, hydroxypropyl cellulose allyl (HA). For galactose conjugation, 1 gram of HA was dissolved in 15 mL anhydrous dimethyl formamide (DMF) in which the hydroxyl groups were activated by addition of 1,1'-carbonyldiimidazole (0.322 g in 2 mL DMF). D-(+)-galactosamine HCl (0.427 g in 30 mL DMF), which was dissolved with addition of

triethylamine, was added to the mixture with two folds molar ratio compared to D-(+)-galactosamine HCl. The reaction was carried out for a further 48 hours at room temperature. To remove impurities, the mixture was further dialyzed in excess methanol and subsequently in deionised water for 3 days each and the final product (hydroxypropyl cellulose allyl galactose, HA Gal) was lyophilized. A schematic diagram with the complete synthesis described, including ^{1}H NMR characterization are shown in **figures 5 and 6.**

3.2.3 Preparation of HA Gal sponges

HA Gal was dissolved in deionised water to a final concentration of 7.5 % wt/vol after which the solution was inserted into tubes (diameter 6 mm, length 3 cm). The tubes were heated in a water bath (40°C) until phase separation occurred, and then crosslinked by γ irradiation for 30 min at a dose of 10 kGray/hour (Gammacell 220, MDS Nordion, Canada). The sponge monoliths were obtained by breaking tubes subsequent to freezing in dry ice. A Krumdieck tissue slicer (Alabama Research & Development USA) was used to cut the sponge uniformly (50 rpm for 1 mm thickness). We fabricated thin sponge slices to reduce possible drug absorption during assays. Sliced sponges were washed extensively with excess amounts of deionised water for 3 days to remove uncross-linked polymers. Finally, slices were lyophilized and sterilized by γ irradiation (1.7 kGray total dose) prior to cell seeding with hepatocytes. A schematic diagram of the sponge preparation is described in **figure 6.**

As a comparison, galactosylated polyethylene terephthalate (PET Gal) membranes were also seeded with hepatocytes. Preparation and synthesis steps of PET Gal membranes have been described previously [175].

3.2.4 Physiochemical characterization of HA Gal macroporous sponges

3.2.4.1 High performance liquid chromatography elution assay

Galactose presence in the sponge was detected by a HPLC elution assay. Sponges were hydrolyzed by 6 N HCl at 110°C for 24 hours. Cooled hydrolyzed solutions were evaporated, re-suspended in 500 µL deionised water and derivatized using the ATTO-TAG™ CBCQA amine-derivatization kit (Molecular Probes, USA) for fluorescence detection on a C-18 column using HPLC (Agilent Technology, place). The mobile phase consisted of A) water + 0.1 % trifluoroacetic acid (TFA), and B) acetonitrile + 0.1 %TFA with an A/B gradient (98:2/ 70:30 in 45 min. The flow rate was 1 mL/min and the fluorescence detector settings were excitation at 450 nm, and emission at 550 nm.

3.2.4.2 X-Ray photoelectron spectroscopy

X-Ray photoelectron spectroscopy was used to qualitatively verify galactose ligand conjugation onto the HA chemical backbone. Measurements were made on a VG ESCALAB Mk II spectrometer with a MgKa X-ray source (1253.6 eV photons) at a constant retard ratio of 40.

3.2.4.3 Scanning electron microscopy

Top and cross section views of the sponge surface morphology and porosity were captured using SEM (JEOL JSM- 5600, Japan) at 10 kV. High magnification of SEM (15,000 folds) was performed to observe the sponge surface structure. Prior to imaging, the dried sponge was sputter coated with platinum for 60 seconds. Pore size distribution of the sponges was quantified with Image J software (version 1.43u) from collective SEM top view images of the sponges.

3.2.4.4 Water uptake and sponge porosity measurements

The lyophilized sponges were soaked in deionised water at room temperature for 48 hours; their water uptake were calculated according to the equation $Water\_uptake = (\frac{W_h - W_d}{W_h})100\%$, where W_h is the hydrated weight and W_d is the dehydrated weight. The porosities of lyophilized HA Gal sponges were determined by solvent replacement. Samples were soaked in absolute ethanol for 24 hours and weighted after excess ethanol on the surface was blotted. It was noted that there were no significant changes in dimension before and after immersion in ethanol. The porosity was calculated as $Porosity = (\frac{M2 - M1}{\rho V})100\%$, where M1 and M2 are the weight of sponge before and after immersion in absolute ethanol, respectively; ρ is the density of absolute ethanol and V is the volume of sponge.

3.2.4.5 Elastic modulus measurement

The elastic modulus of the sponge was measured by atomic force microscopy (Bioscope Catalyst, Veeco Instruments, Santa Barbara, CA) in deionized water. A hybrid Atomic Force Microscopy (AFM) probe consisting of a silicon nitride cantilever and a silicon tip (ScanAsyst-Fluid, Veeco Probes, Camarillo, CA) was used. The deflection sensitivity was calibrated by ramping force-distance curves on a glass surface, and the spring constant was calibrated by the thermal noise method. After calibration, 128 x 128 force-distance curves were recorded over an area of 5 μm x 5 μm by force volume. Each force-distance curve was analyzed by fitting to the Hertz model with conical tip geometry and Poisson ratio of 0.5. The obtained elastic moduli from each force-distance curve were mapped into a bitmap image with 128 x 128 pixels. The curve fitting and statistical analysis was implemented by a self-developed

Fortran program. The relationship between elastic modulus with the measured force is described as $F = \frac{2}{\pi}\frac{E}{1-v^2}\tan\alpha\delta^2$, where F is the measured force, E is Young's elastic modulus, v is the Poisson ratio of the material under measurement (0.5 was used in the data processing), α is the half angle of the probe (22°) and δ is the sample deformation/indentation.

3.2.4.6 Zeta potential measurement

HA Gal solutions in deionized water with different concentrations (0.125 to 2.5 %wt/vol) were heated to 50°C to let the phase separation occur. The zeta potentials were measured using Malvern Zeta Sizer Nano ZS 90 (Malvern Instruments, United Kingdom) normalized to the base potential of water.

3.2.5 Hepatocyte isolation and culture

Hepatocytes were isolated from male Wistar rats weighing 250-300 g using a modified in situ collagenase perfusion method [182]. Animals were handled according to the IACUC protocols approved by the IACUC committee of National University of Singapore. Cells were maintained with Williams' E medium supplemented with 10 mM $NaHCO_3$, 1 mg/mL BSA, 10 ng/mL of EGF, 0.5 mg/mL of insulin, 5 nM dexamethasone, 50 ng/mL linoleic acid, 100 units/mL penicillin, and 100 mg/mL streptomycin and were incubated with 5% CO_2 at 37°C and 95 % humidity. Medium was replenished every two days. Viability of hepatocytes was determined to be >90% by the Trypan Blue exclusion assay. Yields were approximately 10^8 cells per rat. Freshly isolated rat hepatocytes (10^5 cells in 10 μL culture medium) were loaded to the centre of the wells in 48-well plates; the sponges

were immediately inserted into the wells to allow cells to be absorbed into the sponges from the lower surface. Another aliquot of 10^5 cells in 10 μL culture medium was then seeded into the sponge by dropping the cell suspension onto the top sponge surface. The cell suspension was absorbed into the sponge interior due to the inherent hydrophilicity of the sponges. Fresh culture medium was added to the sponge edge after 45 minutes incubation (300 μL per sponge in 48-well plate). Hepatocytes seeded on a collagen sandwich platform (0.29 mg/mL collagen concentration) were used as control as reported previously [183].

3.2.6 Hepatocyte spheroids characterization

3.2.6.1 Spheroids size distribution

Spheroid size distribution was quantified using imageJ software (version 1.43u) from collective phase contrast images of living hepatocyte spheroids cultured on the PET galactose membrane and in the HA Gal sponges on day 1, 3 and 6.

3.2.6.2 Scanning electron microscopy

Hepatocyte spheroids in sponges on day 1, day 3 and day 7 were fixed with 2.5 % glutaraldehyde overnight and stained with 1% OsO_4 for 1 h. Samples were then dehydrated step-wise with ethanol (25 %, 50 %, 75 %, 90 % and 100 %) for 10 minutes each, dried in a vacuum oven and sputter coated with platinum for 60 seconds. The samples were viewed with a scanning electron microscope (JEOL JSM- 5600, Japan) at 10 kV.

3.2.6.3 Live/dead staining

Hepatocytes spheroids were co-stained with Cell Tracker Green (CTG, 20 μM) (Molecular Probes, USA) and propidium iodide (PI, 25 μg/mL) (Molecular Probes, USA) to determine live and dead cells, respectively. Cells were incubated for 30 min at 37°C and then fixed with 3.7 % paraformaldehyde for 30 min at room temperature. Fluorsave (Merck Chemicals) was applied to the stained spheroids to minimize photo-bleaching. Images were acquired by confocal laser scanning microscopy (Zeiss LSM510, Germany) at 488 and 543 nm excitation wavelengths.

3.2.6.4 Time lapse imaging of spheroids formation

The dynamic process of hepatocyte spheroid formation in the sponges was monitored immediately upon cell seeding. Hepatocytes were pre-stained with 20 μM Cell Tracker Green (Molecular Probe, USA) for 20 min prior to seeding. Seeded sponges were imaged consecutively for 12 hours using a Delta Vision system (Applied Precision, USA) equipped with nano-positioning and a controlled temperature chamber set at 37°C and 5 % CO_2. Images were acquired in hourly intervals thereby minimizing light exposure to the cells.

3.2.7 Hepatocyte functional assessments

3.2.7.1 Immunofluorescence microscopy

To stain F-actin, E-cadherin and MRP2/CD147, hepatocytes cultured for 48 hours in the sponges were fixed in 3.7 % paraformaldehyde for 30 min. For staining F-actin, the cells were permeabilized for 5 min in 0.1 % Triton X-100 and incubated with 1 μg/mL TRITC-phalloidin (Molecular Probes, USA) for 20 min. For E-cadherin,

the cells were permeabilized with 0.1 % Triton X-100 for 30 min, blocked with 1 % BSA for 30 min, incubated with mouse anti-rat E-cadherin (BD, USA) overnight at 4°C followed by incubation with a FITC conjugated anti-mouse secondary antibody. For MRP2/CD147 staining, the cells were permeabilized with 0.1% Triton X-100 for 30 min, blocked with 1% BSA for 30 min, incubated with rabbit anti-rat MRP2 (Sigma Aldrich, Singapore and mouse anti-rat CD147 (Serotec, USA) overnight at 4°C and eventually incubated with FITC conjugated anti-mouse and TRITC conjugated anti-rabbit secondary antibodies. For all staining procedures, at the end of staining period Fluorsave (Merck Chemicals) was applied to preserve the dyes from bleaching. Microscopy images were acquired with 20x lens on a Zeiss Meta 510 upright confocal microscope. The 3D image stack was reconstructed using LSM Browser.

3.2.7.2 Transmission electron microscopy

Hepatocyte spheroids in sponges were fixed with 3.7% paraformaldehyde for 30 min and treated with 1% OsO_4 for 2 hours at room temperature. Samples were subsequently dehydrated step-wise with ethanol (25 %, 50 %, 75 %, 95 % and 100 %) for 10 min followed by 100% acetone twice for 20 min each. Upon dehydration, samples were then treated with 1:1 ratio mixture of acetone and araldite resin for 30 min at room temperature followed by overnight treatment at a 1:6 ratio at room temperature**.** On the following day, the samples were placed into araldite resin for 30 min at room temperature before transferring into a 40°C oven for another 30 min**.** Araldite resin was subsequently changed followed by 1 hour subsequent treatments at 45°C and 50°C. Lastly, the samples were embedded with araldite resin at 60°C for 24 hours. Sections of 90-100 nm thickness were sliced using a Leica EM UC6

Ultramicrotome, collected onto 200-mesh copper grids and co-stained with uranyl acetate and lead citrate for 10 min each. Observation was undertaken with a Transmission Electron Microscope (TEM) (JEOL JEM-1010, Japan) at voltage 100 kV.

3.2.7.3 Biliary excretion of fluorescein dye

For monitoring hepatocyte repolarization, we visualized the excretion of fluorescein dye via bile canaliculi. Hepatocytes spheroids were incubated with 15 μg/mL fluorescein diacetate (Molecular Probes, USA) in Williams' E medium at 37 °C for 45 min at different time intervals (16 hours, 24 hours and 48 hours) post-seeding. The cultures were then rinsed and fixed with 3.7 % paraformaldehyde for 30 min before viewing with a 20x lens on a Zeiss Meta 510 upright confocal microscope.

3.2.7.4 Albumin secretion & urea synthesis assays

Albumin secretion by hepatocytes on days 1, 3, 5 and 7 were assayed using a rat albumin enzyme-linked immunosorbent assay quantitation kit (Bethyl Laboratories Inc., Montgomery, Texas). Urea synthesis by cultured hepatocytes in William's E medium spiked with 1 mM NH_4Cl for 90 min was assayed on the same days using a Urea Nitrogen Kit (Stanbio Laboratory, Boerne, Texas). All functional data were normalized by the number of cells seeded in the sponges which was quantified using the Quant-iT™ PicoGreen dsDNA Assay Kit (Invitrogen, Singapore).

3.2.8 Drug inducibility of hepatocyte spheroids

3.2.8.1 Reverse transcriptase polymerase chain reaction

RNA was extracted from hepatocytes cultured as 3D spheroids in HA Gal sponges by TRIzol (Invitrogen, Singapore). Total RNA concentration was quantified by a Nanodrop (Thermoscientific) and 1 µg of RNA was converted to cDNA by High Capacity RNA-to-cDNA (Applied Biosystems). Primers were designed using Primer 3 and real-time PCR was performed by using SYBR green fast master mix on a ABI 7500 Fast Real-Time PCR system (Applied Biosystems). Gene expression was calculated using the ΔΔCT method normalized to GAPDH. The primers used in experiment are shown below.

Table 4. Primer sequences used in RT-PCR experiments

CYPs

Genes	Forward sequence	Reverse sequence	Primer Accession No.	P.S. (bp)
CYP1A2	CACGGCTTTCTGACAGACCC	CCAAGCCGAAGAGCATCACC	NM_012541.3	291
CYP2B2	ACCGGCTACCAACCCTTGAT	TGTGTGGTACTCCAATAGGGACAA	NM_001198676.1	105
CYP3A2	TGGGACCCGCACACATGGACT	TCCGTGATGGCAAACAGAGGCA	NM_153312.2	183
CYP4A1	TCATGAAGTGTGCCTTCAGC	GATGTTCCTCACACGGGAGT	NM_175837.1	116
CYP2E1	AGGCTGTCAAGGAGGTGCTA	ATGTGGGCCCATTATTGAAA	NM_031543.1	114

CYP: Cytochrome P450

Transporters

Genes	Forward sequence	Reverse sequence	Primer Accession No	Product Size (b.p.)
Mdr1a	TCGGAAAGTAGAGACAC GTGAGGT	TCCAGCCAACCTGCA TAGCG	NM_133401.1	165
Mrp2	CGCGAGGAGAGCATTAT	GGCAAGGTAGAATT TGGTTAT	NM_012833.1	213
Ntcp	CATTATCTTCCGGTGCTA TGA	GTTTCTGAGCATCGG GATT	NM_017047.1	421
Bsep	TGACATTCGCTCTCTTAA CAT	TGGGATTCCGTATGA GG	NM_031760.1	281
Oatp1	CTTAAAGCCAACGCAAG ACC	AGAGATACCCAAGG GCACAA	NM_017111.1	127
GAPDH	AGACAGCCGCATCTTCTT GT	TGATGGCAACAATG TCCACT	NM_017008.4	142

Mdr1a: Multi-Drug Resistance 1a, Mrp2: Multidrug Resistance Protein 2, Ntcp: Na/taurocholate Co-transporting Polypeptide, Bsep: Bile Salt Export Pump, Oatp1: Organic Anion Transporting Polypeptide 1

P.S.: Product size, Annealing temperature: 60°C, Cycle numbers: 40

3.2.8.2 CYP450 induction study

Hepatocyte spheroids cultured in the sponges were used to study drug induction of three CYP450 enzymes, i.e. CYP1A2, CYP2B2 and CYP3A2. 72 hours post-seeding, cells were incubated at 37°C with Williams' E medium containing inducers (50 µM β-naphthaflavone, 1A2; 1 mM phenobarbital, 2B2; 50 µM pregnenolone-16α-carbonitrile, 3A2). After 48 hours of induction, medium was removed and the cells were further incubated for 2 hours at 37°C with Krebs-Henseleit- bicarbonate (KHB)

buffer (118 mM NaCl, 1.2 mM $MgSO_4$, 1.2 mM KH_2PO_4, 4.7 mM KCl, 26 mM $NaHCO_3$, and 2.5 mM $CaCl_2$) containing the P450 substrates (200 μM phenacetin, 1A2; 200 μM bupropion, 2B2; and 5 μM midazolam, 3A2) after which the supernatants were collected as samples. The drug metabolite product in the supernatant was assayed from induced and vehicle- (0.1% DMSO) treated hepatocytes cultured in HA Gal sponges or in the collagen sandwich cultures. Detected metabolite products for CYP1A2, CYP2B2 and CYP3A2 were acetaminophen (APAP), hydroxy bupropion (OH-bupropion) and hydroxy midazolam (OH-midazolam), respectively. Cell supernatants (300 μL) were added with 50 μL internal standards (100 ng/mLAPAP-D4 for APAP and 1'-OH-midazolam, 100 ng/mL OH-bupropion-D6 for OH-bupropion) and dried by concentrator under vacuum. The obtained residues were reconstituted in 50 μL methanol containing 0.1 % formic acid and centrifuged at 10000 rpm for 10 min. The supernatants were then analysed by Liquid Chromatography-Mass Spectrometry (LC-MS Finnigan LCQ Deca XP Max, Agilent 1100 series). The LCMS experiments setup consisted of a flow rate of 0.8 mL/min, with solvent A, 0.1% formic acid in water, and solvent B, 0.1% formic acid in methanol. The column used was a Phenomenex Onyx-monolithic C18 with dimensions of 100 x 3.0 mm. The mass spectrometry parameters were spray voltage 5 kV, sheath gas flow rate of 80 L/min, auxiliary gas flow rate set at 20 L/min, capillary temperature of 350°C, tube lens 45 V, and capillary voltage 30 V. Elution schemes for the three different metabolites products were for APAP and OH-midazolam, solvent B gradually increased from 6% to 90% in 6 min while for OH-bupropion, solvent B gradually increased from 10% to 90% in 6 min.

3.2.9 Drug absorption properties of sponge

Sponges were incubated with various hydrophobic and hydrophilic drugs with different net charges dissolved in PBS for 24 hours at 37°C. The concentrations of each compound before and after incubation were recorded with UV Spectrophotometer (Agilent). Percentage of drug absorption was determined by the formula as follows: $\%Absorption = (1 - \frac{Concentration_{Final}}{Concentration_{Initial}})x100\%$

3.2.10 Statistical analysis

Statistical comparisons were undertaken using paired two-tailed Student's t tests. Results are expressed as mean ± standard error of the mean (s.e.m). Confidence interval to be significantly different is 95%.

3.3 Results

3.3.1 Galactosylated macroporous cellulosic sponges have macroporosity for the confinement of hepatocyte spheroids

The first step in the chemical synthesis of the macroporous cellulosic sponges involved the conjugation of allyl groups onto hydroxypropyl groups of hydroxypropyl cellulose to act as crosslinking sites during γ irradiation, as described elsewhere [15]. The galactose conjugation onto the remaining available hydroxypropyl groups was performed using 1,1'-carbonyldiamidazole in anhydrous dimethylformamide (fig 6A). The sponge fabrication is depicted in detail in **figure 5B.**

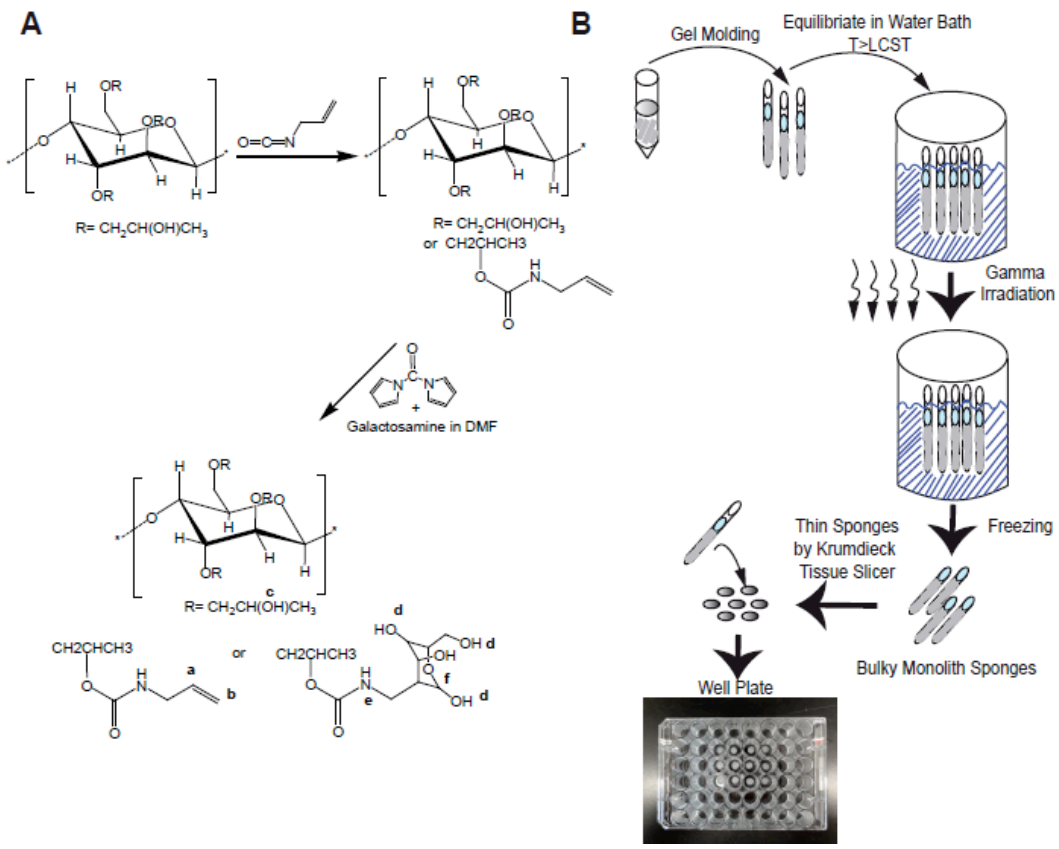

Figure 5. a) Chemical synthesis steps, b) Schematic diagram of galactosylated cellulosic sponge preparation

Galactose presence on the chemical backbone was verified by ^{1}H NMR by identifying additional peaks at ~7 to 8 ppm which indicates additional bonds from the attached galactose (fig 6). The integrated peak area between 2.5 ppm to 5 ppm showed an increase from 2.067 to 2.402 relative amount of the proton, which correlated to the presence of more hydroxyl groups from the conjugated galactose (estimated to be 1 conjugated galactose per 3 subunits of the HA Gal backbone).

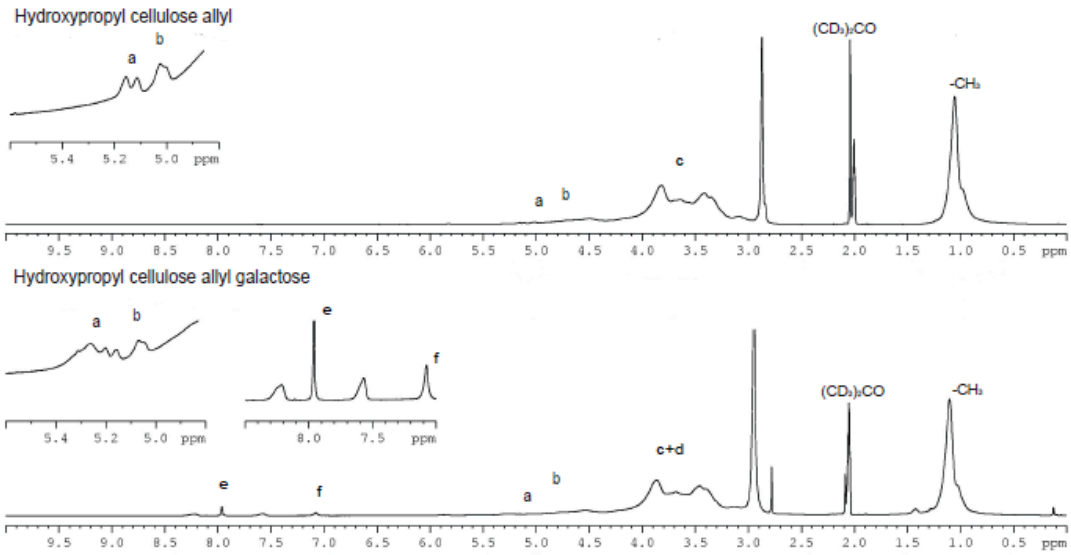

Figure 6. Chemical synthesis validation with ^{1}HNMR spectrum of galactosylated cellulosic sponge in d_6-acetone. Alphabetic labels correspond to **figure 5A.**

To further confirm the presence of galactose in the sponges, we hydrolyzed the sponges with 6N hydrochloric acid at 110°C for 24 hours, derivatized using an amine-derivatization kit and analyzed the products using HPLC. As a comparison, a pure D-(+)-galactosamine sample was also assayed. One eluted peak in the HPLC chromatogram at ~43 min represents the bound galactose (**figure 7A**) [175]. An X-ray photoelectron spectroscopy spectrum showed increased nitrogen atomic counts after conjugation (~1.5 % increase) (**figure 7B**). Lectin conjugated with FITC was also used to specifically stain galactose on the sponge surface and showed increased FITC signal, compared to non-galactose containing HA sponges (data not shown). From the point of view of the galactose conjugate into HA side chain group, this equimolar ratio of added galactosamine was found to be the optimum condition.

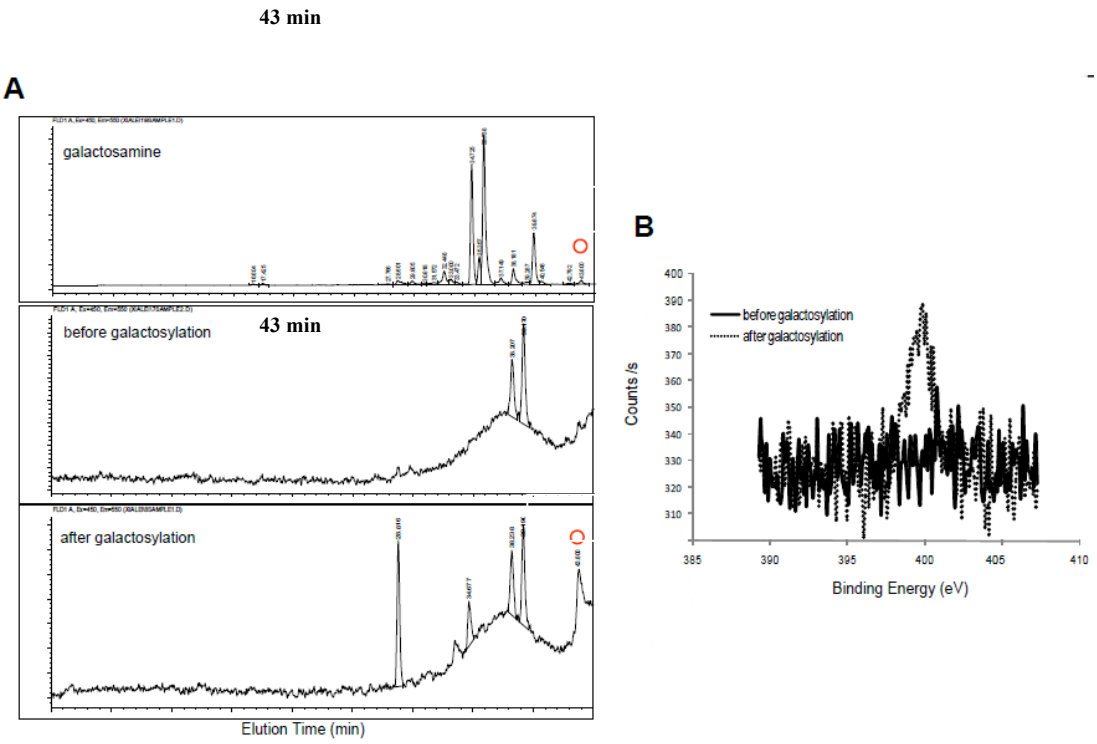

Figure 7. Characterization of cellulosic sponge: a) Galactose elution assay with High Performance Liquid Chromatography (HPLC). Red circle indicates the elution time. b) X-ray Photoelectron Spectroscopy

Surface morphology and porosity of the sponges were characterized using SEM. Image analysis of the sponge porosity showed the average pore size to be between 110 to 130 µm (**figure 8A**) for potentially constraining cellular spheroids within diffusible dimension [29, 184]. Water uptake of the HA Gal sponge is 95.90 ± 0.19 % with porosity 89.76 ± 8.50 %. Measurement of the elastic modulus of the sponges using atomic force microscopy revealed an average modulus of 5.6 kPa (**figure 8B**). This modulus is considered to be soft and close to the modulus of native rat and human livers [185, 186]. The net charge of the HA Gal structure in deionized water was measured through zeta potential measurement of the HA Gal at different concentrations ranging from 0.125 to 2.5 %wt/vol (**figure 8C**). At 2.5% wt/vol the value approached an almost neutral charge (-0.91 mV), which at concentrations beyond 2.5% wt/vol the solution became difficult to measure accurately due to its

high viscosity. Therefore, at the working concentration for cell culture (7.5 %wt/vol), the value is considered to be a neutral net charge.

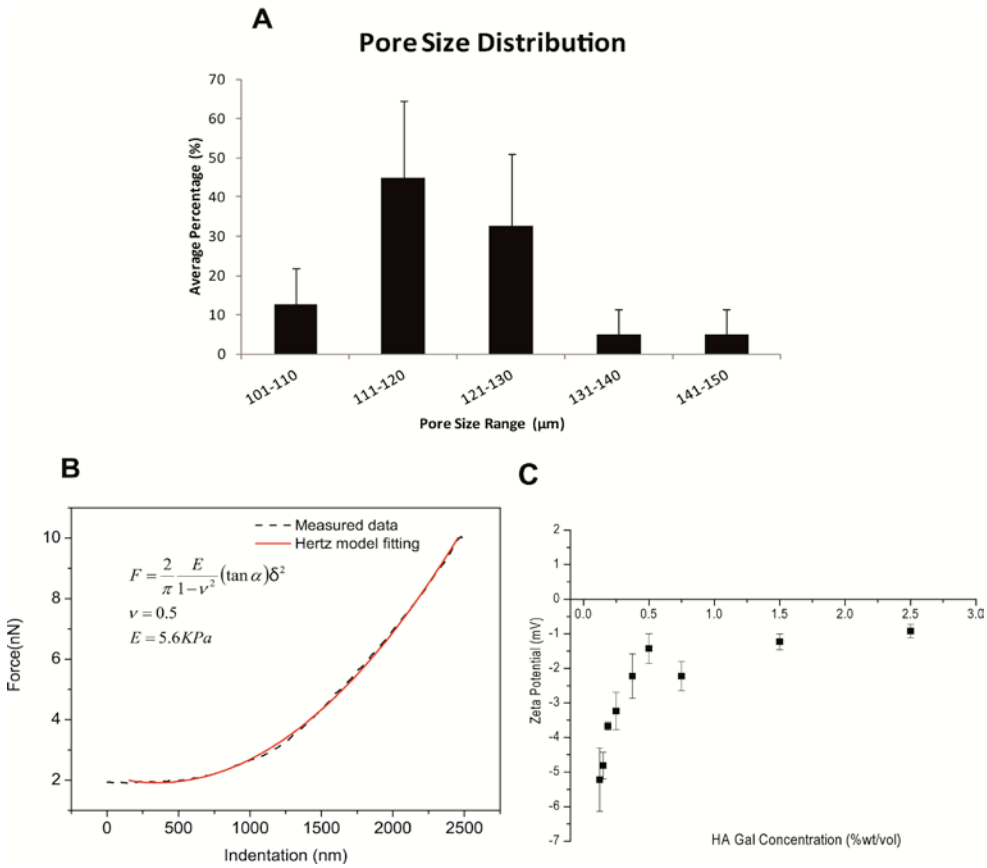

Figure 8. Characterization of cellulosic sponge: a) Sponge pore size distribution (n=40), b) Elastic modulus measurement by Atomic Force Microscope (AFM) (n=3), c) Zeta potential measurement (n=3). Data are average ± standard deviation

In addition to the macroporous structure viewed from the top of the sponges, the porosity also expanded throughout the sponges cross sectional areas (**figures 9A-B**). High magnification images of the sponge surface revealed surface sub-micron features in the nanometer scale which might tether the hepatocyte spheroids to the sponge (**figure 9C**). The dry sponge was incubated in fluorescein isothiocyanate solution to stain the sponge's macroporous structure in aqueous phase. By laser confocal microscopy, we observed that the macroporosity was maintained as a hydrated macroporous network structure in an aqueous environment (**figure 9D**) in contrast to typical hydrogels that lose their porosity in an aqueous environment.

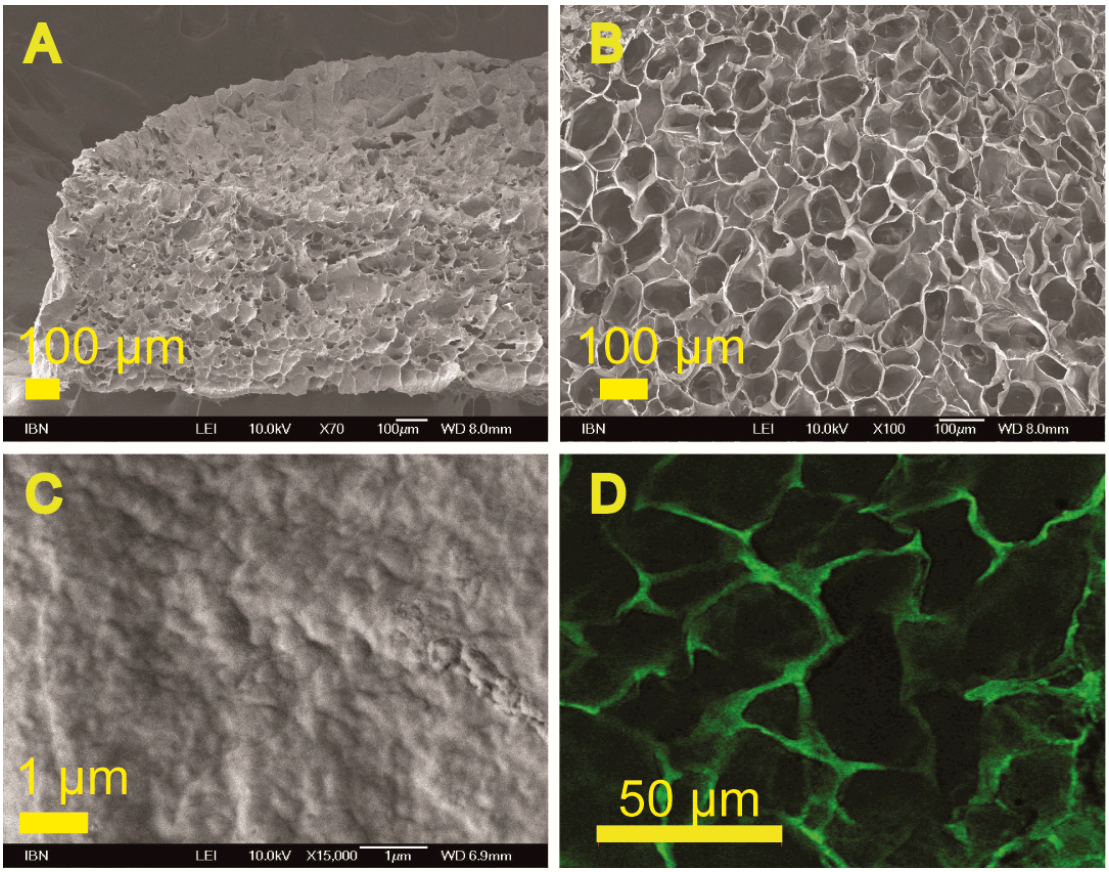

Figure 9. Characterization of cellulosic sponge: a) SEM image of cross section view, b) SEM image of top view, c) SEM image of sponge surface sub-micron features and d) Confocal image of FITC-stained sponge

3.3.2 Characterization of the hepatocyte spheroids cultured in cellulosic sponges

3.3.2.1 Hepatocyte spheroids develop more rapidly in cellulosic sponges and maintain cell viability

Rat hepatocytes cultured on three different platforms revealed platform-dependent cell behaviours (**figure 10**). Hepatocytes cultured on collagen monolayers were relatively flat and spread on day 3 onwards, which correlate with loss of differentiated functions [175]. Hepatocyte spheroids formation on galactosylated polyethylene terephtalate membranes (2D PET Gal membrane) took 3 days to form, and often collided with adjacent spheroids thus forming larger spheroids. In the HA

Gal sponge cultures, hepatocytes immediately organized into 3D spheroids within 1 day of culture, and remained stable in this configuration until at least day 6. Hepatocyte spheroids formed in the HA Gal sponges were smaller than those formed on 2D PET Gal membrane, with spheroid diameter 60.7 ± 15.9 µm and 108.1 ± 19.2 µm, for each platform, respectively. In addition, spheroids formed in HA Gal sponges were constrained by the sponge pores and thus did not easily detach as those plated on 2D PET Gal membranes.

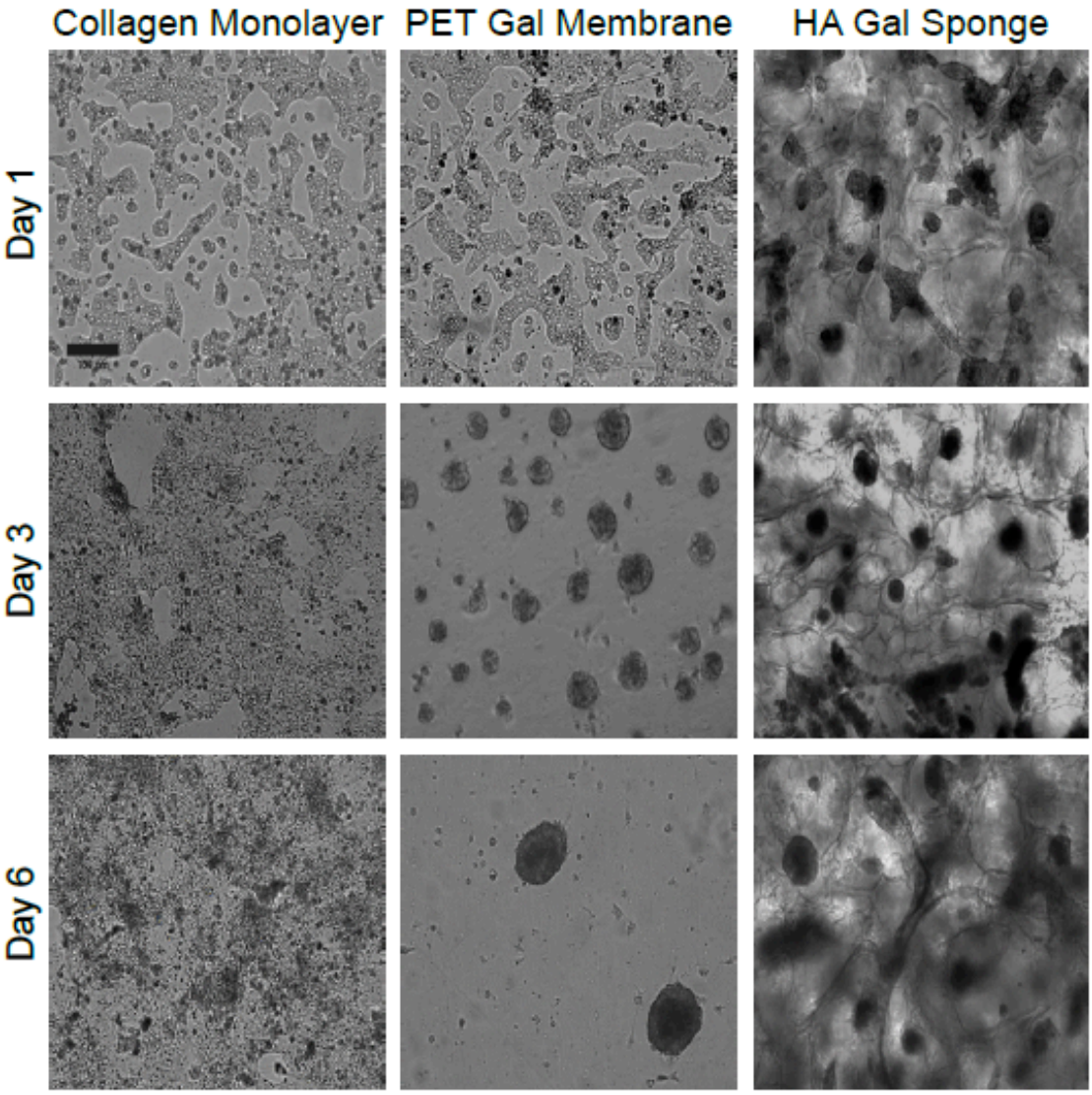

Figure 10. Phase contrast images of rat hepatocyte cultured in 3 different platforms (scale bar 100 µm). Diameter of hepatocyte spheroids formed on PET Gal membrane on day 3: 39.8 ± 8.1 µm, day 6: 108.1 ± 19.2 µm, and in HA Gal Sponge day 1: 46.1 ± 9.3 µm, day 3: 55.7 ± 21.1 µm, day 6: 60.7 ± 15.9 µm. (n=15)

Hepatocyte spheroids cultured between days 1 and 7 showed gradual increases in surface smoothness and disappearance of the cell-cell boundaries (**figure 11**). On day 1, the cell morphology was spherical. The nature of the hydrophilic and soft hydrogel sponges would prevent the cells from spreading, which normally occurs on hard substrates [181]. Tethered spheroids on the sponge surface was observed (**figure 11**). The arrows in the figure show the contact points where the spheroids adhere to the sponge surface sub micron features.

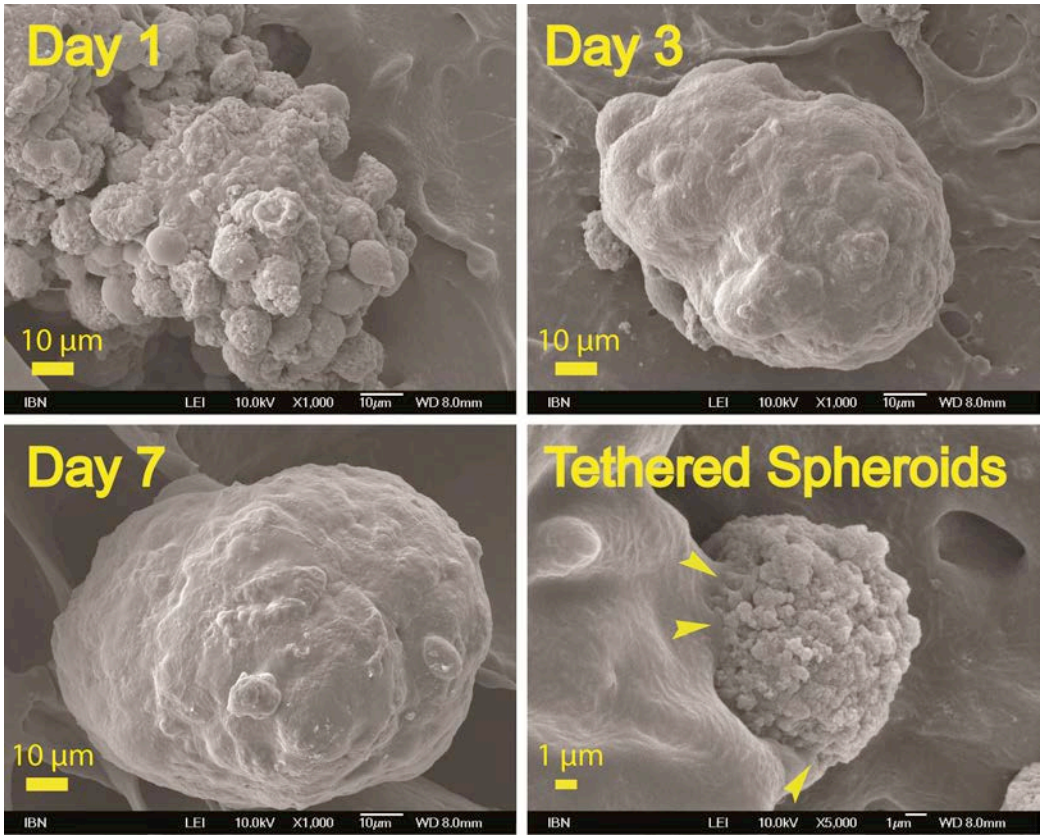

Figure 11. SEM Images of hepatocyte spheroids formed in HA Gal sponge

Hepatocyte spheroid viability, which was assessed by co-staining live and dead cells using Cell-Tracker Green (CTG) and Propidium Iodide (PI), respectively, showed no PI signal which revealed good viability maintenance from day 1 to day 7 in culture (**figure 12**). The CTG signals illustrated indistinguishable borders between single cells in the spheroids, which reflected the tightness of the cell-cell contacts.

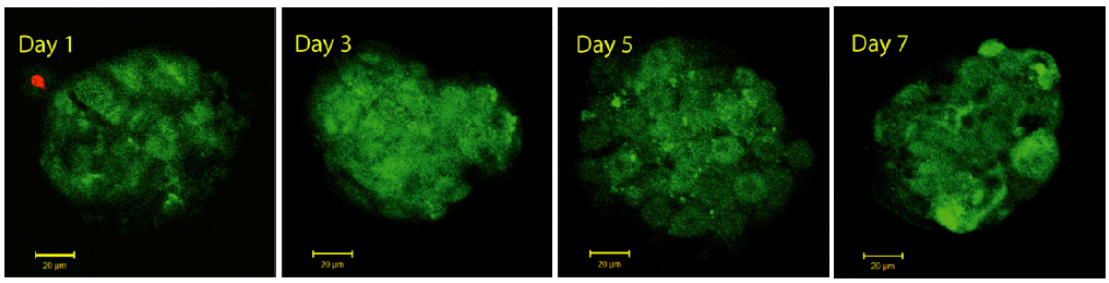

Figure 12. Hepatocyte spheroids viability (projected spheroids images, scale bar 20 µm)

Dynamic observation of hepatocytes upon seeding into the sponges for the first 12 hours showed that by 7 hours, the cells had reorganized themselves into hepatocyte spheroids with no further detectable changes in cell movement (**figure 13**). The spheroid morphology appeared compact and with cell boundaries becoming indistinguishable after 7 hours.

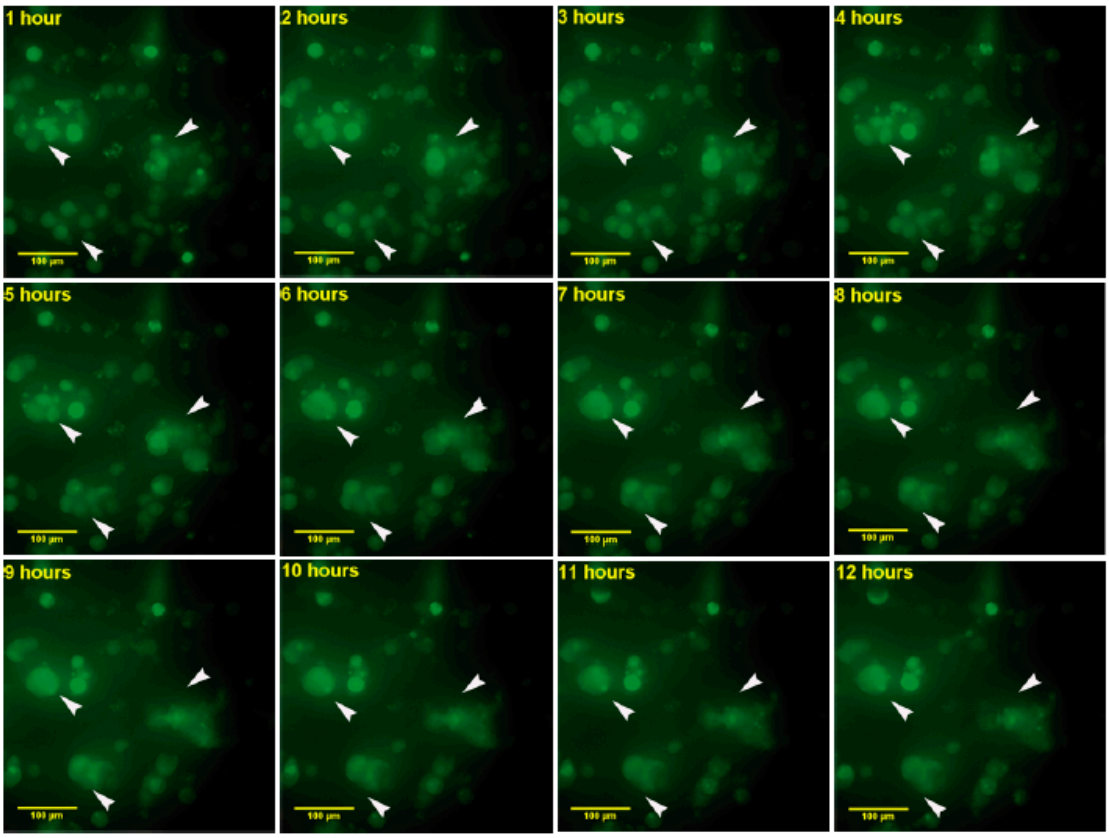

Figure 13. Time-lapse imaging of hepatocyte spheroids formation in HA Gal sponge (scale bar 100 µm)

3.3.2.2 Hepatocyte spheroids in cellulosic sponges maintain polarized phenotypes

Immunofluorescence staining of F-actin, E-cadherin and MRP2/CD147 in the hepatocyte spheroids 48 hours post seeding, in comparison to collagen sandwich control, showed localization of these markers (**figure 14**). As would be expected in non-spreading cells, F-actin staining revealed that the actin cytoskeleton had a predominant cortical localization in both sponge and collagen sandwich cultures and an absence of stress fibers. E-cadherin staining, a marker of cell-cell adhesions demonstrated that cells in the hepatocyte spheroids have tight associations between neighbouring cells. E-cadherin expression also supports the maintenance of cell viability during long-term culture [187]. MRP2/CD147 staining marked the apical and basolateral domains of the hepatocytes, respectively. In MRP2/CD147 staining

image (**figure 14** rightmost panel), the signals showed a comparable and non-colocalized signal as observed in collagen sandwich culture.

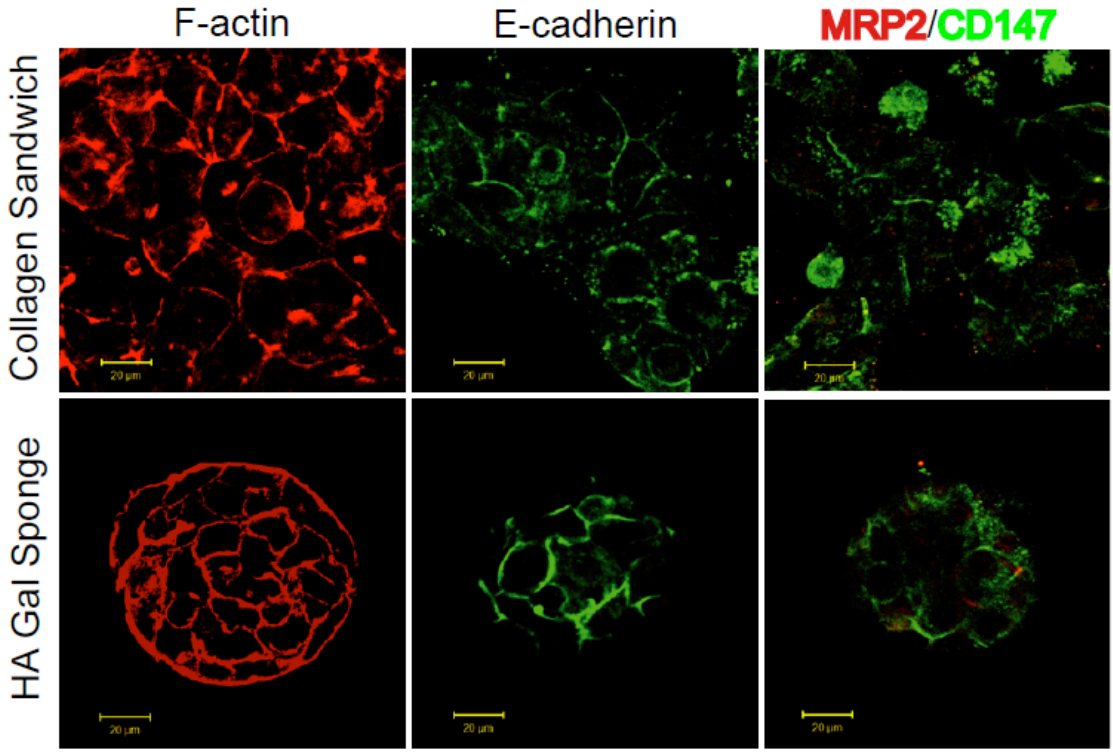

Figure 14. Immunofluorescence staining of polarity markers and cell-cell adhesions of hepatocyte spheroids (projected spheroids images, scale bar 20 µm)

Ultrastructural views observed by transmission electron microscopy illustrated the sub-cellular micro-structures located inside the spheroids. The images of hepatocyte spheroids cultured for 48 hours demonstrated a space between neighbouring cells, reminiscent of the bile canaliculi with the presence of microvilli in rat liver (**figure 15**) [188, 189]. Tight junctions between the two cells were also clearly observed.

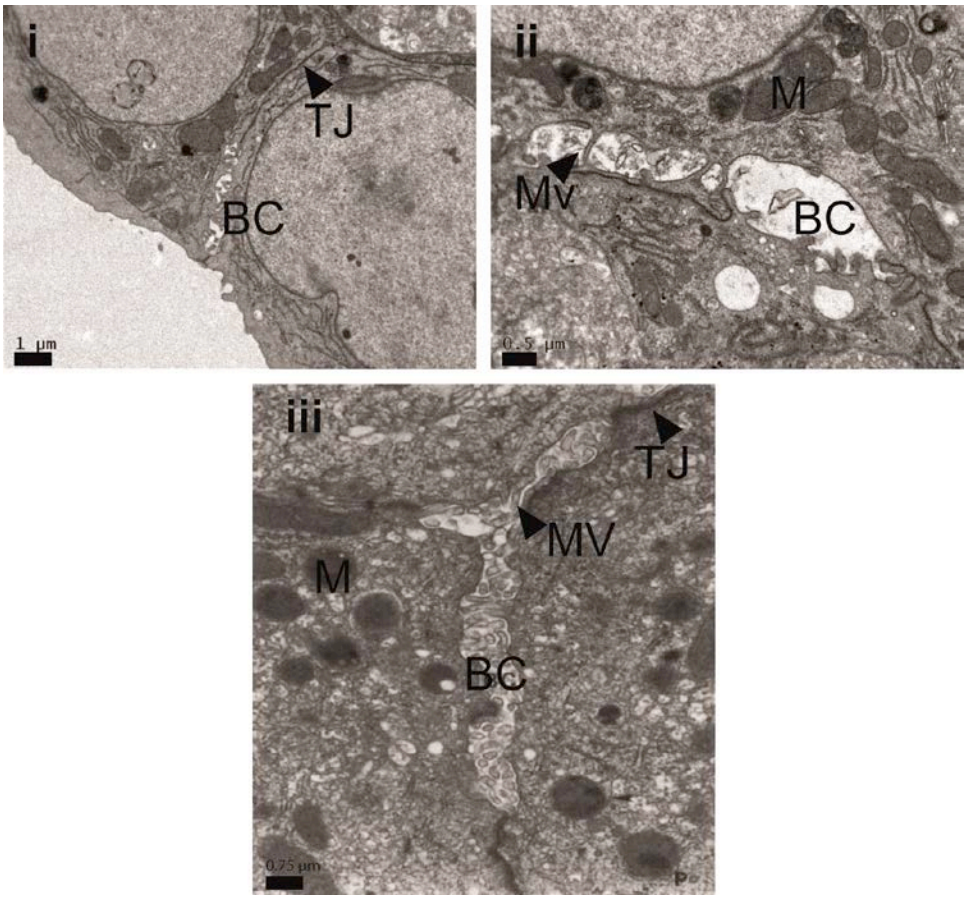

Figure 15. i-ii) Transmission electron microscopy images of hepatocytes spheroid at 48 hours post-seeding and iii) Rat liver transmission electron microscopy image (adapted from [190]). Scale bars for i, ii and iii are 1, 0.5 and 0.75 µm, respectively. TJ: Tight Junction, BC: Bile Canaliculi, Mv: Microvili, M: Mitochondria

3.3.2.3 Hepatocyte spheroids in cellulosic sponges show maintained liver-specific functions over time

Several liver functions are thought to be dependent on the polarized phenotype of the cells, including biliary excretion, albumin secretion and urea synthesis. After we observed an early formation polarity of hepatocytes in the cellulosic sponges, we wanted to address if these functions were also enhanced.

Biliary excretion was examined by the addition of fluorescein diacetate dye at various time intervals, including 16, 24 and 48 hours post seeding (**figure 16**).

Polarized hepatocytes formed bile canaliculi structures between neighbouring cells that contain the MRP2 transporter (see **figure 14**). Viable cells in the spheroids will cleave FDA into fluorosecein dye by intracellular esterases which then be excreted by MRP2 into the bile canaliculi. FDA staining in the hepatocyte spheroids formed in the sponge showed an accumulation in the bile canaliculi between two cells, starting from 16 hours post seeding, significantly faster than has been reported in collagen sandwich which normally occurs between 48-72 hours post-seeding [191]. Morphology of the FDA signal resembled the mouth-like shape of bile canaliculi described elsewhere [2, 192], confirming its proper excretion.

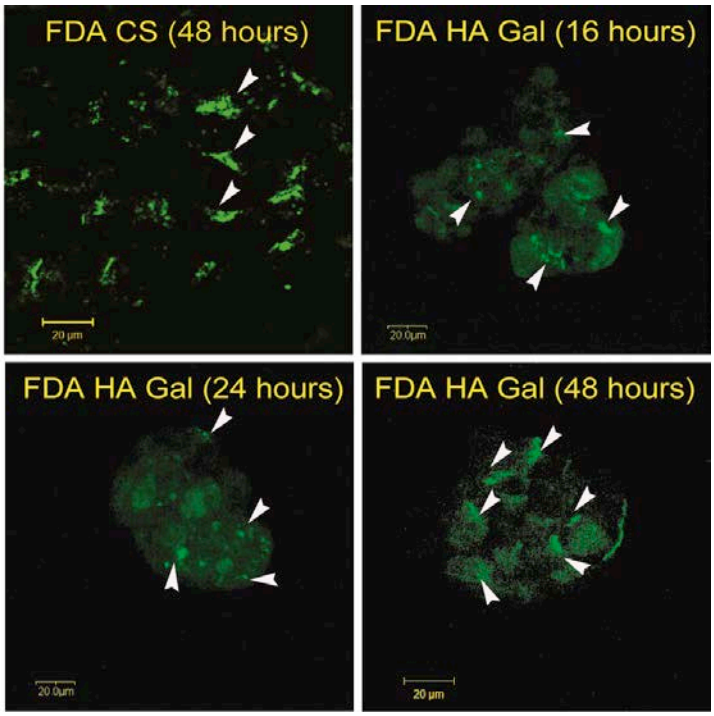

Figure 16. Fluorescein diacetate excretion of hepatocytes in collagen sandwich (CS) and sponge (HA Gal) at different time intervals (projected spheroid images, scale bar 20 µm)

Maintenance of albumin secretion and urea synthesis, markers of mature differentiated hepatocytes, during extended culture is a prerequisite for drug safety testing applications [193]. **Figure 17** demonstrates that these functions were generally

better maintained in hepatocytes cultured in the HA Gal sponge compared to the collagen sandwich for at least 7 days. When the hepatocytes were cultured in collagen sandwich, they had albumin secretion rate ranging from 57.74 μg/ million cells/ day to 219.70 μg/ million cells/ day for 7 days of culture. Hepatocytes cultured in the sponge on average secreted albumin at the rate ranging from 127.51 μg/ million cells/ day to 1,145 μg/ million cells/ day, showing their peak on day 5 (**figure 17** left panel). There was a decrease of secretion to 908.95 μg/ million cells/ day on day 7. Urea synthesis capability of hepatocytes cultured in the sponge showed an increasing trend from day 1 to day 7 of culture (**figure 17** right panel), ranging from 71.31 μg/ million cells/ 90 min to 666.44 μg/ million cells/ 90 min. On average, hepatocytes cultured in collagen sandwich showed relatively stable and lower urea synthesis rate at the range of 30.52 μg/ million cells/ 90 min to 40.52 μg/ million cells/ 90 min.

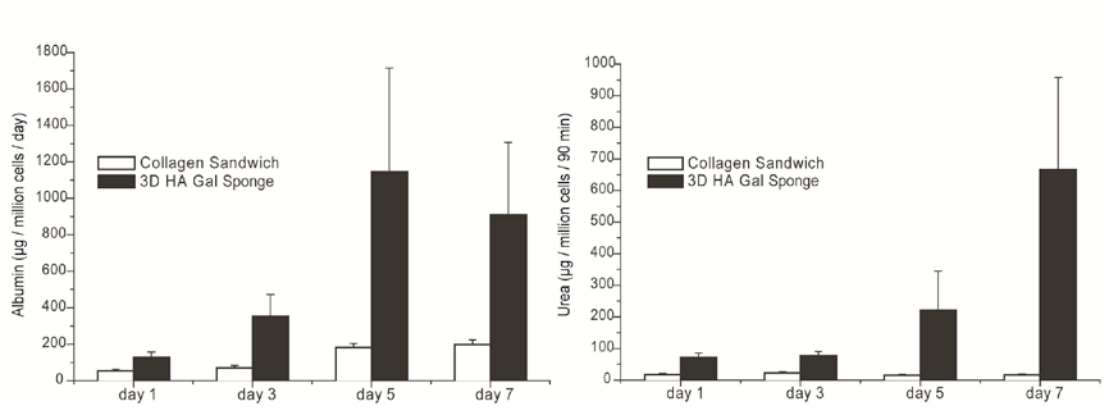

Figure 17. Albumin secretion and urea synthesis function of hepatocyte in the sponges and collagen sandwich. Data are average ± standard error of the mean from 3 independent experiments

3.3.2.4 Drug-metabolizing enzymes and transporters are maintained over time in hepatocytes cultured in cellulosic sponge

Maintenance of drug-metabolizing enzymes (CYP1A2, CYP3A2, CYP4A1, CYP2B2 and CYP2E1) and drug transporter expression (Mdr1a, Mrp2, Ntcp, Bsep

and Oatp1) was examined in hepatocyte spheroids and compared to sandwich culture. Hepatocyte spheroids showed higher expression of CYP1A2, CYP3A2 and CYP4A1 than the hepatocytes cultured in collagen sandwich (**figure 18** upper panel). The expression of CYP2B2 on day 5 was similar for both culture configurations. For CYP2E, collagen sandwich culture slightly outperformed the hepatocyte spheroids culture on day 3; however on day 5, the spheroid culture showed a 3.42 folds higher expression of CYP2E than in collagen sandwich.

In addition to drug-metabolizing enzymes, various drug transporters known to be expressed in liver were analysed. These transporters are involved in the influx of endogenous substances and xenobiotics into liver, or conversely the efflux of endogenous substances and xenobiotics into the bile or blood [194]. Together with CYPs, these transporters mediate clearance of drugs from liver. Bsep, Mdr1a, and Mrp2 are efflux transporters which are present on the apical canalicular membrane [195, 196]. Oatp1 and Ntcp are located in the basolateral membrane and act as influx transporters. On day 3 and 5 in culture, we observed a modest upregulation of Mrp2 in the hepatocyte spheroids at 2.6 folds and 1.7 fold, respectively (**figure 18** lower panel). On day 3, Oatp1 had similar expression in hepatocytes cultured in both culture configurations. On day 5, however, there was a drastic upregulation (13 folds) in the sponge culture. Mdr1a expressions for both culture configurations were similar for both days 3 and 5. For both Ntcp and Bsep expression on both day 3 and day 5, hepatocyte spheroids exhibited lower level expression than the collagen sandwich culture.

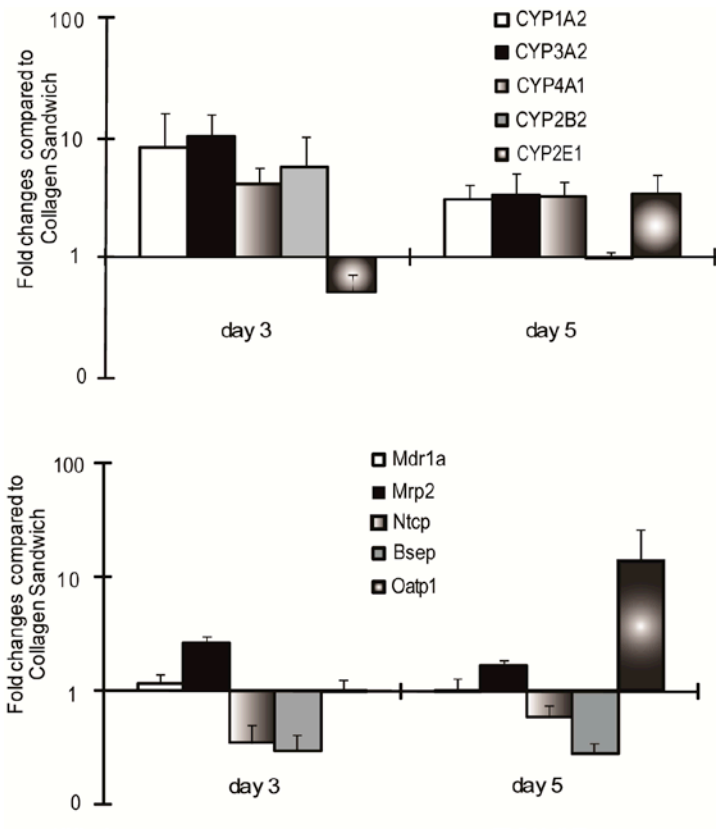

Figure 18. Gene expression of CYP450s enzymes and drug transporters. Data are average ± standard error of the mean from 4 independent experiments

For all three cytochrome P450s in the drug induction experiments, the basal levels in the sponge-cultured hepatocyte spheroids showed relatively higher metabolite production than the collagen sandwich (**figures 19A-C**). This reflected an improved ability of hepatocyte spheroids in metabolizing drugs and correlated with the upregulation of drug-metabolizing enzyme expression in hepatocyte spheroids at basal level (**figure 18** upper panel). Metabolite production CYP1A2 induced hepatocyte spheroids showed a higher absolute amount than the hepatocytes in collagen sandwich, 4,973 ± 1327 ng/million cells per 2 hours and 1,449 ± 173 ng/million cells per 2 hours, respectively, as well as a higher fold of metabolite production activity between induced and basal levels, 18.67 folds for spheroids versus 6.66 folds for collagen sandwich (**figure 19A**). For CYP2B2 induction, induced

hepatocyte spheroids and collagen sandwich exhibited an absolute value of metabolite production of 73.91 ± 1.90 ng/million cells per 2 hours and 43.96 ± 7.18 ng/million cells per 2 hours, respectively, but reflecting a similar 4.53 and 4.64 folds change over basal levels in both culture configurations (**figure 19B**). For CYP3A2 induction, the C absolute value of metabolite production of the induced spheroids culture showed a lower value than collagen sandwich culture, 139.85 ± 9.14 ng/million cells per 2 hours and 541.38 ± 132.83 ng/million cells per 2 hours, respectively (**figure 19C**). This translated into a 6.53 and 31.98 folds induction over basal levels for each of the culture configurations. The 6.53 folds induction of metabolic activity for CYP3A2 over basal levels is still considered significant.

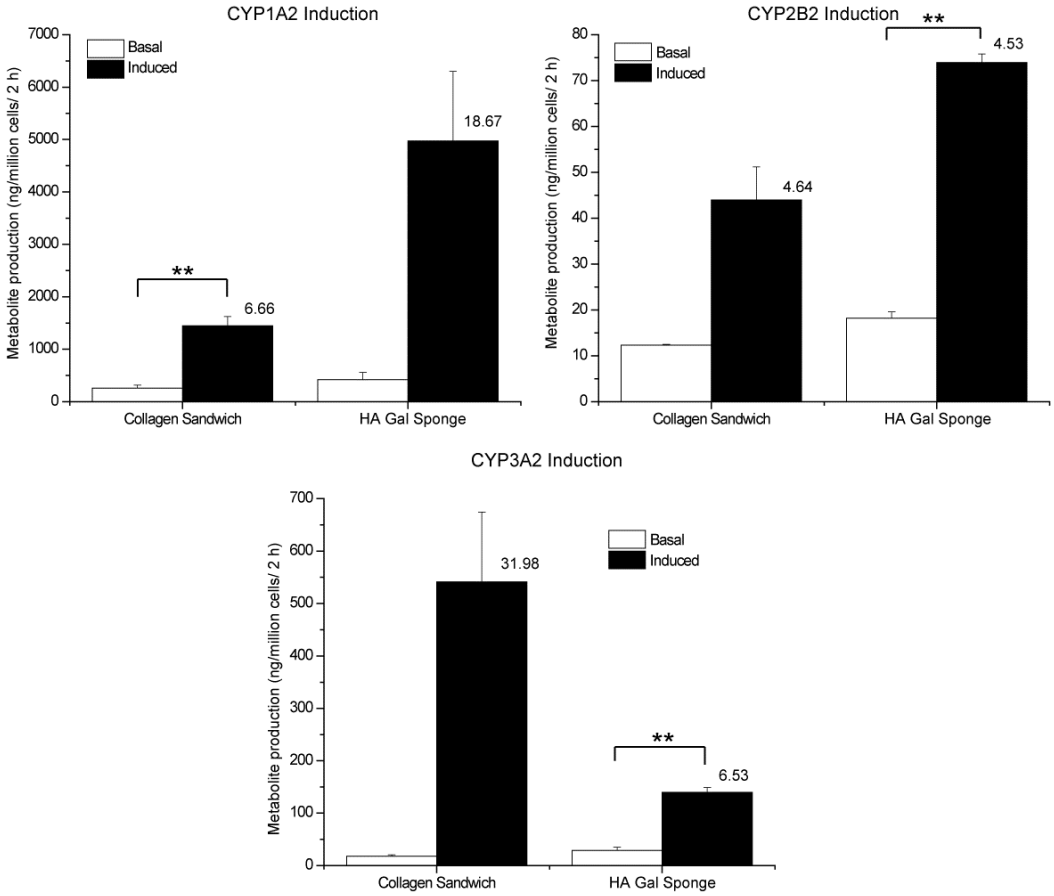

Figure 19. Drug induction of a) CYP1A2, b) CYP2B2 & c) CYP3A2 (numbers on top of induced level bar denote fold induction activity changes. Data are average ± standard error of the mean from 3 independent experiments. ** p value < 0.05

3.3.3 Cellulosic sponge has had exhibits comparable or better drug absorption properties compared to other frequently commonly-used hepatocyte platforms

To be useful in drug safety testing it is important to characterize absorption of different classes of commonly used drugs in the sponge platform. Eight drugs with differing hydrophilicity and net charges were chosen. The definition of hydrophobic and hydrophilic drugs was determined based on drug partition coefficients (log P), where hydrophobic drugs have log P>>0 and hydrophilic drugs have P □ 0. For comparison, drug absorption experiment was performed with three other scaffolds for hepatocyte culture *in vitro*, i.e. collagen gel, PuraMatrix™ gel, and Reinnervate polystyrene scaffolds [95, 107, 197]. The drug absorption properties of two tested hydrophobic drugs were found to be dependent on the solubility limit of each drug (**figure 20**). Testosterone with low water solubility (23.4 µg/mL) and bulky chemical structure was found to be severely absorbed by all four tested scaffolds. WY14643, another hydrophobic drug with higher water solubility (40 µg/mL), showed 9 %, 14 %, 24% and 0% drug absorption to the HA Gal sponge, collagen gel, PuraMatrix™ gel and Reinnervate scaffold, respectively. For the hydrophilic drugs with positive and negative charges, HA Gal sponge absorbed at most 10 % of the tested drugs, which was less than the collagen gel and PuraMatrix™ gel but more than Reinnervate scaffold. Hydrophilic drugs with neutral net charges such as nicotine and caffeine were 29 % and 19 % absorbed in the HA Gal sponge, respectively. This was comparable to the extent of adsorption by collagen gels, 23% and 29%, respectively. PuraMatrix™ gel absorbed 45% and 32% of nicotine and caffeine, respectively. Reinnervate scaffold absorbed 5% and 11% of nicotine and caffeine, respectively. The significant absorption of hydrophilic drugs with neutral net charges to the sponge

correlated with the net neutral charge of the sponge (shown by its Zeta potential in **figure 9C**). In most of the tested drugs for drug absorption, the HA Gal sponge outperformed the collagen sandwich, which is the commonly used biomatrix for hepatocyte culture.

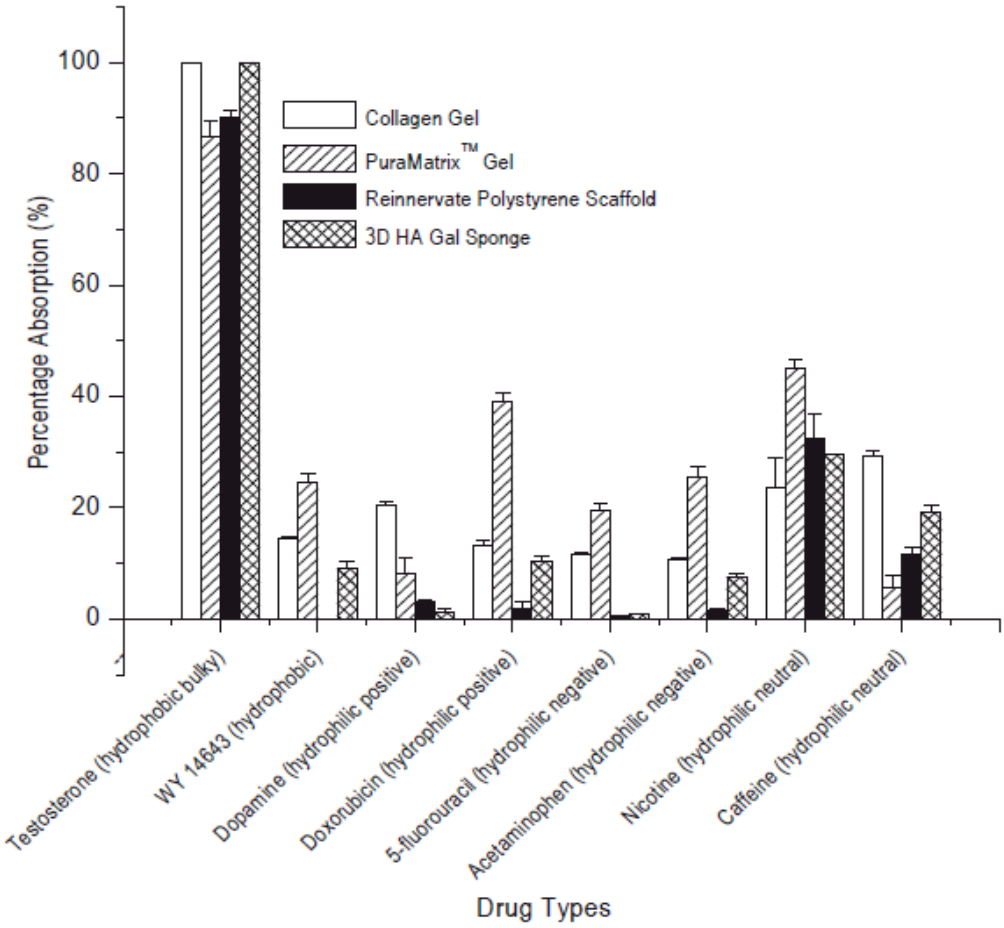

Figure 20. Drug absorption properties of cellulosic sponge compared to other commercial cell culture platforms. Data are average ± standard error of the mean from 3 independent experiments.

3.4 Discussion

We have conjugated galactose ligands onto cellulosic sponges by using D-(+)-galactosamine, which is commercially available, more cost effective and readily useful for large-scale synthesis than customized 1-O-(6-aminohexyl)-D-

galactopyranoside (AHG), which has been used previously [34, 86, 175]. The absence of a hexyl spacer in galactosamine compared to AHG was found only critical in the early stage of cell attachment kinetics, as shown by the comparison of HepG2 cells adhesion energy on the polyethylene membrane conjugated with AHG and lactobionic acid [198]. Unlike other hydrogels, the macroporous networks in our cellulosic sponge support the in situ formation and maintenance of polarized hepatocyte spheroids in the diffusible porosity dimension [33, 199, 200]. The cellulosic sponge, which acts as a hepatocyte substratum anchor, did not prevent cell aggregation, as would normally happen in cell culture platforms with excessive extracellular matrix presentation [201]. In addition, galactose presented chemical cues to the hepatocytes to reorganize into 3D spheroids, while the macroporous structure constrained and tethered them physically. Since the galactose ligand only interacts weakly with ASGPR receptors in the hepatocyte cell membrane [175], it is the combination of the physical and chemical cues in the sponge which is important in establishing stable constrained hepatocyte spheroids.

Cellulosic sponges were fabricated in large-scale with thin dimensions to reduce drug absorption. Compared to other scaffolds used for cultivation of hepatocyte spheroids, our sponge has a lower mechanical stiffness ($E<10$ kPa) [107, 202], durable macroporosity and is fabricated without chemical cross-linkers, yet cross-linked through stable chemical bonds [15]. The soft stiffness of the sponge will prevent cell spreading, which is important for maintenance of the mature hepatocyte phenotypes [181].

Hepatocytes cultured as 3D spheroids in the cellulosic sponge were tethered onto the sponge surface, which has sub-micron features, and constrained within the

macroporosity of the sponge. Hepatocyte spheroids started to form at 7 hours post-seeding with a gradual increase in cell boundary tightness. They exhibited maintenance of cell viability for 7 days in culture, polarity markers and 3D cell morphology including a cortical F-actin cytoskeleton and tight cell-cell adhesions. At 16 hours post-seeding they have excreted fluorescein dyes into bile canaliculi-like structures, which was faster than the other platforms used to form hepatocyte spheroids or collagen sandwich cultures [176, 191, 203]. These translated into high level of albumin secretion and urea synthesis, which were significantly higher than collagen sandwich culture. Compared to other galactosylated scaffolds used for culturing primary rat hepatocytes, hepatocytes cultured in cellulosic sponges also showed relatively higher maintenance of albumin secretion and urea synthesis at least two fold [24, 60, 204]. Hepatocyte spheroids constrained in the sponge expressed multiple phase 1 CYP450 enzymes and drug transporters at the same or higher level than hepatocytes cultured in collagen sandwich with the exception of Ntcp and Bsep.

When these spheroids were incubated with known P450 inducers such as β-naphthoflavone (CYP1A2), phenobarbital (CYP2B2), or pregnenolone-16α-carbonitrile (CYP3A2), the absolute value of metabolite production of CYP1A2, CYP2B2 and CYP3A2 were elevated, respectively. Levels of drug metabolites under basal conditions, as measured by LC/MS, in the hepatocyte spheroids cultured in the sponge were higher compared to the collagen sandwich (fig 19A-C). Upon drug inductions, the amount of metabolites increased even more in the hepatocytes cultured in HA Gal sponge, while only true for CYP1A2 and CYP2B2, the major CYPs in rat hepatocytes [205-207]. Similar induction folds of CYP2B2 in sponge and collagen sandwich culture were correlated to the reduction of CYP2B2 expression in

hepatocyte spheroids between day 3 to day 5 to a similar level with the collagen sandwich culture on day 5 (**figure 18** upper panel). CYP3A2 showed lower but still significant level of induction. The sponge exhibited lower or comparable drugs absorbency than collagen gel, Puramatrix™ gel and Reinnervate scaffold. Overall, the galactosylated cellulosic sponge supports the uniform formation, maintenance and functions of hepatocyte spheroids that are useful for drug safety testing.

3.5 Conclusion

We have synthesized and fabricated a galactosylated macroporous cellulosic hydrogel sponge as a platform to culture hepatocytes as 3D spheroids for drug safety testing applications. The soft and diffusible dimension macroporous cellulosic sponge with conjugated galactose facilitates the formation of hepatocyte spheroids by presenting both the mechanical cues (via matrix rigidity) and chemical cues for the hepatocytes to reorganise into 3D spheroids within 7 hours post-seeding. The constrained hepatocyte spheroids maintain cell viability, cell polarity markers, and 3D cell morphology. These translate into maintained hepatocyte-specific functions and expression of drug metabolic enzymes and drug transporters. Furthermore, hepatocyte spheroids grown in the sponge show inducibility of various drug metabolizing enzymes including CYP1A2, CYP2B2 and CYP3A1. The sponge has comparable or lower drug absorbency as other cell culture scaffolds. Importantly, sponge fabrication is amenable for large-scale production and high-throughput screening. Cell seeding into the sponge involves simple steps similar to high-throughput 2D cell cultures. Together, this platform provides a promising tool for hepatocyte-based drug safety testing. As other cells such as stem cells, neuroblasts and cardiomyocytes also show

more mature phenotypes when cultured as spheroids, cellulosic sponges may have broad applications in other areas of pharmaceutical research.

CHAPTER 4

GALACTOSYLATED CELLULOSIC SPONGE AS PLATFORM TO STUDY HCV INFECTION

4.1 Introduction

Hepatitis C virus (HCV) has currently infected 130-200 million human populations in the world, with 3-4 million new cases reported annually [208]. This *flaviviridae* family virus can lead to chronic hepatitis, cirrhosis then eventually hepatocellular carcinoma [114]. One of the most commonly found HCV strains is genotype 1 (~70%) [209]. The ribonucleic acid (RNA) of the virus encodes 3,000 amino acid length-single polyprotein, which upon infecting the host, structural and non-structural proteins are formed [121]. Therefore, anti viral candidates has been developed to target these proteins. The only currently available registered choice to treat HCV infection is by administering ribavirin and PEG interferon 2α, which could lead to side-effects such as harsh, flu-like symptoms, anaemia and depression [113]. Worse, upon drug administration the patient became too weak to work or enjoy family life, and the virus often manages to survive under these conditions [113]. Moreover, PEG interferon 2 α and ribavirin are only effective against genotype 2 HCV [210]. Patients with genotype 1 had the lowest drug response levels (42-46% for PEG interferon 2 α plus ribavirin in the two trials) and patients with genotype 2 or 3 had the highest levels of drug response response (76-82% for PEG interferon 2 plus ribavirin in the two trials) [211].

The host specificity of HCV in human and chimpanzee liver has challenged the study to be done *in vitro* to observe how virus enters the cells and infect the hosts

[212]. Recent developments to propagate HCV in human hepatoma cell lines have shown some features but these cell lines, however, display abnormal proliferation, peculiar gene expression, as well as deregulated signaling and endocytic functions [213-216]. Primary human hepatocytes are considered the most physiologically relevant cells to study HCV infection and replication *in vitro*, but they are difficult to handle upon isolation from *in vivo* environment; the cells viability and functions started to drop if not preserved or cultured properly [217]. Currently there are not many robust *in vitro* 3D models to culture human hepatocytes to maintain the cells polarity for prolonged culture to let the HCV stains keep re-infecting the host cells. iPS-derived human hepatocytes can also be used to study HCV entry and infections *in vitro* but are normally specific to fetal hepatocyte [165]. Researchers have performed several strategies to culture primary human hepatocytes by manipulating extracellular matrix, formulating proper cell culture media composition, culturing the cells using bioreactors, co-culturing with non-parenchymal cell and culturing hepatocytes by enhancing cell-cell interactions through 3D spheroids formation [92, 94, 151, 217]. However, until now it is still unclear whether these platforms could support HCV glycoprotein mediated entry and persistent replication *in vitro*.

Previously, we have shown that our galactosylated cellulosic sponge platform has salient features such as rapid formation of spheroids, facilitates homotypic interaction, controlled spheroids dimensions, easily scalable multi-well format and mechanical properties suitable for soft tissue culture. Therefore we hypothesized that this could preserve difficult-to-culture human hepatocytes by presenting mechanical and chemical cues to be polarized cells. Rapid hepatocyte spheroids formation (within 7 hours) could help in restoring hepatocyte functions. This thin sponge to be used as

HCV infection study platform also offers its capability towards large scale antiviral screening.

Here we demonstrated the utility of our thin macroporous galactosylated cellulosic sponge (1 mm thickness, 6 mm diameter) to culture cryopreserved primary human hepatocytes and Huh 7.5 cells as spheroids in a multi-well plate to support HCV infection. Both human hepatocytes and Huh 7.5 cells formed compact spheroids within 1 day post-seeding and maintained their tight spheroid configuration over prolonged culture of up to 40 and 21 days, respectively. These spheroids maintained good cell viability, expressed polarity markers (MRP2 and CD147) and displayed HCV entry markers such as CD81, SCARB1 and Claudin1. Upon incubation with HCV pseudoparticles (HCVpp), these spheroids showed high level of infectivity with no visible mass transfer barrier. Dose-dependent response of HCV entry inhibition was also observed upon co-incubating HCVpp with CD81 antibody. Overall, this platform is useful to culture primary human hepatocyte and hepatocyte cell line to study HCV infection and to screen HCV antiviral candidate.

4.2 Materials and methods

4.2.1 Materials

All chemicals and reagents were purchased from Sigma Aldrich (Singapore), unless otherwise stated.

4.2.2 Synthesis and fabrication of galactosylated cellulosic sponge (HA Gal sponge)

The detail synthesis has been described previously in chapter 3 and in [80]. Hydroxypropyl cellulose (HPC), Mw = 80,000 g/mol and ~3.4 degree of etherification was dehydrated by azeotropic distillation in toluene at 70°C. 4 grams of dried HPC was dissolved in anhydrous chloroform (100 mL), to which 2.095 mL allyl isocyanate 98% and 1 mL dibutyltin dilaurate 95% were added dropwise. The mixture was stirred vigorously for 48 hours at room temperature, after which it was precipitated in an excess amount of anhydrous diethyl ether. Following vacuum drying, the product was dissolved in deionized water (DI H_2O), purified by dialysis for 3 days, and finally lyophilized to the intermediate product, HA. For galactose conjugation, 1 gram of HA was dissolved in 15 mL anhydrous dimethyl formamide (DMF) in which the hydroxyl groups were activated by addition of 1,1'-carbonyldiimidazole (0.322 g in 2 mL DMF). D-(+)-galactosamine HCl (0.427 g in 30 mL DMF), which was dissolved with addition of triethylamine, was added to the mixture with two folds molar ratio compared to D-(+)-galactosamine HCl. The reaction was carried out for a further 48 hours at room temperature. To remove impurities, the mixture was further dialyzed in excess methanol and subsequently in deionised water for 3 days each and the final product (HA Gal) was lyophilized.

HA Gal was dissolved in deionised water to a final concentration of 10 % wt/vol after which the solution was inserted into tubes (diameter 6 mm, length 3 cm). The tubes were heated in a water bath (40°C) until phase separation occurred, and then crosslinked by γ irradiation for 1 hour at a dose of 10 kGray/hour (Gammacell 220, MDS Nordion, Canada). The sponge monoliths were obtained by breaking tubes

subsequent to freezing in dry ice. A Krumdieck tissue slicer (Alabama Research & Development USA) was used to cut the sponge uniformly (40 rpm for 1 mm thickness). Thin sponge slices were fabricated to reduce possible anti viral absorption during assays. Sliced sponges were washed extensively with excess amounts of deionised water for 3 days to remove uncross-linked polymers. Finally, slices were lyophilized and sterilized by γ irradiation prior to cell seeding.

4.2.3 Cell culture

4.2.3.1 Cryopreserved primary human hepatocyte culture

Primary human hepatocytes were maintained in Williams' E media supplemented with human hepatocyte maintenance supplements from Invitrogen containing dexamethasone, penicillin streptomycin, insulin, transferrin, selenium complex, bovine serum albumin (BSA), linoleic acid, GlutaMAX and 4-(2-hydroxyethyl)-1-piperazineethanesulfonic acid (HEPES). 0.1 millions human hepatocytes were seeded into each HA Gal sponge (6 mm diameter, 1 mm thickness) in total 16 μL culture medium. Fresh culture medium was added to the sponge edge after 30 minutes incubation (300 μL per sponge in 48-well plate).

4.2.3.2 Huh 7.5 cell culture

Aside from primary human hepatocytes, as a known control for the HCV infection study, we also cultured Huh 7.5 cells in the sponge. Previous research findings have shown that Huh 7.5 cells were highly permissive to HCV infection and replication [218]. Huh 7.5 cells were propagated in DMEM (high glucose) media supplemented with 1x minimal essential amino acids and 10% FBS. Cells were

passaged at 80% confluence. 0.1 millions Huh 7.5 cells were seeded into each HA Gal sponge (6 mm diameter, 1 mm thickness) in total 16 μL culture medium. Fresh culture medium was added to the sponge edge after 30 minutes incubation (300 μL per sponge in 48-well plate).

4.2.4 Human hepatocyte and Huh 7.5 spheroids characterizations and functional assessments

4.2.4.1 Spheroids size distribution

Spheroid size distribution was quantified using imageJ software (version 1.43u) from collective phase contrast images of living human hepatocyte and Huh 7.5 spheroids cultured in the HA Gal sponges on day 3 (week 0), day 7 (week 1), and day 14 (week 2).

4.2.4.2 Live/dead staining

Human hepatocyte and Huh 7.5 spheroids were co-stained with Cell Tracker Green (CTG, 20 μM) (Molecular Probes, USA) and propidium iodide (PI, 25 μg/mL) (Molecular Probes, USA) to determine live and dead cells, respectively. Cells were incubated for 30 min at 37°C and then fixed with 3.7 % paraformaldehyde for 10 min at room temperature. Fluorsave (Merck Chemicals) was applied to the stained spheroids to minimize photo-bleaching. Images were acquired by confocal laser scanning microscopy (Zeiss LSM510, Germany) at 488 and 543 nm excitation wavelengths.

4.2.4.3 Scanning electron microscopy

Hepatocyte spheroids in sponges were fixed with 3.7% paraformaldehyde overnight and stained with 1% OsO4 for 1 hour. Samples were then dehydrated step-wise with ethanol (25%, 50%, 75%, 90% and 100%) for 10 min each, dried in a 37°C dry oven and sputter-coated with platinum for 90 seconds. The samples were viewed with a scanning electron microscope (JEOL JSM-5600, Japan) at 10 kV.

4.2.4.4 Reverse transcriptase polymerase chain reaction

RNA was extracted from hepatocytes cultured as 3D spheroids in HPCSS Gal sponges by RLT lysis buffer (Qiagen, Singapore). Total RNA concentration was quantified by a Nanodrop (Thermoscientific) and 1 μg of RNA was converted to cDNA by High Capacity RNA-to-cDNA (Applied Biosystems). Primers were designed using Primer 3 and real-time PCR was performed by using SYBR green fast master mix on a ABI 7500 Fast Real-Time PCR system (Applied Biosystems). Gene expression was calculated using the ΔΔCT method normalized to GAPDH. The primers used in experiment are shown below.

Table 5. Primer sequences used in RT-PCR experiments

Genes	Forward sequence	Reverse sequence	Primer Accession No.	P.S. (bp)
AAT	GTCAAGGACACCGAGGAAGA	TATTTCATCAGCAGCACCCA	NM_001127707.1	134
CYP1A1	CTTCACCCTCATCAGTAATGGTC	AGGCTGGGTCAGAGGCAAT	NM_000499.3	125
CYP3A4	TGCTTTGTCCTTCCGTAAGGG	CAGCATAGGCTGTTGACAGTC	NM_017460.5	100
HNF4α	TGTACTCCTGCAGATTTA	CTGTCCTCATAGCTT	NM_178849.2	163

	GCC	GACCT		
Albumin	TGGCACAATGAAGTGGGTAA	CTGAGCAAAGGCAATCAACA	NM_000477.5	166
GAPDH	GAGTCAACGGATTTGGTCGT	GACAAGCTTCCCGTTCTCAG	NM_002046.4	185

AAT: α-1-antitrypsin, CYP: Cytochrome P450, HNF4α: Hepatocyte Nuclear Factor 4α
P.S.: Product size, Annealing temperature: 60°C, Cycle numbers: 40

4.2.4.5 Immunofluorescence microscopy of spheroids

Cells were fixed with 3.7% paraformaldehyde for 10 minutes followed by washing with PBS. Following washing and blocking with 2% BSA/0.2% Triton-X 100, the spheroids were incubated overnight at 4°C with primary antibodies: mouse anti-human CD81 (clone JS-81, BD Pharmingen; 1:100), rabbit anti-SCARB1 (NB110-57591, Novus Biologicals; 1:100), rabbit anti-Claudin1 (51-9000, Zymed; 1:100), rabbit anti-MRP2 (Clone M2III-6, Sigma Aldrich; 1:50) and rabbit anti-firefly luciferase (AbCam, 1:100). Secondary antibodies used were goat anti-mouse and goat anti-rabbit 488 and 555, respectively. Nuclei stain was captured using mounting medium containing DAPI stain (Vecta Shield). Images were captured using Olympus fluoview FV1000 with a 60x water lens. Images were analysed using IMARIS and images assembled using Adobe illustrator CS2.

4.2.5 HCV pseudoparticles (HCVpp) synthesis

The HCVpp were synthesized at Roche Nutley Virology Department, USA by co-transfection of plasmids encoding E1 and E2 HCV glycoproteins, HIV lacking nef and env genes and containing luciferase gene into 293T cells.

4.2.6 HCVpp entry and inhibition assays

Human hepatocytes and Huh 7.5 spheroids were cultured for 3 days post-seeding before proceeded into HCVpp entry experiments. These spheroids were subjected to treatment with 100 µL of media containing 2% DMSO and 2x penicillin streptomycin containing antiviral drugs at various concentrations. To this media 50 µL of HCVpp solution was added. The spheroids were incubated for 3 days. End points of viral entry were measured post infection by immunofluorescence staining and luciferase assay measuring total luminescence using Promega Steady Glo kit. Additionally, the infection experiments were performed in human hepatocyte spheroids on day 10 and 14 post-seeding to observe prolonged infection.

4.2.7 Statistical analysis

Statistical comparisons were undertaken using paired two-tailed Student's t tests. Results are expressed as mean ± standard deviation. Confidence interval to be significantly different is 95%.

4.3 Results

4.3.1 Characterization of the human hepatocyte and Huh 7.5 spheroids cultured in cellulosic sponges

4.3.1.1 Human hepatocyte and Huh 7.5 spheroids are formed in galactosylated cellulosic sponge and maintained for over 2 weeks of culture

We first analysed the ability of galactosylated cellulosic sponge in inducing human hepatocytes and Huh 7.5 cells to form spheroids and we found that the cells formed spheroids within the first 24 hours post-seeding (**figure 21**). Both human hepatocytes and Huh 7.5 cells formed tight spheroids within 3 days post-seeding and maintained their spheroid configuration over prolonged culture of up to 40 days and 21 days, respectively.

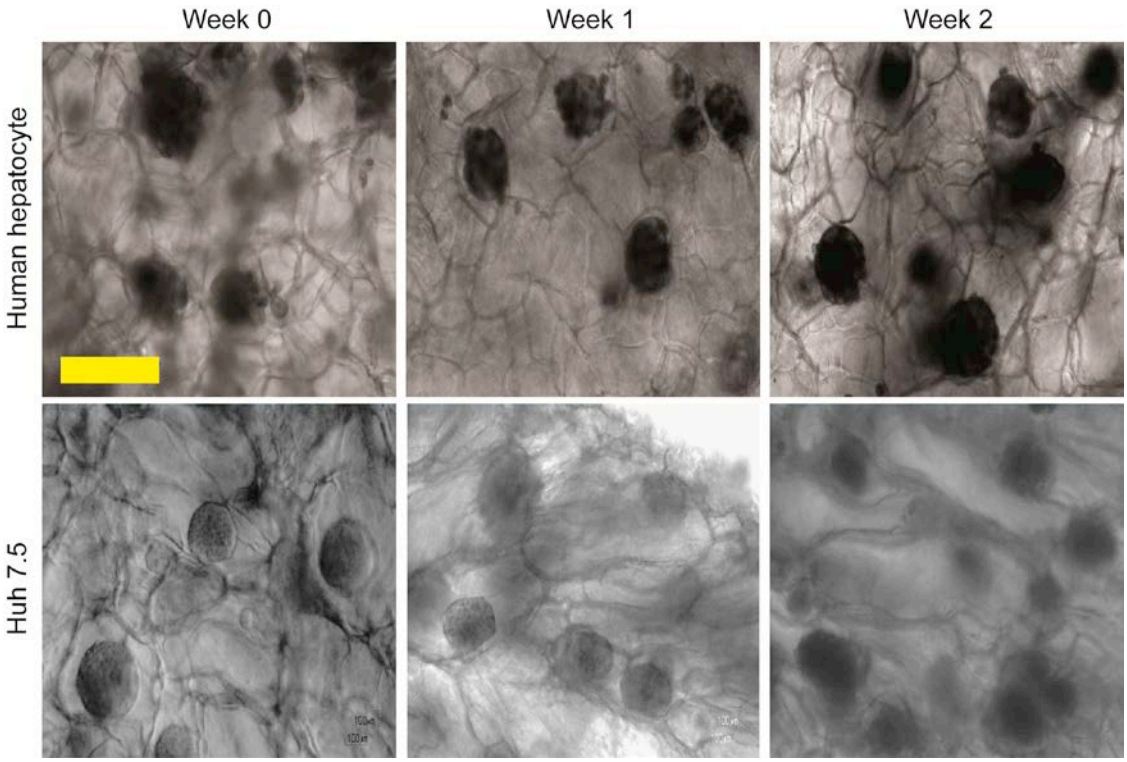

Figure 21. Phase contrast images of human hepatocyte spheroids (upper panel) and Huh 7.5 spheroids (lower panel) at different weeks of culture (scale bar 100 µm)

We characterized the size distribution of human hepatocyte and Huh 7.5 spheroids in culture and we found that most human hepatocyte spheroids formed were between 50-80 µm in size (~45%) from day 3 until Day 14 in culture (**figure 22**). Whereas, due to proliferative nature of Huh 7.5 cells, most Huh 7.5 spheroids were between 80-120 µm in size (~ 63%) on day 3 of culture and there was an increase in number of spheroids between 150-200 µm in diameter over 14 days in culture (~27% increase) (**figure 22**).

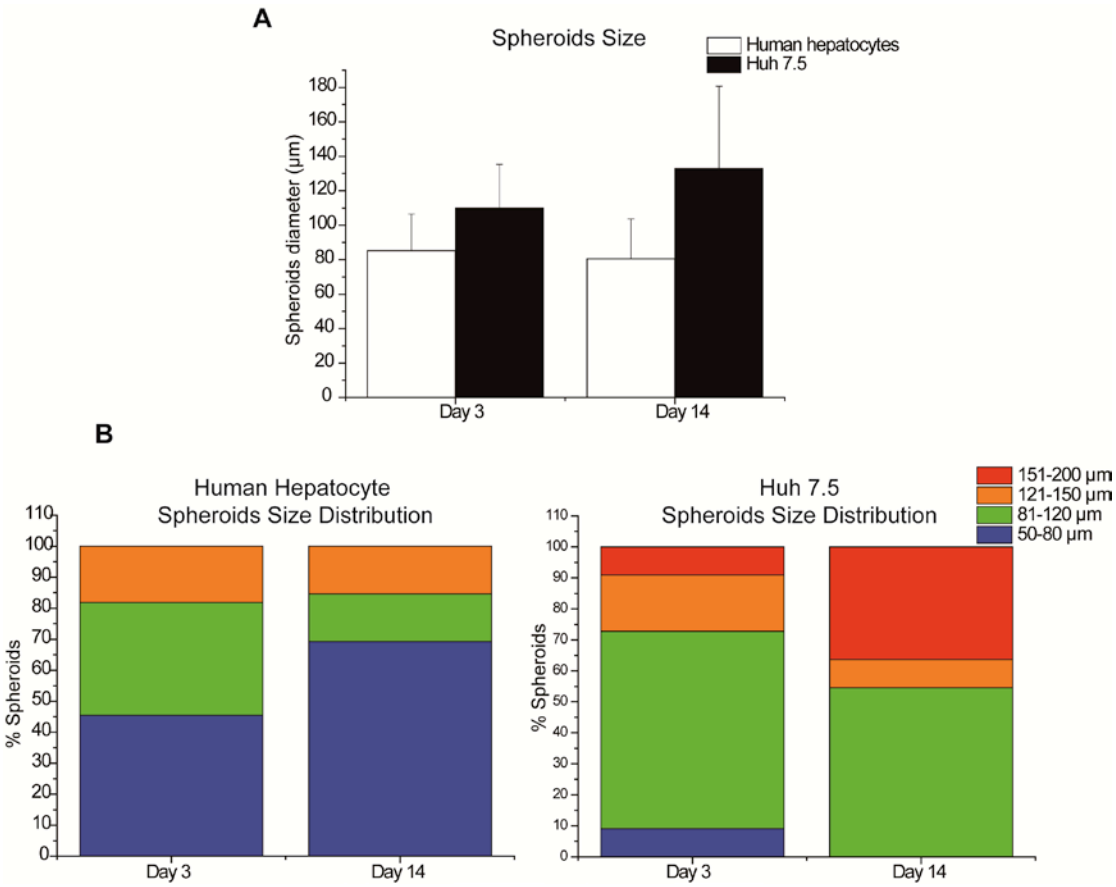

Figure 22. Human hepatocyte and Huh 7.5 spheroids size analysis and distributions. Data are average ± standard deviation (n = 11)

We further determined the viability of the spheroids for both cell types over 40 days of culture and found that human hepatocytes remained highly viable (~80%

viability) in spheroids over 40 days in culture while the Huh 7.5 spheroids lost most of their viability after 3 weeks in culture which could be due to hypoxia in the centre of the spheroid as a result of proliferating Huh 7.5 cells and increase in spheroid size (**figure 23**).

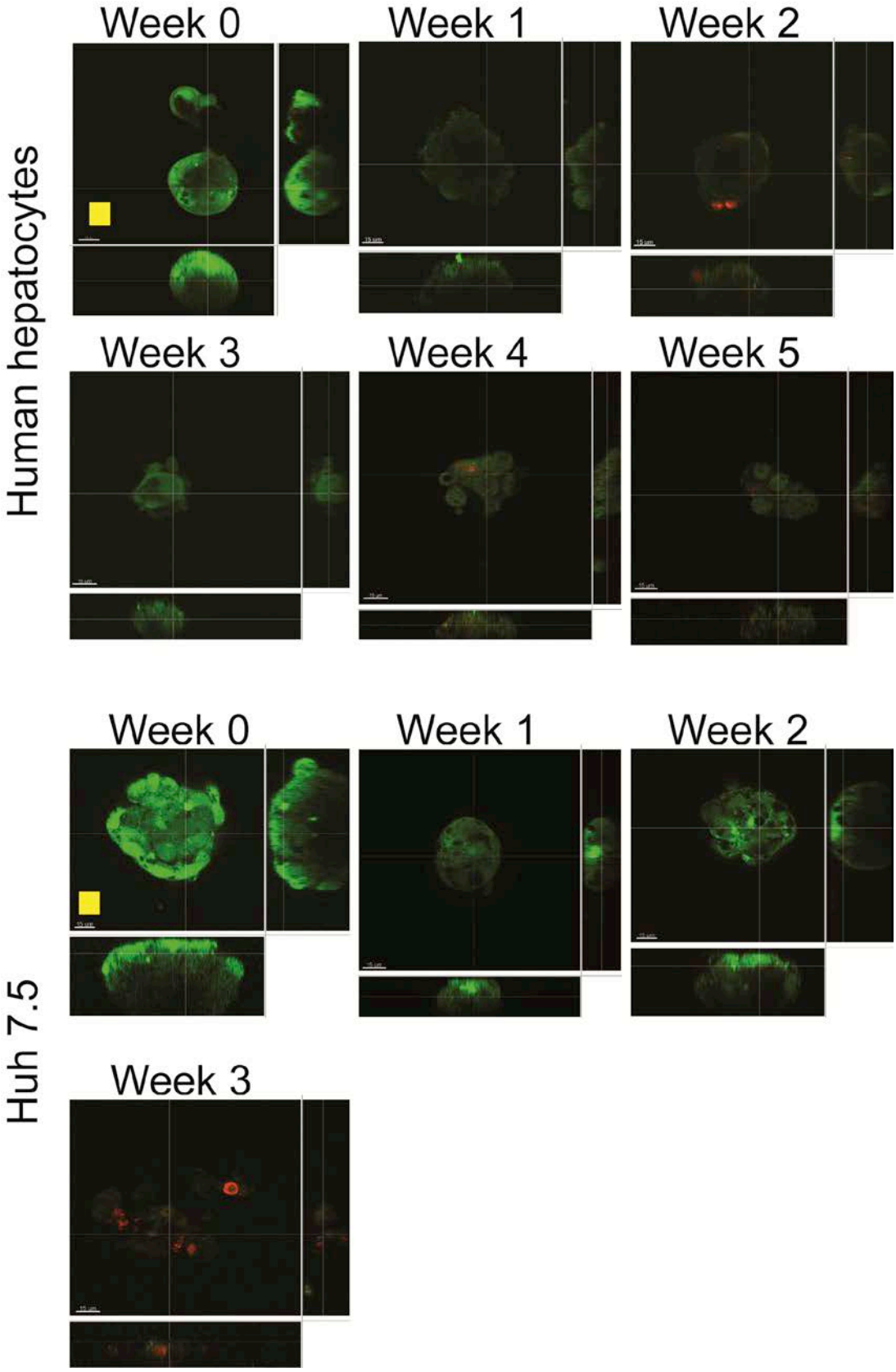

Figure 23. Live/dead staining of human hepatocyte and Huh 7.5 spheroids (projected spheroids images, scale bar 15 μm)

SEM images of both cell types' spheroids portrayed tight spheroids formation and maintenance of the spheroids compact morphology over prolonged culture; 6 weeks for human hepatocytes and 3 weeks for Huh 7.5 spheroids (**figure 24**). Interestingly, SEM images of human hepatocyte spheroids showed 1-2 µm size holes on the spheroid surface of the spheroids (see the arrows) which was reported before to be bile canaliculi-like structures extending from the surface to the interior of the [219]. These holes also commonly appear in mammalian liver (**figure 25**).

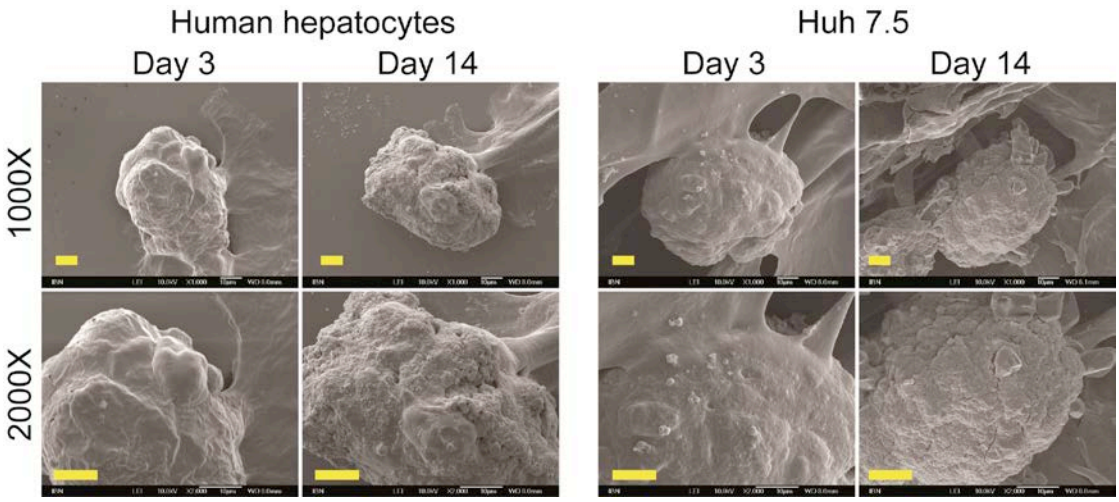

Figure 24. SEM images of human hepatocytes and Huh 7.5 spheroids (scale bar 10 µm)

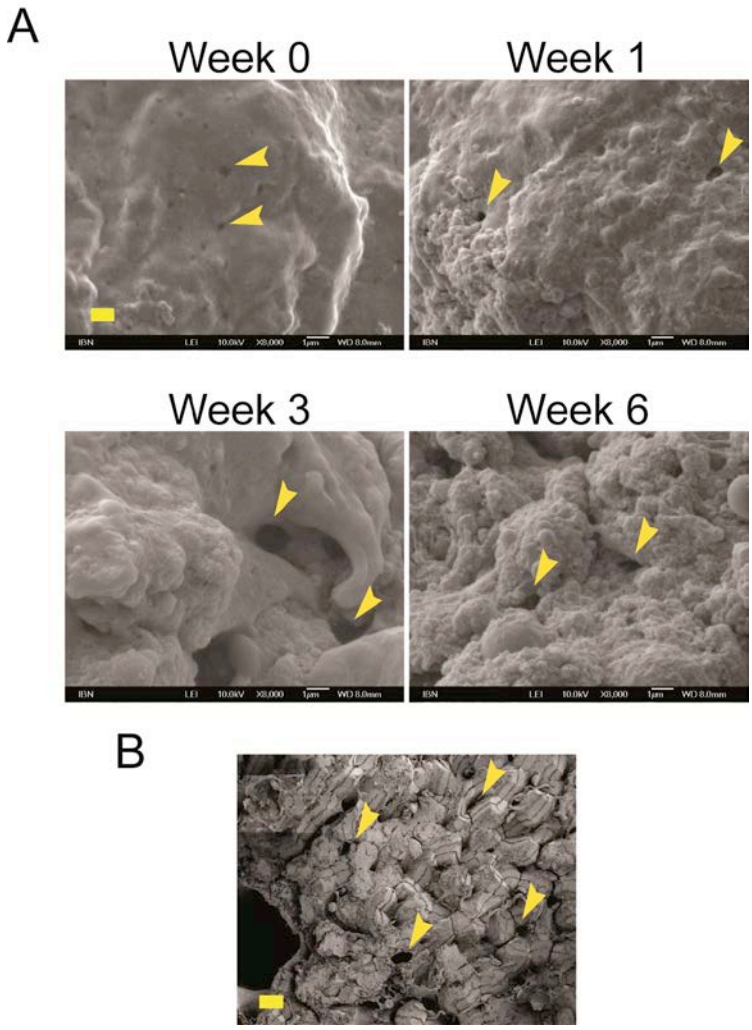

Figure 25. a) High magnification SEM images of human hepatocytes spheroids at different weeks of culture and b) Mammalian liver SEM image adapted from [220]. Scale bar 1 µm

4.3.1.2 Human hepatocyte and Huh 7.5 spheroids maintain polarized phenotypes and express HCV entry markers

Phenotypic differentiations of the two kinds of spheroids were assessed by analyzing liver specific genes over 14 days of culture. Primary human hepatocytes cultured as spheroids exhibited minimal dedifferentiation compared to freshly thawed cryopreserved human hepatocytes for various lots (**figure 26A**). Mature human hepatocyte genes like CYP1A1, CYP3A4, HFN4α and Albumin were upregulated in

the spheroid culture at 1,024, 4, 5,700 and 90 folds, respectively. AAT gene was 45 folds downregulated. For Huh 7.5 spheroids, we observed a significant increase in the transcript levels of CYP3A4 and Albumin genes (256 and 16,384 folds, respectively after 7 days of culture) (**figure 26B**). These important mature hepatocyte genes showed significant increase over 7 days of culture and maintained similar levels of expression until 14 days in culture. The other genes like AAT, CYP1A1 and HNF4α were maintained from day 1 to day 14 of culture.

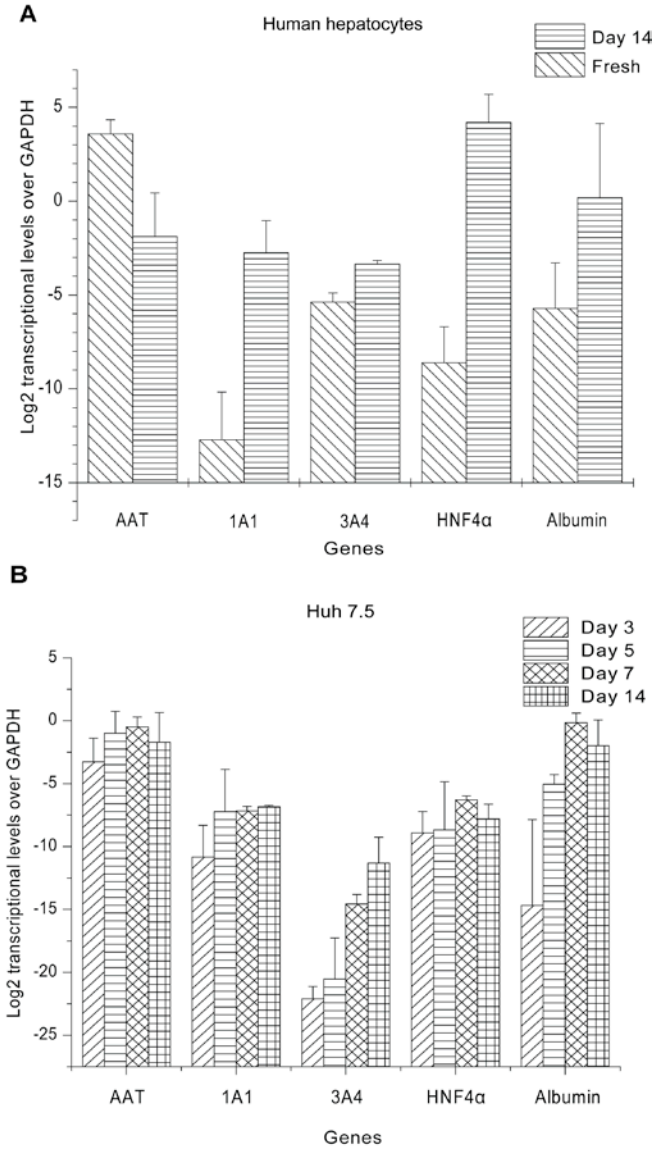

Figure 26. Gene expression analysis of human hepatocyte and Huh 7.5 spheroids. Data are average ± standard deviation of 3 independent experiments.

Hepatocyte polarity was found to significantly contribute to HCV entry [4]. And it has been discussed in chapter 2 that HCV enters hepatocytes via binding with various receptors [110]. We characterized the expression and localization of these markers and receptors in our spheroid cultured cells by immunofluorescence staining. Hepatocyte polarity markers such as MRP2 and CD147 were visualized at the tight junctions and at the basolateral domain, respectively (**figure 27**).

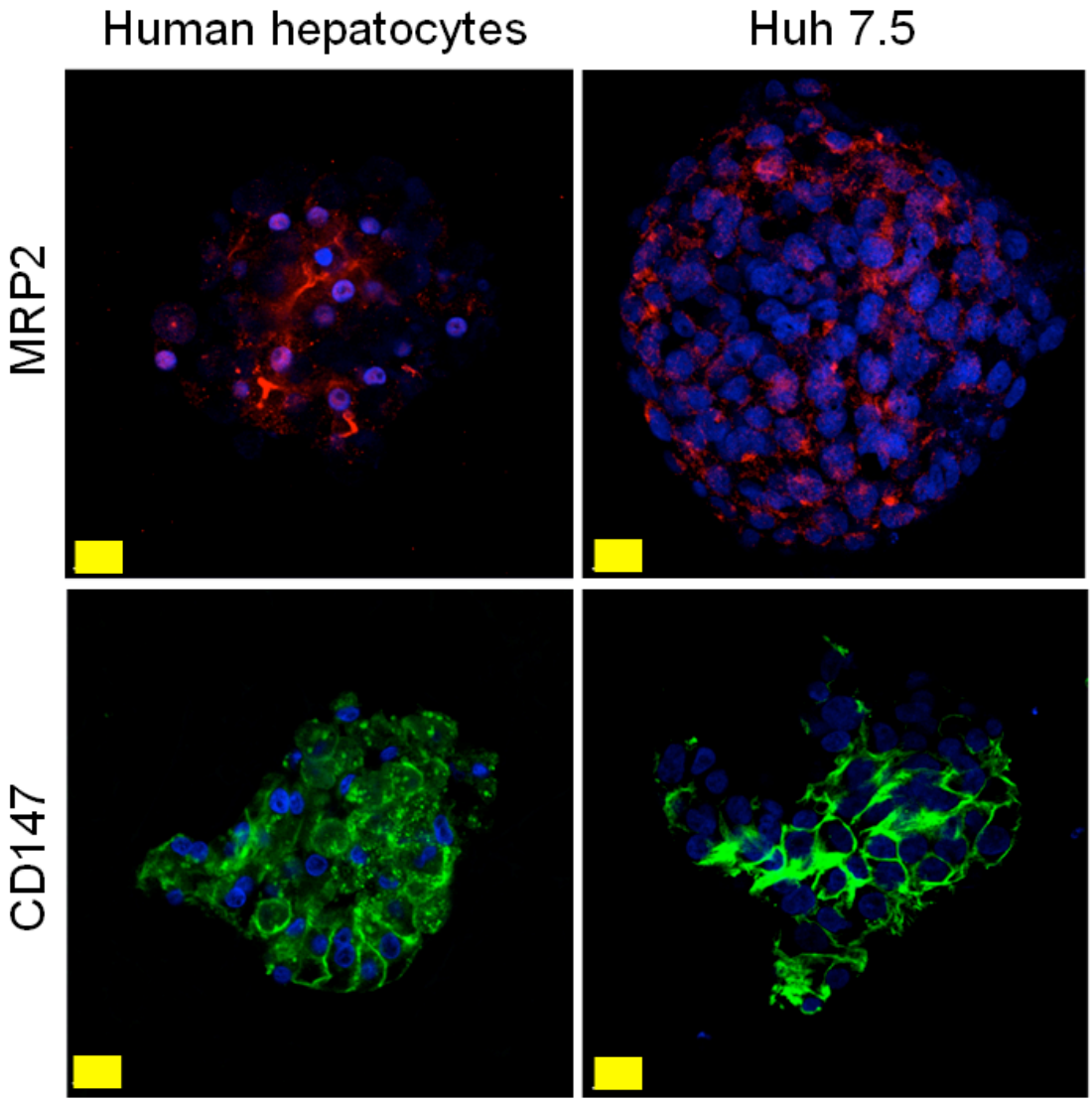

Figure 27. Liver polarity markers of human hepatocyte and Huh 7.5 spheroids (2 µm slice image of spheroid, scale bar 20 µm)

Various HCV entry markers namely CD81, SCARB1 and Claudin1 were also characterized in the spheroids. CD81 was visualized at the basolateral domain of the cells. SCARB1 and Claudin1 were visualized at the tight junction regions of the spheroid (**figure 28**). We observed these markers expression in the spheroids over extended culture of up to 14 days.

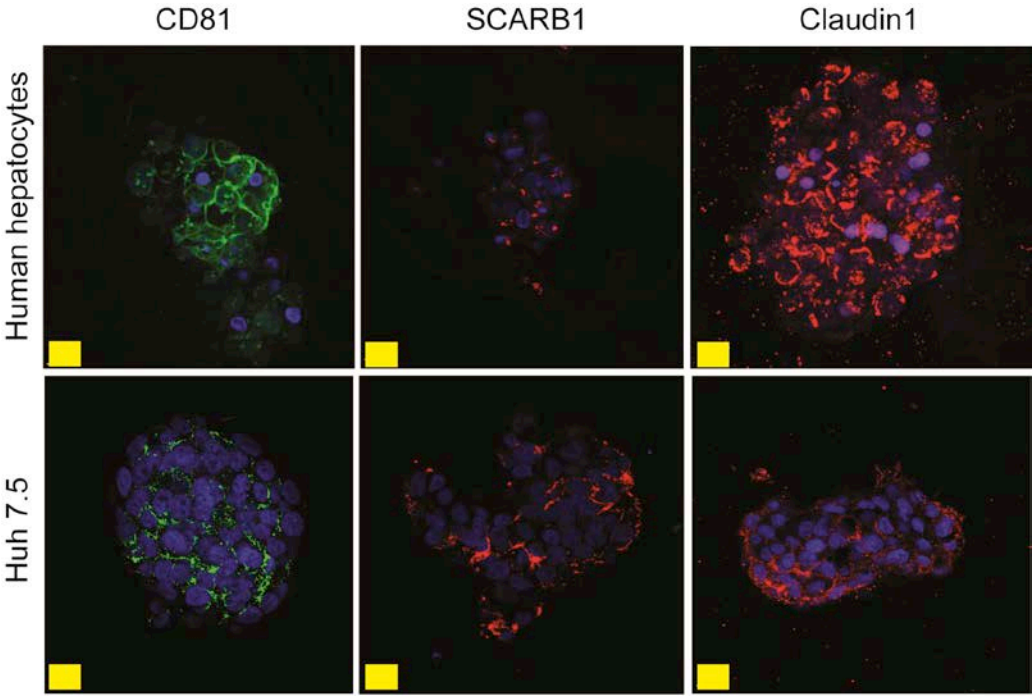

Figure 28. HCV entry markers stained in human hepatocyte and Huh 7.5 spheroids (2 µm thickness slice image of spheroid core, scale bar 20 µm)

4.3.2 HCV infection susceptibility study of the spheroids

4.3.2.1 Human hepatocyte and Huh 7.5 spheroids are susceptible to HCV infection demonstrated through HCV pseudoparticles

In order to further test the susceptibility of our human hepatocytes and Huh 7.5 spheroids system to glycoprotein-mediated HCV entry, we inoculated the spheroids with HCV pseudoparticles (HCVpp). HCVpp were the first available *in vitro* infection model for investigation of the entry of this major human pathogen [221]. We

found high levels of infectivity in both human hepatocytes and Huh 7.5 spheroids. The levels of infectivity was found to be much higher than the previously reported 3D culture model; ~80% of the spheroids were infected compared to just 1% cells infectivity in previously reported HCV culture model [3]. The cells at the centre of the spheroid were also infected with pseudoparticles indicated by the luciferase staining, which showed that this spheroid system is not subjected to mass transfer limitation at the spheroid core (**figure 29**). The ability of human hepatocyte spheroids to support HCVpp entry at prolonged culture (day 3, day 10 and day 14 post-seeding) further substantiated the findings that the HCV entry receptors were present and localized in the spheroids over prolonged culture periods (**figure 30**).

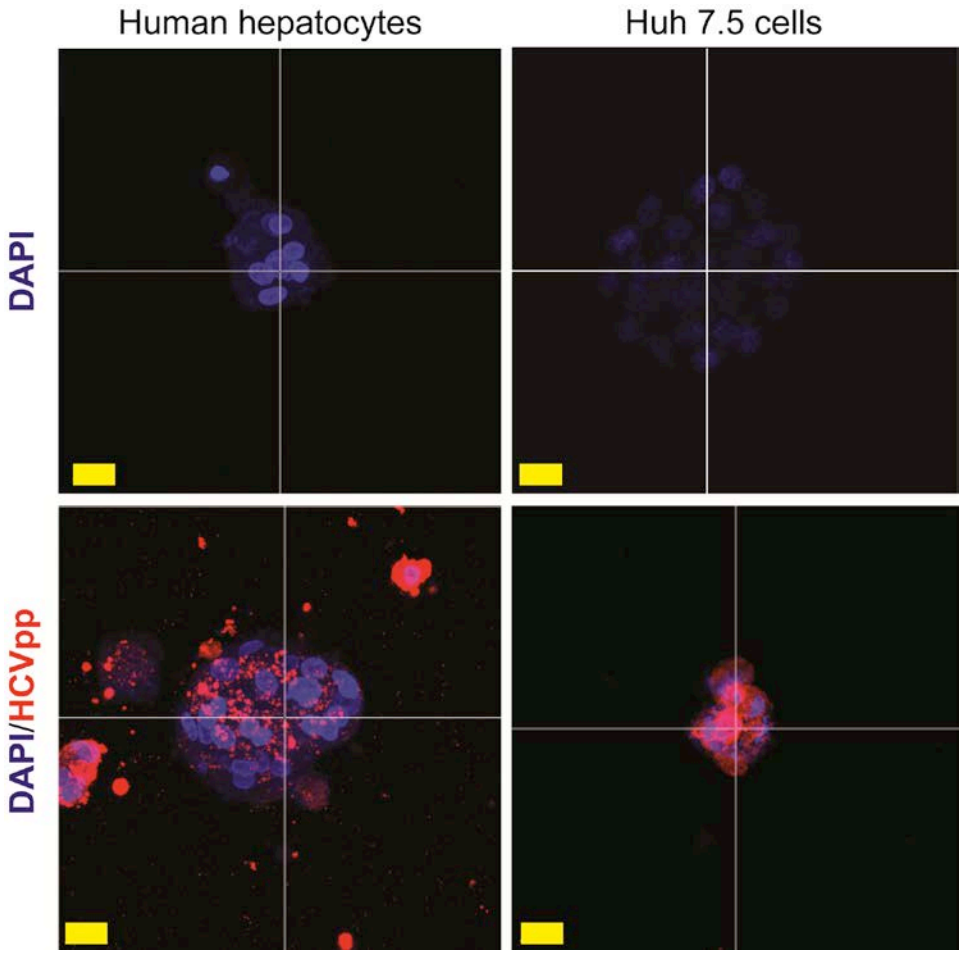

Figure 29. Immunofluorescence of HCVpp-infected human hepatocyte and Huh 7.5 spheroids (projected spheroid images, scale bar 20 μm)

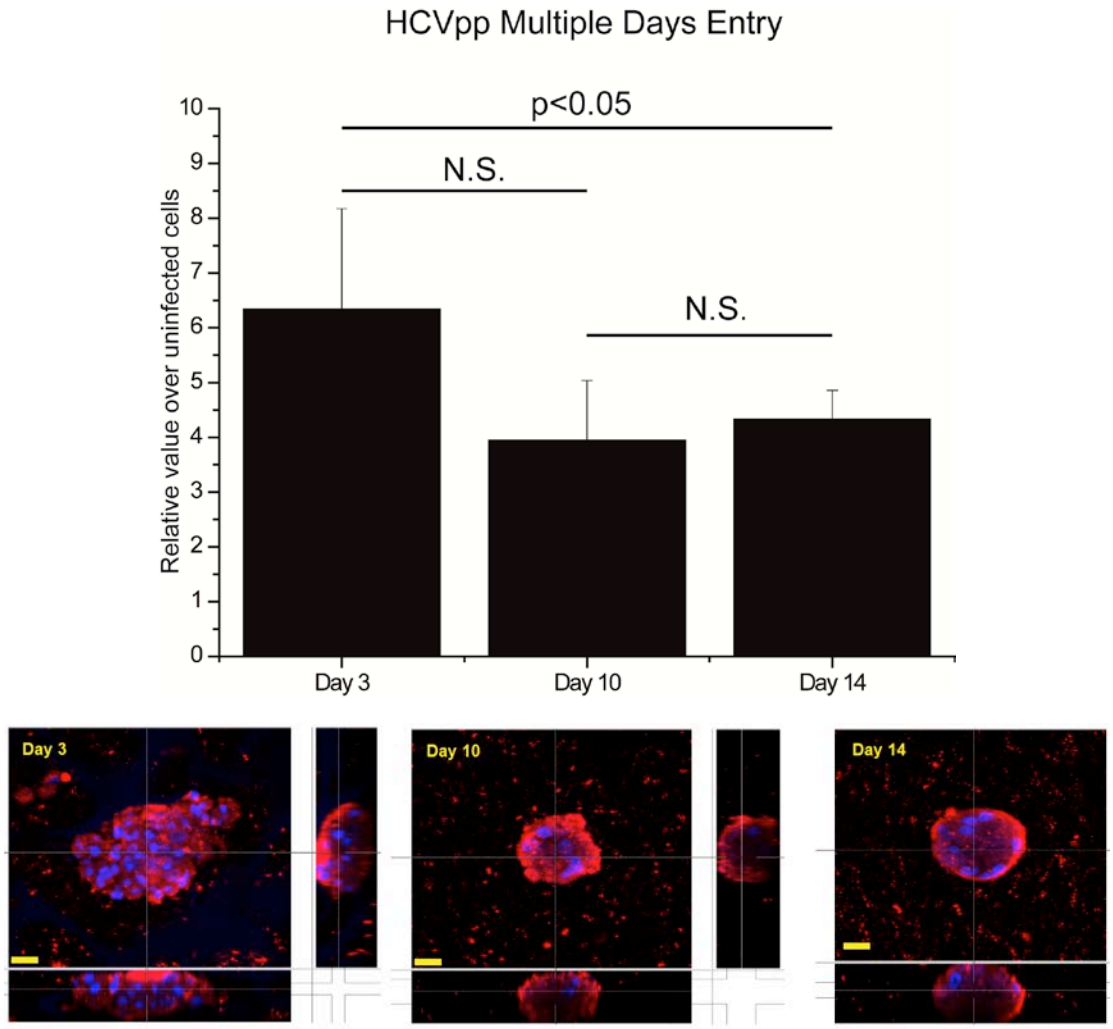

Figure 30. HCVpp entry in human hepatocyte spheroids in prolonged culture (projected spheroid images, scale bar 20 µm). N.S.: not significantly different

4.3.2.2 The entry of HCV pseudoparticles into human hepatocyte and Huh 7.5 spheroids can be inhibited by JS-81 in dose-dependent manner

To demonstrate the utility of our spheroids model to screen antiviral compound we co-incubated HCVpp with CD81 antibody. CD81 antibody was reported previously to inhibit HCV entry by reducing the availability of CD81 receptors to mediate HCV entry [222]. The presence of CD81 antibody inhibited HCVpp entry in a dose dependent manner (**figure 31**). The CD81 antibody concentration when 50% of

HCVpp entry was inhibited, labelled as IC_{50}, was estimated to be 500 ng/mL for human hepatocytes and 100 ng/mL for Huh 7.5 cells (**figure 31** left and right panel, respectively). These IC_{50} values were close to the previously reported values i.e. < 1 µg/mL [118].

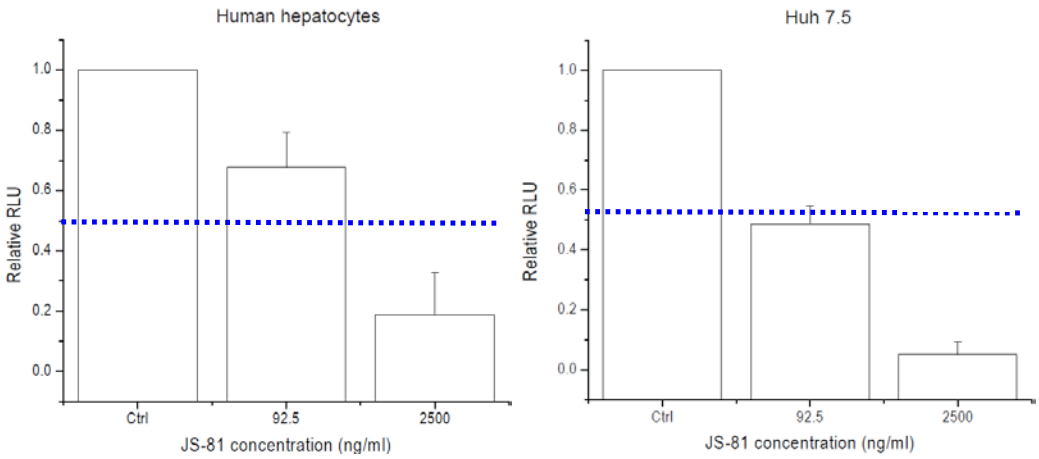

Figure 31. Inhibition assay of HCVpp entry in human hepatocyte and Huh 7.5 spheroids with CD81 antibody (JS-81). Data are average ± standard deviation of 3 independent experiments.

4.4 Discussion

We have demonstrated the utility of our galactosylated cellulosic sponge (HA Gal sponge) to culture human hepatocyte and Huh 7.5 cells as 3D spheroids in multi-well format for HCV infection (entry and inhibition) study. Within 24 hours post-seeding, both types of cells had reorganized to form compact spheroids morphology. Galactose conjugated on the sponge presented chemical cues to the cells to reorganize into 3D spheroids, while the macroporous structure constrained them physically. Since galactose ligand only interacts weakly with ASGPR receptors in the hepatocyte cell membrane, it is the combination of the physical and chemical cues in the sponge which are important in establishing stable constrained 3D hepatocyte spheroids [80].

Human hepatocyte spheroids size was maintained at the size of mass transfer barrier-free (majority size 50-80 µm) while proliferative Huh 7.5 spheroids reached 150-200 µm range. Spheroid viability of human hepatocyte spheroids maintained at least up to 5 weeks of culture however Huh 7.5 spheroids viability decreased significantly beyond 3 weeks of culture due to the increase in spheroids size limiting the mass transfer into the spheroids core. The spheroids morphology observed by SEM revealed tight spheroids morphology of these two types of spheroids and their maintenance over prolonged culture; 6 weeks and 3 weeks for human hepatocytes and Huh 7.5 spheroids, repectively. Human hepatocyte spheroids exhibited additional spheroids feature observed at higher magnification that is the 1-2 µm size hole located on spheroids surface which was reported before to be bile canaliculi-like structures extending from the surface to the interior of the spheroid [219].

Spheroids morphology correlated well with the expression of various mature differentiated hepatocyte genes being upregulated and or maintained over prolonged culture. Human hepatocytes spheroids exhibited minimal dedifferentiation compared to freshly thawed cryopreserved human hepatocytes. Mature human hepatocyte genes like CYP1A1, CYP3A4, HFN4α and Albumin were upregulated in the spheroid culture at 1,024, 4, 5,700 and 90 folds, respectively. For Huh 7.5 spheroids, we observed a significant increase in transcript levels of CYP3A4 & Albumin genes (256 and 16384 folds, respectively after 7 days of culture). These important mature hepatocyte genes were further maintained at similar levels of expression until 14 days in culture. The other genes like AAT, CYP1A1 and HNF4α were maintained from day 1 to day 14 of culture.

Both human hepatocyte and Huh 7.5 spheroids displayed hepatocyte polarity markers such as MRP2 and CD147 (visualized at the tight junctions and at the basolateral domain, respectively). Hepatocyte polarity markers were previously reported to be one of the requirements for HCV entry and propagation [4]. These spheroids also showed HCV entry markers namely CD81, SCARB1 and Claudin1. These HCV markers were reported to be important in the early phase of HCV infection [110]. CD81 was visualized at the basolateral domain of the cells while SCARB1 and Claudin1 were expressed at the tight junction regions of the spheroid. We observed these markers expression in the spheroids over extended culture of up to 14 days.

When these spheroids were inoculated with HCVpp to study the HCV entry, they exhibited high infection level throughout the whole spheroid region (~80% of total spheroids were infected). This infection level was significantly higher compared to other previously reported model to study HCV entry in human hepatocyte [118]. These spheroids cultured in the thin sponge were amenable to be inoculated with HCVpp in 96-well plate format, which brings the high throughput feature of our system. Importantly for human hepatocyte spheroids, HCVpp were able to infect the spheroids on a prolonged culture which secures our hypothesis for further investigation in HCV replication study. When both types of spheroids were co-incubated with HCVpp with CD81 antibody, we observed a dose-dependent inhibition of the HCV infection. 50% of HCVpp entry was inhibited by CD81 antibody at concentration of ~500 ng/mL for human hepatocytes and ~100 ng/mL for Huh 7.5 cells. These IC50 values were close to the previously reported values [118].

4.5 Conclusion

We have elucidated the usefulness of our galactosylated cellulosic sponge for human hepatocyte and Huh 7.5 cell 3D culture as spheroids for multi-well HCV entry and inhibition study. Human hepatocyte and Huh 7.5 spheroids are formed in the sponge within 24 hours post-seeding and constrained in the sponge macroporosity for prolonged culture. The size of the spheroids lies within mass transfer barrier-free range. Spheroids viability is well maintained up to 5 and 2 weeks for human hepatocyte and Huh 7.5, respectively. The compact spheroids morphology is observed at least up to 2 weeks of culture. Compact spheroids morphology correlates well with gene expression showing minimal dedifferentiation of human hepatocyte spheroids and upregulation of mature hepatocyte genes in Huh 7.5 spheroids. Both types of spheroids express liver polarity markers and HCV entry markers. When these spheroids are inoculated with HCVpp, an available *in vitro* model to study HCV entry, ~80% of the spheroids are infected with HCVpp distributed throughout whole spheroids region. Human hepatocyte spheroids have shown the ability to be infected at prolonged culture indicating the maintenance of HCV entry markers. By co-incubating both types of spheroids with HCVpp and CD81 antibody, HCVpp entry is inhibited at dose-dependent manner. Together, this spheroids model provides a useful platform to study HCV entry and inhibition *in vitro* and to screen HCV antiviral candidates.

CHAPTER 5

CLEAVABLE CELLULOSIC SPONGE DEVELOPMENT FOR 3D CELL CULTURE AND SPHEROIDS RETRIEVAL

5.1 Introduction

In tissue engineering scaffold design, it is ideal to have the scaffold to be biodegradable because three dimensional scaffolds serves only as temporary support for cell growth [223]. Upon study completion or for further downstream cell assays, the bulk amount of the scaffold materials need not to be present hence biodegradability is important. Ideally, scaffold degradation products should not elicit cytotoxicity or immunological responses and it is desired to have water soluble degradation product for easy by products removal. As shown previously, cellulosic sponge has shown many salient features for cell culture applications such as high water uptake, excellent hydrophilicity, diffusible and aqueous macroporosity, versatility for ligand conjugation, soft mechanical stiffness suitable for soft tissue culture, induces quick hepatocyte repolarization through accelerated spheroids formation, ease of cell seeding procedure and capability for large scale cell culture and drug/anti viral screenings [15, 80, 166]. Macroporous hydrogel sponge made of cellulose derivative could entrap cells, induce spheroids formation and maintain these constructs within the macroporous networks over extended culture period. However the current cellulosic sponge design is non-degradable during cell culture thus impose challenges to retrieve living spheroids from the sponge for further analysis and further use. Addition of trypsin or other dissociating enzymes to retrieve these spheroids is unable to achieve good spheroids harvesting yield. Biodegradation capability of this

class of novel cellulosic sponge has not been investigated. The reason is probably due to its rare application as tissue engineering scaffold.

To our knowledge, others have explored a way to degrade cellulose derivative materials using cellulase enzyme from *Aspergillus niger* to hydrolyze 1,4-β-D-glycosidic linkages but it might not be suitable for cell culture applications involving sensitive cells e.g. primary hepatocyte and stem cells [224]. Our attempt has also proven that this enzyme did not cleave our cellulosic sponge in which γ ray-crosslinked polymer has a rather strong covalent bond. Other class of polymeric scaffold such as polyester has been explored as hydrolysis induced-degradable scaffold but the degradation mechanism is rather slow and sometimes unpredictable [225]. Although the degradation occurs physiologically, they only exhibit gradual degradation kinetics with degradation times ranging from days to months [226]. In addition, this continuous hydrolysis process leads to the gradual weakening of the system during tissue growth. It is desirable to maintain the scaffold mechanical stiffness to support the cell/tissue growth throughout the culture that still allows on demands degradation kinetics upon completion of the study. The possibility to attach UV-sensitive bond in the scaffold chemical construct is an option to make the scaffold degradable on demand, as it has shown robust application for cell culture, but the use of high power and intensity of UV to cleave the labile bond might be detrimental to mature and sensitive cells we are mainly using [227]. With this respect, disulfide bonds are of our particular interest since they are stable against hydrolysis but can be cleaved on demand in the presence of reducing agents. The applications of disulfide bonds as cleavable bond have been investigated for various applications ranging from drug delivery to tissue engineering researches [228, 229]. In particular for soft tissue

culture, disulfide-containing scaffold was found to be suitable in 3D environment of *in vitro* tissue culture to be utilized for replacing diseased tissue *in vivo* [226].

Disulfide bond cleavability has been known for years in protein synthesis mechanism. When cysteine is oxidized it will form cystine, which is actually two cysteine residues joined by a disulfide bond (cysteine-S-S-cysteine) between the -SH group [230]. In recent years, there is an increasing interest to prepare scaffold matrices containing disulfide crosslinked bonds since cleaving these bonds is controllable under physiological condition by altering the concentration of reductant used [231-234]. Through chemical cleaving, disulfide bond (-S-S-) would readily decompose into thiol groups (-SH HS-). These thiol groups also do not decrease the local pH like what it was commonly observed in polyester hydrolysis mechanism [235]. Various chemical reductants are known to cleave disulfide bonds e.g. dithiothreitol (DTT), glutathione (GSH), L-cysteine (Cys) and tris(2-carboxyethyl) phosphine (TCEP) [232, 236-239]. The insertion of this disulfide bond into the hydrogel construct has been known to induce cleavage in physiological condition by incubating with reductants. Soluble decomposed products were easily removed by washing with excess cell culture medium or buffer [240]. Various disulfide-containing hydrogels were already reported as temporary hydrogel template, ECM-mimicry matrix and 3D cell encapsulation platform [223, 232, 238, 240]; however we found that there is still no exploration on cleavable macroporous disulfide-containing cellulosic sponge as hydrogel template for spheroids culture and retrieval.

The disulfide-containing cellulosic sponge is designed to be used as 3D spheroids hepatocyte culture and retrieval of these spheroids. Other cell types that show good functionality if cultured as spheroids are also explored e.g. cancer and

stem cells. Therefore careful polymer design and choice of less cytotoxic reductant were performed. Tris(2-carboxyethyl) phosphine (TCEP), a known less cytotoxic chemical reductant, is used to cleave the disulfide bonds in the cellulosic macroporous sponge. Compared to a known and strong chemical reductant dithiothreitol (DTT), TCEP is found to be more chemically stable, more effective in cleaving disulfide bond and able to reduce disulfide bonds at wider pH range; TCEP is effective at wider range of pH, 1.5-8.5, while DTT is only effective at pH 7-8.1 [241-243]. In terms of cytotoxicity, although 10 mg/mL TCEP was found to reduce cell viability upon 24 hours of exposure to the cells but still in the acceptable range of 60% remaining viable cells [244]. In our attempt to develop disulfide-containing cellulosic sponge, we aim to synthesis a sponge which can be cleaved less than 1 hour thus reducing the exposure time between the cells and reductant.

Here, we have demonstrated by conjugating reducible disulfide bond into hydroxyl groups at the side chain of hydroxypropyl cellulose prior to attaching the double bond for crosslinking, we can tailor the cellulosic sponge to be readily cleavable on-demand upon addition of suitable disulphide bond reductant that works best under a range of cell-compatible conditions. The sponge cleavage occurs at physiological condition (pH 7.4, 37°C, in cell culture medium and or buffer) within 30 minutes without inducing significant cell toxicity, disruption of cell-cell adhesions, primary hepatocyte polarity markers and cytochrome P450 enzymes. The insertion of disulfide bond at the side chain of hydroxypropyl cellulose also does not interfere with the formation of macroporous network of cellulosic sponge as well as the crosslinkability of the hydrogel with γ irradiation. Moreover this modification does

not inhibit the ligand conjugation process onto the sponge for subsequent cell culture application.

Comparing our disulfide-containing cellulosic sponge to the other disulfide-containing hydrogel systems, our technology shows the importance of having macroporous networks with mechanically and chemically tunable properties of the sponge for 3D cell culture within diffusible construct rather than cell encapsulated in hydrogel system. The presence of macroporous networks is hypothesized to accelerate the sponge cleavage. Sponge macroporosity helps in the formation of cell-dense construct i.e. spheroids. Our disulfide-containing sponge also shows significantly faster cleavage rate at the addition of comparable reductants concentration than other disulfide-containing hydrogels (which cannot form spheroids as in our sponge likely due to blockage of cell-cell interactions by hydrogels) i.e. spheroids can be easily retrieved from our sponge as fast as 30 minutes [223, 240]. Compared with the prior art of cellulosic sponge [15], this cleavable disulfide-containing cellulosic sponge has been designed and synthesized with novel chemistry that is not obvious. The reduction condition importance for cytocompatibility with rapid sponge cleavage for intended applications with utilities have been explored and experimentally determined.

5.2 Materials and methods

5.2.1. Materials

All chemicals and reagents were purchased from Sigma Aldrich (Singapore), unless otherwise stated.

5.2.2 Chemical synthesis of disulfide-containing hydroxypropyl cellulose polymer (HPCSS)

Hydroxypropyl cellulose (HPC) Mw = 80,000 g/mol and degree of etherification ~3.4 was dehydrated by azeotropic distillation in toluene at 70°C. The chemical synthesis consists of 2 steps. The first step of the reaction was inspired by the Steglich esterification reaction with 4-dimethylaminopyridine (DMAP) as the catalyst to conjugate carboxylic group into alcohol group [245]. 1 gram of dried HPC was dissolved in 30 mL anhydrous dimethylformamide (DMF), to which 5.95 mmol of DMAP was added. In a separate flask, 5.95 mmol of dithiodipropionic acid (DTDP) was dissolved in 30 mL anhydrous DMF. Completely dissolved DTDP was activated with 2.98 mmol of each 1-ethyl-3-(3-dimethylaminopropyl) carbodiimide (EDC) and N-hydroxy succinimide (NHS) for 10 minute. The activated DTDP solution was added to HPC/DMAP mixture and reacted for 24 hours at room temperature under N_2 blanket. The mixture was then dialyzed in excess methanol and water, subsequently, and lyophilized. The end product is denoted as HPCDTP.

The second step of the reaction is an esterification reaction to conjugate amino group into carboxylic group. HPCDTP was dissolved in 30 mL deionized water and activated with two molar ratio of each EDC and N-hydroxysulfosuccinimide (sulfo-NHS) for 10 minute. In a separate flask, two molar ratio of 2-amino ethyl methacrylate hydrochloride was dissolved in 30 mL deionized water. 2-amino ethyl methacrylate hydrochloride solution was added to the activated HPCDTP mixture and reacted for 24 hours at room temperature under N_2 blanket. The mixture was then dialyzed in excess water subsequently and lyophilized. The end product is denoted as

HPCSS. A schematic diagram with the complete synthesis described, including ^{1}H NMR characterization are shown in **figures 32 and 33.**

5.2.3 Preparation of HPCSS sponges

Firstly, HPCSS was dissolved in deionised water to a final concentration of 10% wt/vol after which the solution was inserted into glass tubes (diameter 10 mm, length 6 cm). The tubes were heated in a 40°C water bath until phase separation occurred and then crosslinked by γ irradiation for 1 hour at a dose of 10 kGray/hour (Gammacell 220, MDS Nordion, Canada). The sponge monoliths were obtained by breaking tubes subsequent to freezing the frozen glass tubes in dry ice. A Krumdieck tissue slicer (Alabama Research & Development USA) with set speed 50 rpm was used to cut the sponge uniformly. Sliced sponges were further washed extensively with excess amounts of deionised water for 3 days to remove uncross-linked polymers. These sponges were lyophilized prior to further galactosylation.

5.2.4 Galactosylation of HPCSS sponges (HPCSS Gal sponges)

The lyophilized pre-sliced HPCSS sponge was immersed in acetone three times within 20 min interval each (1 mL of acetone per 10 mm diameter 1 mm thickness sponge). The sponge was further activated with 2 mM 1,1'-carbonyldiimidazole (CDI) dissolved in acetone for 30 min and shaken at 4°C. The activated sponge was washed with acetone three times to remove the excess CDI. 2 mg/ml of D-(+)-galactosamine dissolved in carbonate bicarbonate buffer pH 10 was added and reacted at 4°C for 24 hour. This concentration of added galactose was found to be the optimum in the

chemical synthesis. The reacted sponge was subsequently washed with excess of Dulbecco`s Phosphate Buffered Saline (DPBS) and deionized water three times each. Upon washing, sponge was lyophilized. The cleavability of the sponge was confirmed by further incubation of the sponge in 10 mM tris(2-carboxyethyl) phosphine (TCEP) in cell culture medium adjusted to pH 7.4.

5.2.5 Physiochemical characterization of HPCSS Gal macroporous sponges

5.2.5.1 X-Ray photoelectron spectroscopy

X-Ray photoelectron spectroscopy was used to qualitatively verify galactose ligand conjugation onto the HPCSS sponge. Measurements were made on a VG ESCALAB Mk II spectrometer with a MgKa X-ray source (1253.6 eV photons) at a constant retard ratio of 40.

5.2.5.2 Elastic modulus measurement

The elastic modulus of the sponge was measured by atomic force microscopy (Bioscope Catalyst, Veeco Instruments, Santa Barbara, CA) in deionized water. A hybrid Atomic Force Microscopy (AFM) probe consisting of a silicon nitride cantilever and a silicon tip (ScanAsyst-Fluid, Veeco Probes, Camarillo, CA) was used. The deflection sensitivity was calibrated by ramping force-distance curves on a glass surface, and the spring constant was calibrated by the thermal noise method. After calibration, 128 x 128 force-distance curves were recorded over an area of 5 μm x 5 μm by force volume. Each force-distance curve was analyzed by fitting to the Hertz model with conical tip geometry and Poisson ratio of 0.5. The obtained elastic moduli from each force-distance curve were mapped into a bitmap image with 128 x 128

pixels. The curve fitting and statistical analysis was implemented by a self-developed Fortran program. The relationship between elastic modulus with the measured force is described as $F = \frac{2}{\pi}\frac{E}{1-v^2}\tan\alpha\delta^2$, where F is the measured force, E is Young's elastic modulus, v is the Poisson ratio of the material under measurement (0.5 was used in the data processing), α is the half angle of the probe (22°) and δ is the sample deformation/ indentation..

5.2.5.3 Scanning electron microscopy

Top and cross section views of the sponge surface morphology and porosity were captured using SEM (JEOL JSM- 5600, Japan) at 10 kV. High magnification of SEM (15,000 folds) was performed to observe the sponge surface sub-micron features. Prior to imaging, the dried sponge was sputter coated with platinum for 90 seconds. Pore size distribution of the sponges was quantified with imageJ software (version 1.43u) from collective SEM top view images of the sponges.

5.2.5.4 Water uptake and sponge porosity measurements

The lyophilized sponges were soaked in deionised water at room temperature for 48 hours; their water uptake were calculated according to the equation $Water\_uptake = (\frac{W_h - W_d}{W_h})100\%$, where W_h is the hydrated weight and W_d is the dehydrated weight. The porosities of lyophilized HA Gal sponges were determined by solvent replacement. Samples were soaked in absolute ethanol for 24 hours and weighted after excess ethanol on the surface was blotted. It was noted that there were no significant changes in dimension before and after immersion in ethanol. The porosity was calculated as $Porosity = (\frac{M2 - M1}{\rho V})100\%$, where M1 and M2 are the

weight of sponge before and after immersion in absolute ethanol, respectively; ρ is the density of absolute ethanol and V is the volume of sponge.

5.2.5.5 Fourier transform infrared spectroscopy

Infrared spectra were recorded on a Perkin Elmer Spectrum 100 FTIR (Fourier transform infrared) spectrometer. The disulfide to thiol exchange upon sponge cleavage was identified at wavenumber 2550 cm^{-1} [240].

5.2.5.6 Ellman's thiol analysis

Crosslinked HPCSS gel was completely cleaved with 25 mM DTT in DPBS at room temperature for 90 min and was further dialyzed using a Spectra/Pore membrane (molecular weight cutoff 12-14,000) for 3 days to remove DTT. The dried decomposed product was obtained by lyophilizing the solution for 3 days. The decomposed product (0.15 mM) was dissolved in 2.4 mL of 0.1 M Tris–HCl/0.01 M EDTA buffer (pH=8.0) and 100 μL of 0.01 M 5,5′-dithio-bis(2-nitrobenzoic acid) (DTNB) (Sigma, USA)/0.05 M DPBS (pH=7.0) was added to the solution. The absorbance of the solution at 412 nm was measured by Agilent 8453 UV Visible System and readings were compared with 0.05 mM TCEP (as positive control), 0.15 mM cystamine (as negative control) and 0.15 mM uncleaved pre-crosslinked HPCSS polymer.

5.2.5.7 Sponge cleavage condition optimization

For easy visualization during cleavage, HPCSS Gal sponges were pre-soaked in 0.25 mg/mL propidium iodide overnight (Molecular Probes, USA). The stained sponges were incubated with 3 mL of TCEP per sponge at various concentrations (25,

10, 5, 3 and 1 mM) in 37°C, 5% CO_2 and 95 % incubator. The morphological changes of the sponge were monitored visually every 15 minutes.

5.2.5.8 Dynamic visualization of sponge cleavage with time lapse imaging

The propidium iodide-prestained HPCSS Gal sponges were incubated with 10 mM TCEP and its macroporosity changes were monitored by Olympus fluoview FV1000 equipped with 37°C heated chamber with a 60x water lens for 30 minute with 2 minute time interval. Images were analysed using IMARIS and images assembled using Adobe illustrator CS3.

5.2.6 Cell culture

Hepatocytes were isolated from male Wistar rats weighing 250-300 g using the in situ collagenase perfusion method [182]. Animals were handled according to the IACUC protocols approved by the IACUC committee of National University of Singapore. Viability of hepatocytes was determined to be >90% by the Trypan Blue exclusion assay. Yields were approximately 10^8 cells/rat. Freshly isolated rat hepatocytes were seeded onto the sponge by simply dropping the cell suspension on the sponge surface (0.5 x 10^6 cells per 55 μL cell suspension per 10 mm diameter 1 mm thick sponge). The cell suspension was slowly absorbed into the sponge interior due to the inherent hydrophilicity of the sponges. Fresh cell medium was added slowly to the sponge edge after 45 minutes incubation (500 μL per sponge in 24-well plate). Hepatocytes seeded on a collagen monolayer platform (0.29 mg/mL collagen concentration) were used as control. Cells were maintained with Williams' E medium supplemented with 10 mM $NaHCO_3$, 1 mg/mL BSA, 10 ng/mL of EGF, 0.5 mg/mL

of insulin, 5 nM dexamethasone, 50 ng/mL linoleic acid, 100 units/mL penicillin, and 100 mg/mL streptomycin and were incubated with 5% CO_2 at 37°C and 95 % humidity. Medium was replenished every day.

5.2.7 TCEP toxicity study in primary rat hepatocyte

Primary rat hepatocyte was seeded on collagen coated well in 24-well plate format (0.3 x 10^6 cell per well). The culture was maintained for 3 days and the medium was replenished every day. On the 3rd day, the cells were incubated with TCEP solution in Williams' E medium at pre-determined concentrations and time; 5 mM for 1.5 hour, 10 and 25 mM for 1.5 hour each. The duration of the incubation was chosen based on the ability of the associated TCEP concentrations to completely cleave HPCSS Gal sponge. Upon incubation, the morphology of the cells was monitored and followed with further incubation of 1 mg/mL (3-(4,5-dimethylthiazol-2-yl)-2,5-diphenyltetrazolium bromide (MTT) solution for 3 h. The formed formazan product in each well was dissolved with 300 μL of 0.04 M HCl in isopropanol and its optical density was measured by TECAM Infinite M1000 microplate reader at 570 nm. Cell viability was determined by calculating the ratio of treated sample absorbance against untreated sample absorbance.

5.2.8 Hepatocyte spheroids characterization and functional assessment

5.2.8.1 Spheroids size distribution

Spheroid size distribution was quantified using imageJ software (version 1.43u) from collective phase contrast images of living hepatocyte spheroids cultured in the HPCSS Gal sponges on day 1, 3, 5 and 7.

5.2.8.2 Hepatocyte spheroids retrieval by cleaving the HPCSS Gal sponge

Rat hepatocyte spheroids were retrieved from the sponge by incubating cell seeded-cleavable sponge with 3 mL of 10 mM TCEP in respective cell culture mediums in each well of 12-well plate for 30 min at 37°C (incubator set up 5% CO_2 and 95 % humidity). The cleaved sponge solution from each well was mixed thoroughly by 3 mL plastic dropper and then transferred into 15 mL falcon tube. This solution was further diluted with 3 mL pre-warmed DPBS and centrifuged at 100 x *g* for 10 minutes. This washing step was repeated three times to remove TCEP solution completely. Eventually, the retrieved hepatocyte spheroids were resuspended in fresh mediums and replated on collagen coated dish or poly-L-lysine coated dish for further assays or spheroids manipulation.

5.2.8.3 Live/dead staining

Spheroids were co-stained with Cell Tracker Green (CTG, 20 μM) (Molecular Probes, USA) and propidium iodide (PI, 25 μg/mL) (Molecular Probes, USA) to determine live and dead cells, respectively. Cells were incubated for 30 min at 37°C and then fixed with 3.7 % paraformaldehyde for 10 min at room temperature. Fluorsave (Merck Chemicals) was applied to the stained spheroids to minimize photo-

bleaching. Images were acquired by confocal laser scanning microscopy (Zeiss LSM510, Germany) at 488 and 543 nm excitation wavelengths.

5.2.8.4 Reverse transcriptase polymerase chain reaction

RNA was extracted from hepatocytes cultured as 3D spheroids in HPCSS Gal sponges by RLT lysis buffer (Qiagen, Singapore). Total RNA concentration was quantified by a Nanodrop (Thermoscientific) and 1 μg of RNA was converted to cDNA by High Capacity RNA-to-cDNA (Applied Biosystems). Primers were designed using Primer 3 and real-time PCR was performed by using SYBR green fast master mix on a ABI 7500 Fast Real-Time PCR system (Applied Biosystems). Gene expression was calculated using the ΔΔCT method normalized to β-actin. The primers used in experiment are shown below.

Table 6. Primer sequences used in RT-PCR experiments

CYPs

Genes	Forward sequence	Reverse sequence	Primer Accession No.	P.S. (bp)
CYP1A2	CACGGCTTTCTGACAGACCC	CCAAGCCGAAGAGCATCACC	NM_012541.3	291
CYP2B2	ACCGGCTACCAACCCTTGAT	TGTGTGGTACTCCAATAGGGACAA	NM_001198676.1	105
CYP3A2	TGGGACCCGCACACATGGACT	TCCGTGATGGCAAACAGAGGCA	NM_153312.2	183
β-actin	ACCCACACTGTGCCCATCTA	GCCACAGGATTCCATACCCA	NM_031144.3	342

CYP: Cytochrome P450
P.S.: Product size, Annealing temperature: 60°C, Cycle numbers: 40

5.2.8.5 Immunofluorescence microscopy

To stain F-actin, E-cadherin and MRP2, hepatocytes spheroids cultured for 72 hours post-seeding in the sponges and retrieved from HPCSS Gal sponges were fixed in 3.7 % paraformaldehyde for 10 min. For staining F-actin, the cells were permeabilized for 5 min in 0.1 % Triton X-100 and incubated with 1 μg/mL TRITC-phalloidin (Molecular Probes, USA) for 20 min. For E-cadherin and MRP2 staining, following washing and blocking with 2% BSA/0.2% Triton-X 100 the spheroids were incubated overnight at 4°C with primary antibodies: anti-rat E-cadherin (BD, USA) and rabbit anti-rat MRP2 (Sigma Aldrich, Singapore), respectively. Secondary antibodies used were goat anti-mouse and goat anti-rabbit 488 and 555 (Molecular Probes, USA), respectively. Nuclei stain was captured using DAPI stain (Vecta Shield, UK). Images were captured using Olympus fluoview FV1000 with a 60x water lens. Images were analysed using IMARIS and assembled using Adobe illustrator CS3.

5.2.8.6 Biliary excretion of fluorescein dye

For monitoring hepatocyte repolarization, we visualized the excretion of fluorescein dye via bile canaliculi. Hepatocytes spheroids retrieved from the cleaved sponge were incubated with 15 μg/mL fluorescein diacetate (Molecular Probes, USA) in Williams' E medium at 37 °C for 45 min. The cultures were then rinsed and viewed with a 63X water lens on a Zeiss Meta 510 confocal microscope.

5.2.8.7 Scanning electron microscopy

Hepatocyte spheroids retrieved from cleavable HPCSS Gal sponge and non cleavable HA Gal sponge control on day 3 were fixed with 3.7 % paraformaldehyde overnight and stained with 1% OsO4 for 1 hour. Samples were then dehydrated step-

wise with ethanol (25 %, 50 %, 75 %, 90 % and 100 %) for 10 minutes each, dried in a vacuum oven and sputter coated with platinum for 90 seconds. The samples were viewed with a scanning electron microscope (JEOL JSM- 5600, Japan) at 10 kV.

5.2.9 Statistical analysis

Statistical comparisons were undertaken using paired two-tailed Student's t tests. Results are expressed as mean ± standard deviation or standard error of the mean. Confidence interval to be significantly different is 95%.

5.3 Results

5.3.1 Versatility of hydroxypropyl cellulose chemistry facilitates conjugation of cleavable disulfide bonds

The first step in the chemical synthesis of the cleavable cellulosic sponges (HPCSS sponge) involved the conjugation of dithiodipropionic acid onto hydroxypropyl groups of hydroxypropyl cellulose to provide carboxylic acid group (-COOH) to further react with 2-amino ethyl methacrylate hydrochloride. This reaction was inspired by the Steglich esterification reaction with 4-dimethylaminopyridine (DMAP) as the catalyst to conjugate carboxylic group into alcohol group [245]. The second step in the synthesis was the conjugation of 2-amino ethyl methacrylate hydrochloride onto carboxylic acid group. Conjugated methacrylate group acted as crosslinking site during γ irradiation, similar function as the allyl group described previously [15]. The galactose conjugation onto the remaining available

hydroxypropyl groups was performed using 1,1'-carbonyldiamidazole in acetone. The sponge chemical synthesis and fabrication are depicted in detail in **figure 32.**

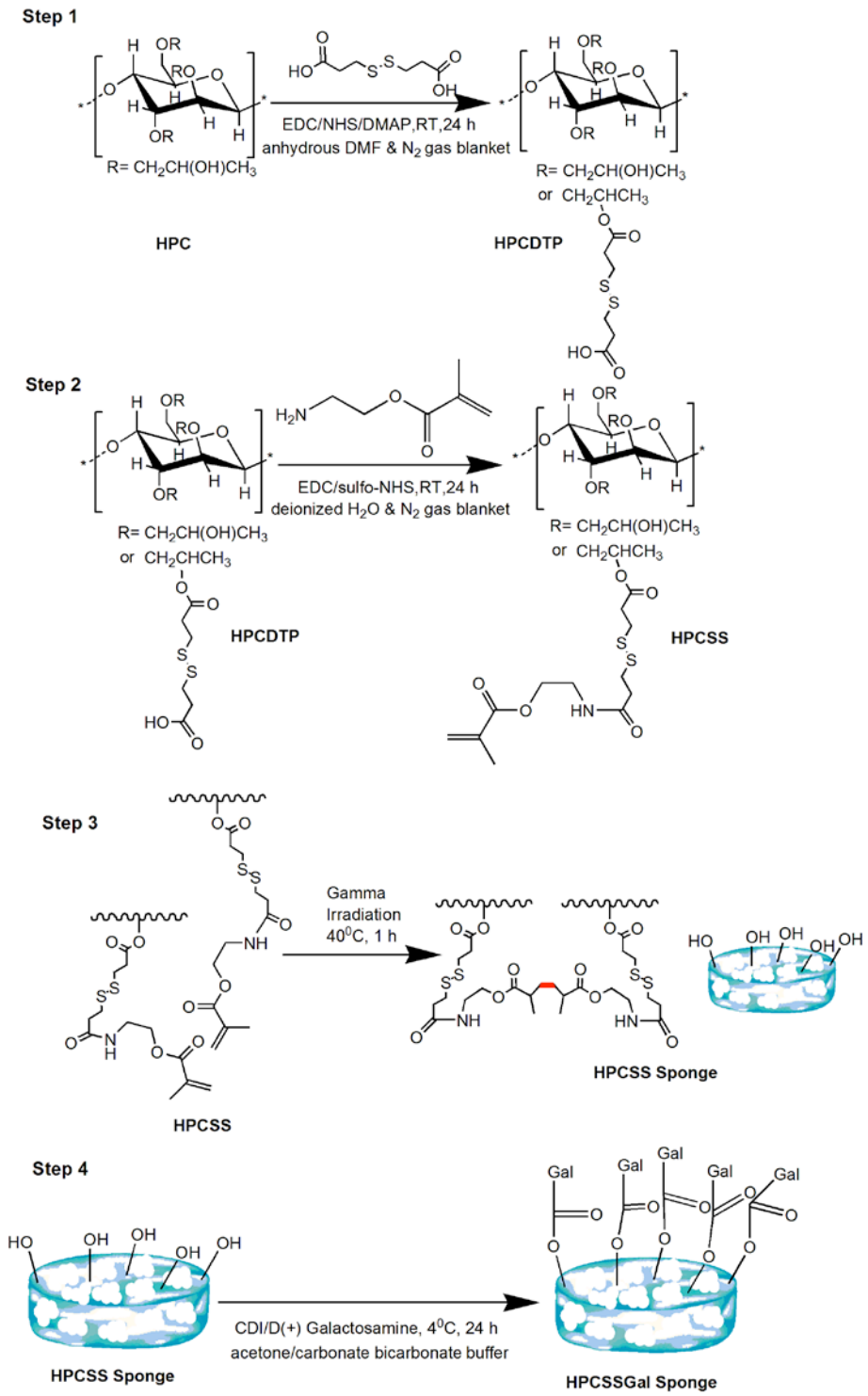

Figure 32. Schematic diagram of cleavable cellulosic sponge synthesis and fabrication

Conjugated dithiodipropionic acid presence on the chemical backbone was verified by ^{1}H NMR by identifying singlet peak at ~9.5 to 10 ppm (Step 1, **figure 33**). In estimation, there was at least 1 conjugated dithiodipropionic acid group in every 6 subunits of HPC. Upon further conjugation of 2-amino ethyl methacrylate hydrochloride in the step 2, this singlet peak disappeared. Based on calculation, the conjugated methacrylate group appeared in every 16 subunits of HPC. Multiplet peaks appeared at ~5 to 5.5 ppm indicated successful conjugation of methacrylate group (Step 2, **figure 33**).

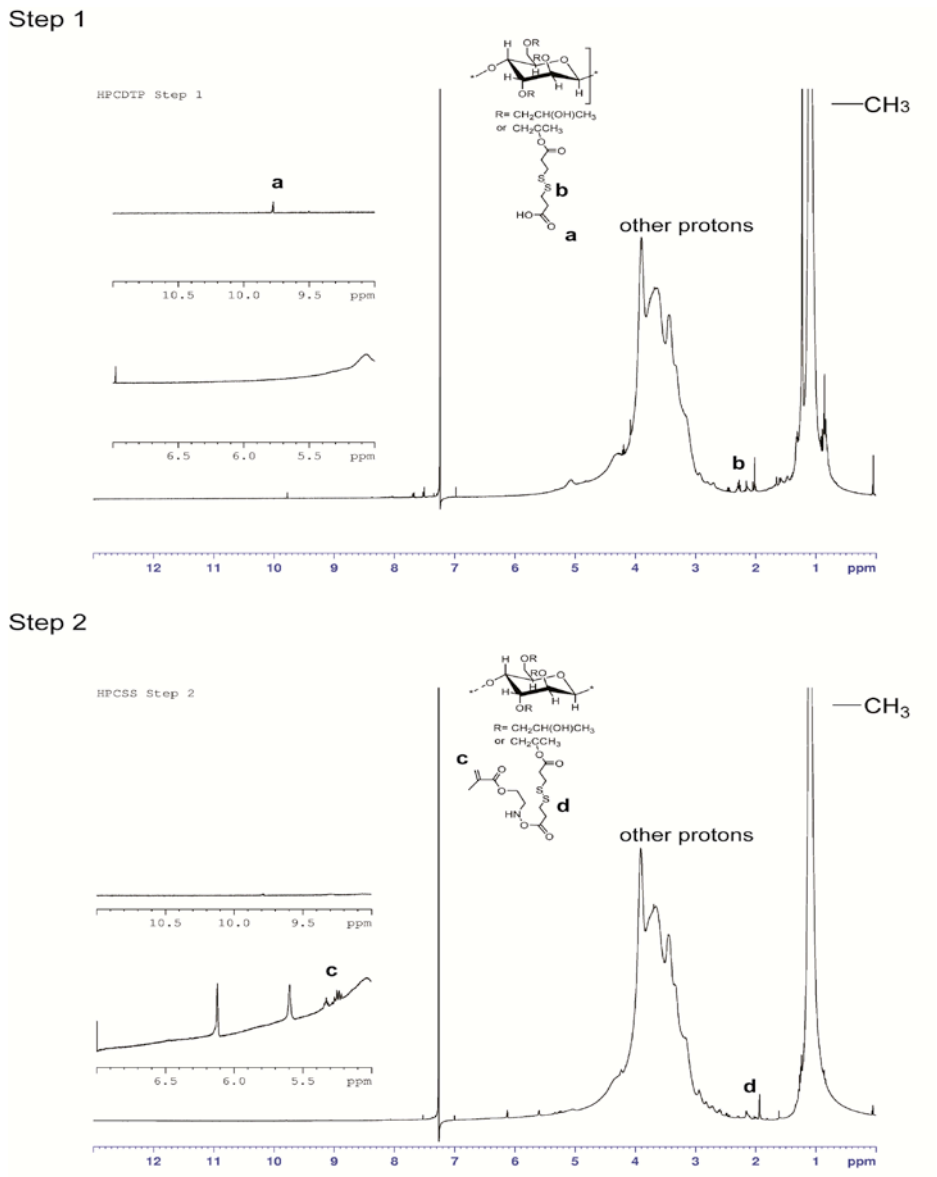

Figure 33. Cleavable sponge chemical structure validation by ^{1}H NMR

Galactose presence on the chemical backbone was quantified by N1s scan XPS. An XPS spectrum showed increased nitrogen atomic counts after conjugation (~0.6 % increase) (**figure 34**).

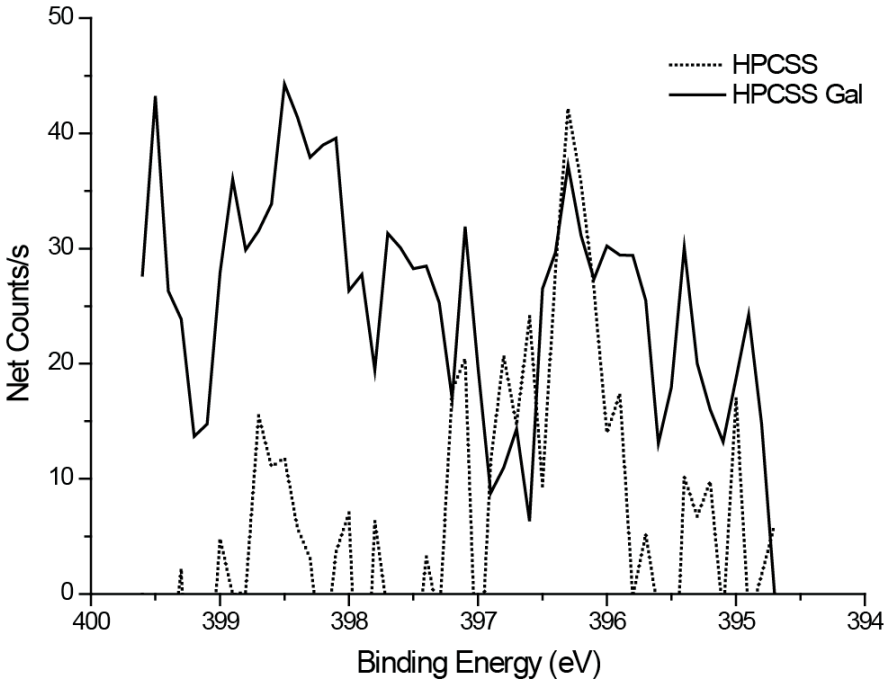

Figure 34. N1s XPS analysis of conjugated galactose indicates the net increase of N1s counts after conjugation

Surface morphology and porosity of the sponges were characterized using SEM images. Image analysis of the sponge porosity revealed the majority of pore size to be between 71 to 90 μm; ~22% and ~28% of pores were 71-80 μm and 81-90 μm, respectively (**figure 35D**). These pores were then within diffusible dimension (< 200 μm). The sponge also had considerably high water uptake (96.8 ± 0.14%) with porosity 88.69 ± 5.92%. Measurement of the elastic modulus of the sponges using atomic force microscopy revealed an average modulus of 30 kPa. This modulus was found to be slightly higher compared to the previous non-cleavable sponge but still considered to be as soft matrix. High magnification images of the sponge surface revealed surface sub-micron features in the range of 0.5 μm scale which was proven previously to help tethering the hepatocyte spheroids to the sponge (**figure 35B** insert) [80]. The dry sponge was soaked in 0.25 mg/mL propidium iodide solution to stain

the sponge's macroporous structure. By laser confocal microscopy, we observed that the macroporosity was maintained as a hydrated macroporous network structure in an aqueous environment (**figure 35C**) in contrast to typical hydrogels that lose their porosity in an aqueous environment.

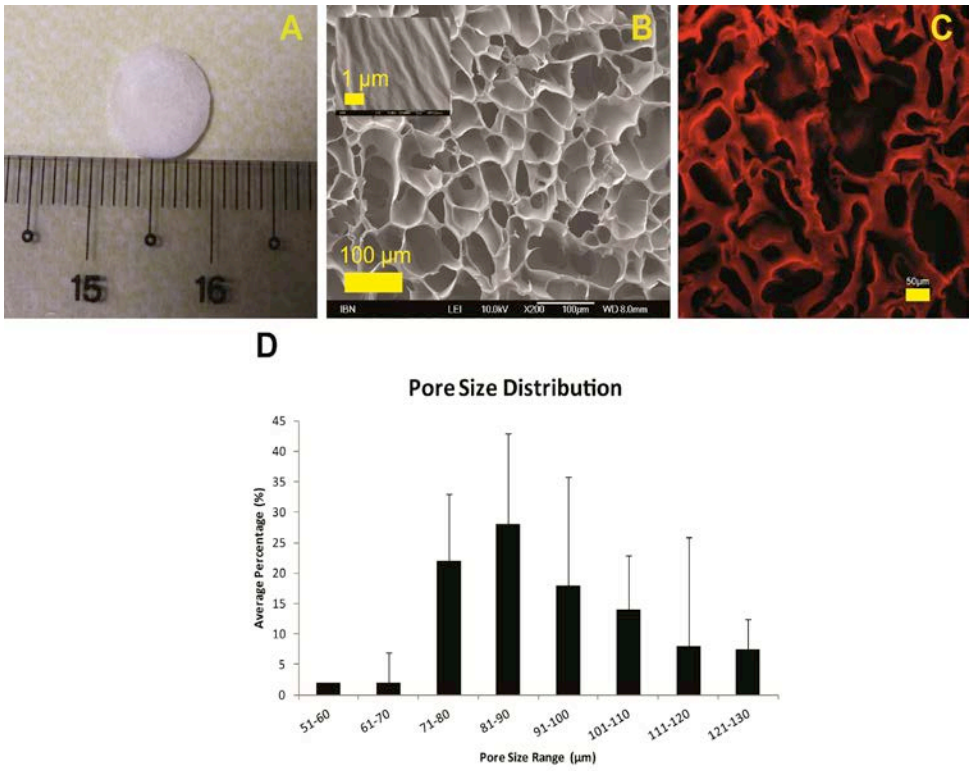

Figure 35. Sponge physical characteristics: a) Sponge top view (scale bar in cm), b) SEM images of the sponge surface porosity (insert image is the surface sub-micron features view), c) Sponge aqueous macroporosity (scale bar 50 µm) and d) Sponge pore size distribution (Data are average ± standard deviation, n=50)

5.3.2 Conjugated disulfide bonds on the side chain of hydroxypropyl cellulose induces cleavability of macroporous cellulosic sponge rapidly at physiological condition

Upon successfully inserting disulfide bond onto hydroxypropyl cellulose side chain, the cleavability of the sponge in reductants was tested. Sponge samples before and after cleavage were compared and analyzed by FTIR. FTIR spectra showed the valley-like peak appearance at 2550 cm^{-1}, similarly as it was reported previously in

another disulfide-containing hydrogel (**figure 36A**) [240]. This peak corresponded to thiol group (-SH) formation from disulfide group (-S-S-) upon cleavage. The thiol group formed was further confirmed by Ellman's thiol analysis in terms of its ability to further cleave a known disulfide-containing dye 5,5'-dithiobis-(2-nitrobenzoic acid) (DTNB) to be UV-detectable compound. The cleaved sponge sample was found to be able to cleave DTNB at 1/3rd strength of the positive control, TCEP (**figure 36B**).

C

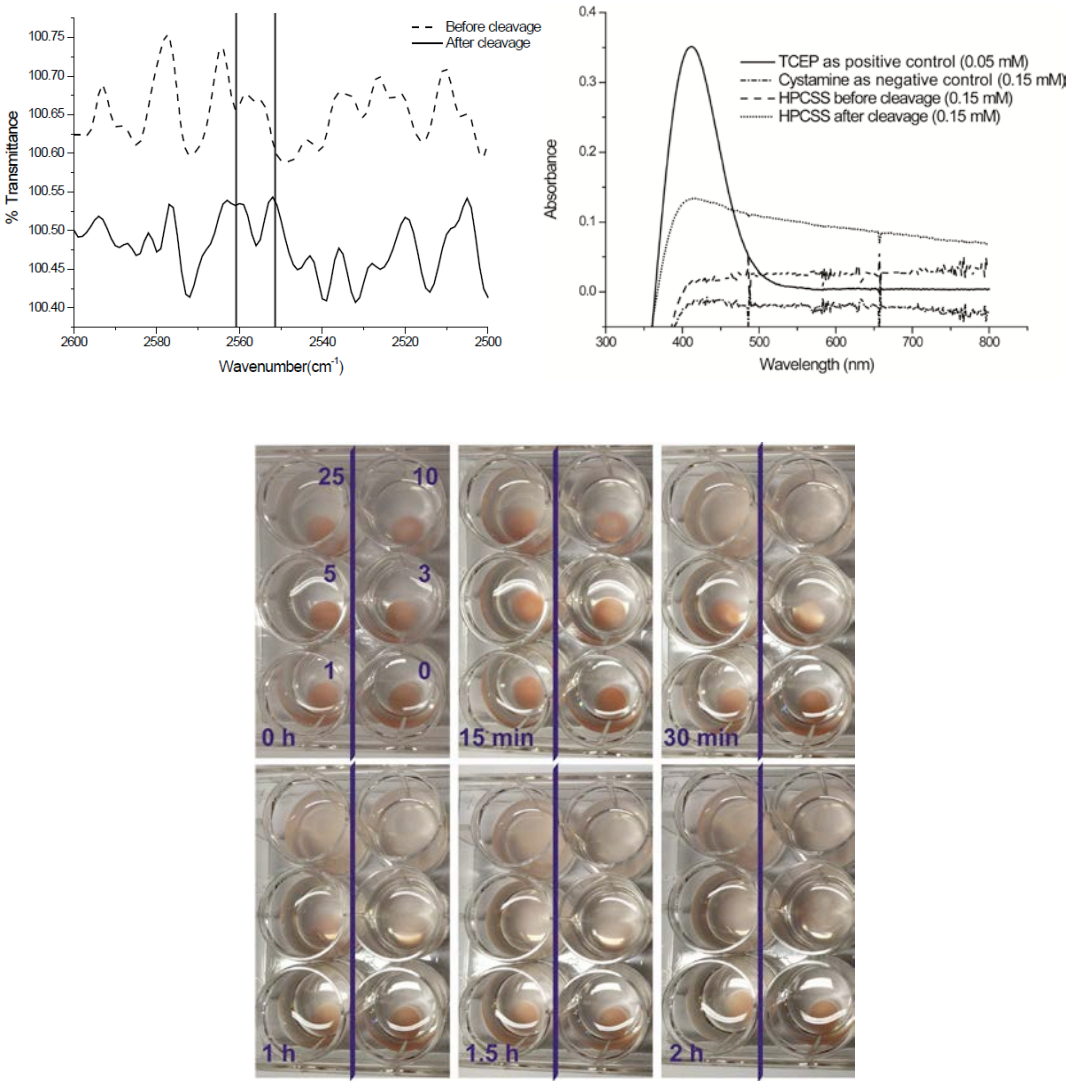

Figure 36. Sponge cleavage characterizations: a) FTIR analysis indicates the presence of valley at 2550 cm^{-1}, b) Ellman's thiol analysis shows the ability of thiol groups of the cleaved HPCSS sponge to further cleave 5,5'-dithiobis-(2-nitrobenzoic acid) indicated by UV absorbance at 412 nm and c) Physical morphology changes of HPCSS Gal sponge upon addition of tris(2-carboxyethyl) phosphine (TCEP) at various concentrations (in mM unit)

After confirming the formation of thiol groups from disulfide groups upon cleavage, the optimum cleavage condition was determined by incubating the sponge with serial concentrations of TCEP. Physical morphology changes of the sponge were monitored visually (**figure 36C**). To ease the monitoring process, the sponges were pre-soaked overnight with 0.25 mg/mL propidium iodide. TCEP could cleave the sponge as fast as 30 min (**table 7**). The optimum cleavage condition was determined by the time taken for cleavage as well as reductant concentration used. TCEP, a reductant without thiol group, had been favoured over thiol-based reductants due to its less cytotoxicity and less ability to penetrate cell membrane [246, 247]. Therefore, 10 mM TCEP was chosen as optimum condition for further sponge cleavage (~30 min cleavage).

Table 7. Optimization of cellulosic sponge cleavage using different concentrations of reductant

TCEP concentrations in William's E medium	Remarks
25 mM	Sponge is cleaved within 30 minute
10 mM	Sponge is cleaved within 30 minute
5 mM	Sponge is cleaved within 1.5 hour
3 mM	Sponge is cleaved within 2 hours
1 mM	Sponge not cleaved

Sponge aqueous macroporous network disappearance was monitored dynamically by time lapse imaging in confocal microscopy. This salient feature of the cellulosic sponge was monitored within 30 minutes duration with image taken every 2 minute time interval. As it is shown in **figure 37**, 6 minutes after adding 10 mM TCEP, the sponge macroporous networks had shrunken significantly. At 20 minutes,

macroporosity had completely vanished with significant drop in the total signal intensity. This decrease corresponded to sponge thinning and dissolution during cleavage.

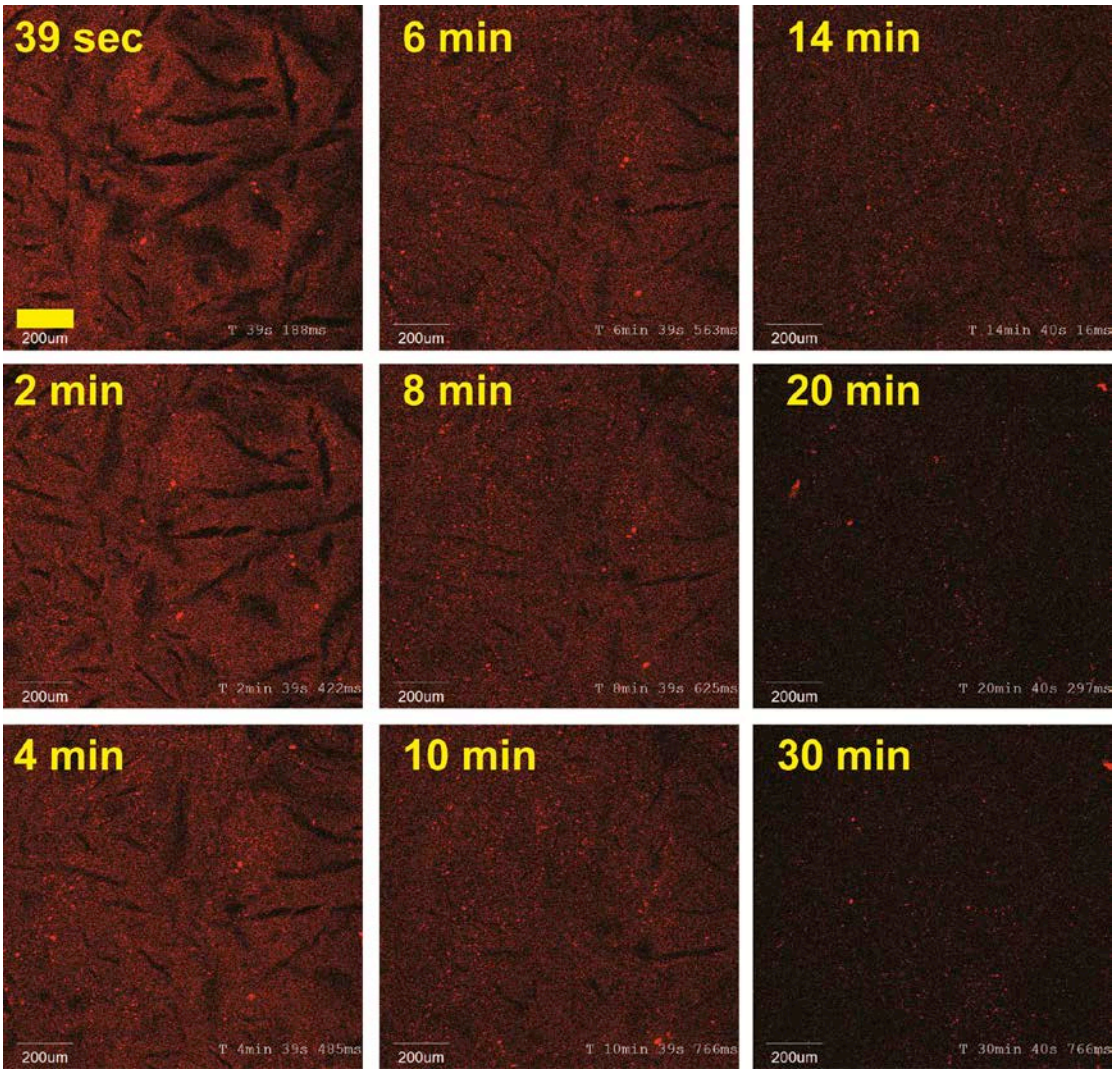

Figure 37. Dynamic observation of sponge cleavage with 10 mM TCEP. Aqueous macroporosity disappears after 30 minute incubation with 10 mM TCEP (scale bar 200 µm)

The intended applications of this cleavable cellulosic sponge were for 3D spheroids culture as well as its cleavability to retrieve the spheroids for further manipulations. This proposed mechanism is show in **figure 38**. During cleavage, disulfide bonds exchanged into thiol bonds, loosen up the crosslinked bond and made

the sponge soluble. The cleavage should only occur on-demand upon adding the disulfide bond reductant.

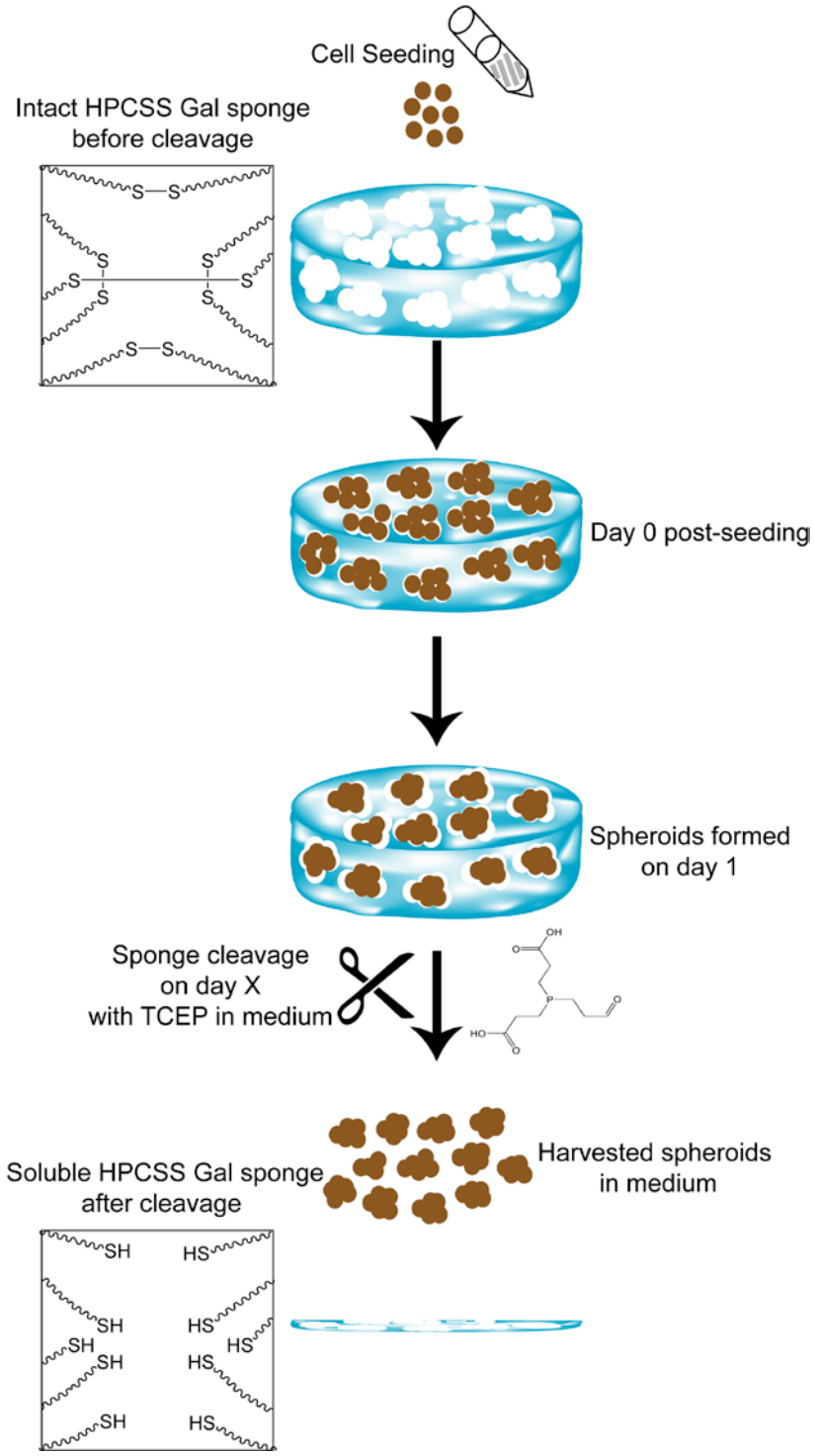

Figure 38. Schematic drawing of cleavable cellulosic sponge cleavage mechanism

5.3.3 Reductant used to cleave the sponge is relatively non-cytotoxic even into sensitive cell type (primary hepatocytes)

The cytotoxicity of TCEP was investigated by incubating TCEP with the associated time needed to completely cleave the sponge; 10 mM in 30 min. Since the application for this cleavable sponge was mainly for primary cell culture, primary rat hepatocyte cultured in collagen monolayer was used in the cytotoxicity study.

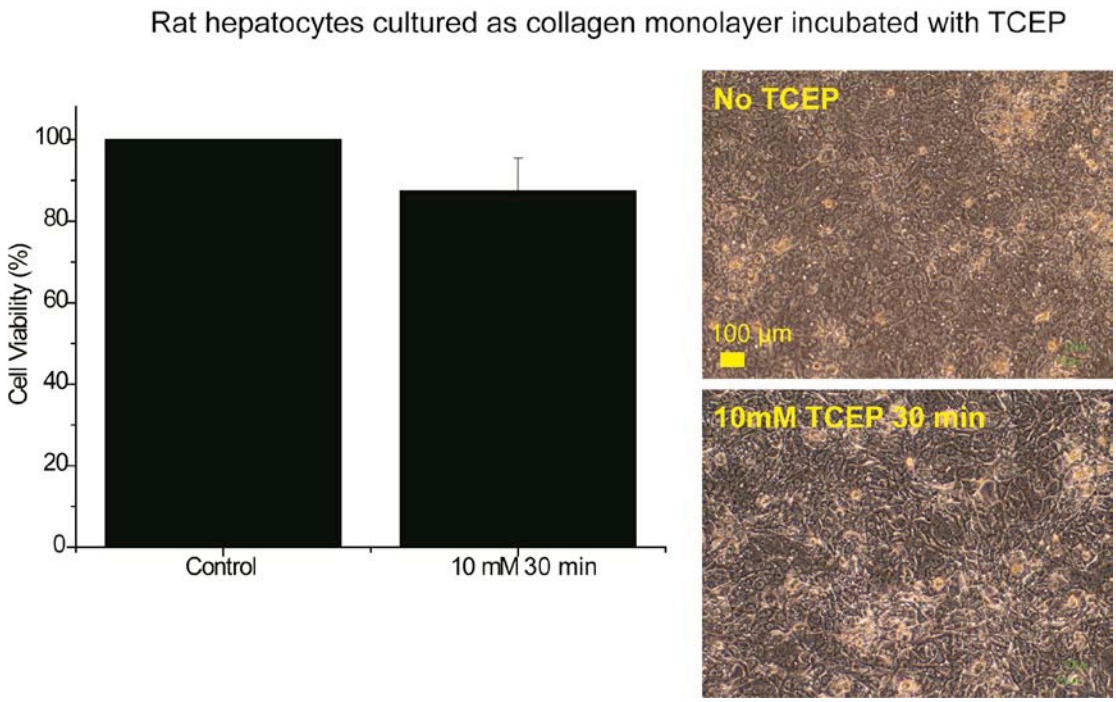

Figure 39. TCEP toxicity in rat hepatocyte indicates good maintenance of cell viability (> 80%) (scale bar 100 µm). Incubation time was determined by the associated time needed to completely cleave the sponge. Data are average ± standard deviation of 3 independent experiments.

As it is shown in **figure 39** left panel, primary rat hepatocyte viability upon 30 minutes incubation of 10 mM TCEP is 87.42 ± 8.03 %. Phase contrast images of hepatocytes with and without TCEP incubation at the right panel clearly show the maintenance of cuboidal cell shape and bile canaliculi-like structure at cell-cell contact. No significant cell damage was observed.

5.3.4 Characterization of the hepatocyte spheroids cultured in cellulosic sponges

5.3.4.1 Primary rat hepatocytes form compact hepatocyte spheroids in the cleavable cellulosic sponge within 24 hours post-seeding

Similarly as it was shown previously in non-cleavable sponge (HA Gal sponge), in cleavable HPCSS Gal sponge, primary rat hepatocytes also immediately reorganized into 3D spheroids within 1 day of culture and remained stable in this configuration until at least day 7 (**figure 40**). Hepatocyte spheroids formed in the HPCSS Gal sponges were 88.77 μm in average diameter. The spheroids formed in HPCSS Gal sponges were constrained in the sponge macropores and thus did not easily detach as those previously shown on 2D PET Gal membranes [80].

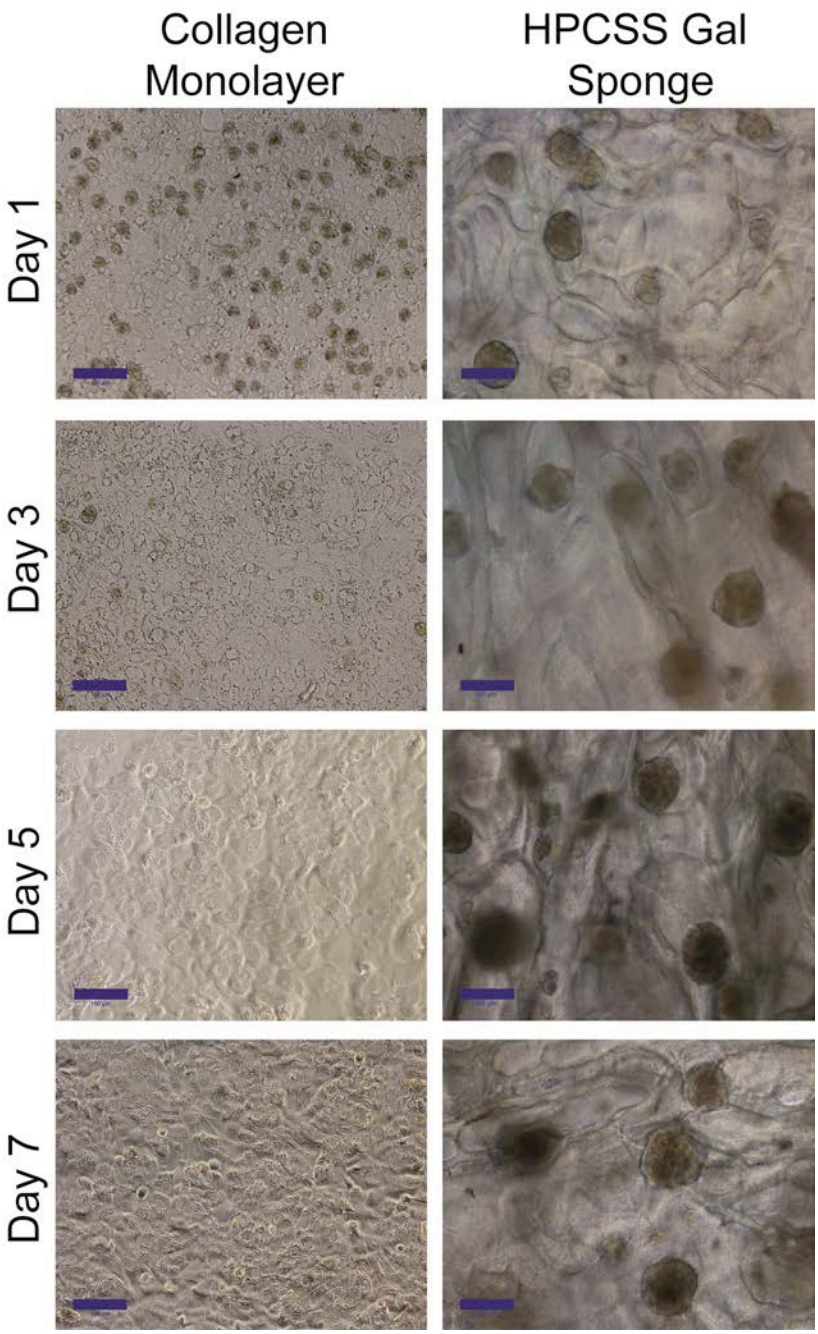

Figure 40. Rat hepatocytes cultured in cleavable HPCSS Gal sponge. Compact spheroids are formed within one day post-seeding (scale bar 100 µm). Average spheroids size on day 1: 75.58 ± 16.61 µm, day 3: 84.68 ±17.64 µm, day 5: 96.95 ± 13.52 µm and day 7: 97.88 ± 11.84 µm (Data are average ± standard deviation of 20 spheroids)

Hepatocyte spheroids viability, which was assessed by co-staining the cells with Cell-Tracker Green (CTG) and Propidium Iodide (PI), showed majority of green signals which revealed good viability maintenance at least 7 days in culture (**figure**

41). The CTG signals illustrated indistinguishable borders between single cells in the spheroids, which reflected the tightness of the cell-cell contacts.

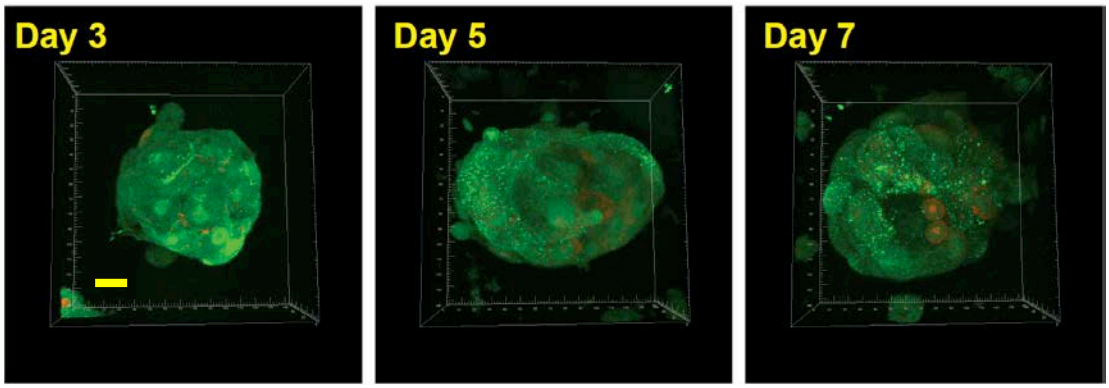

Figure 41. Live/dead staining of rat hepatocyte spheroids in the cleavable sponge (projected spheroid images, scale bar 20 µm)

5.3.4.2 Retrieved hepatocyte spheroids from cleavable cellulosic sponges could be retrieved by cleaving the sponge without imposing cytotoxicity

The effect of sponge cleavage to the characteristics of retrieved spheroid was investigated towards the downstream effects e.g. maintenance of cytochrome P450 genes, polarity marker, tight cell junction, spheroids compactness and bile excretory function. The maintenance of important rat cytochrome P450 genes (CYP1A2, CYP2B2 and CYP3A2) was analyzed based on the effect of TCEP incubation into short term and long term culture/post-replating. Hepatocyte spheroids cultured in non-cleavable sponge (HA Gal sponge) were used as a comparator.

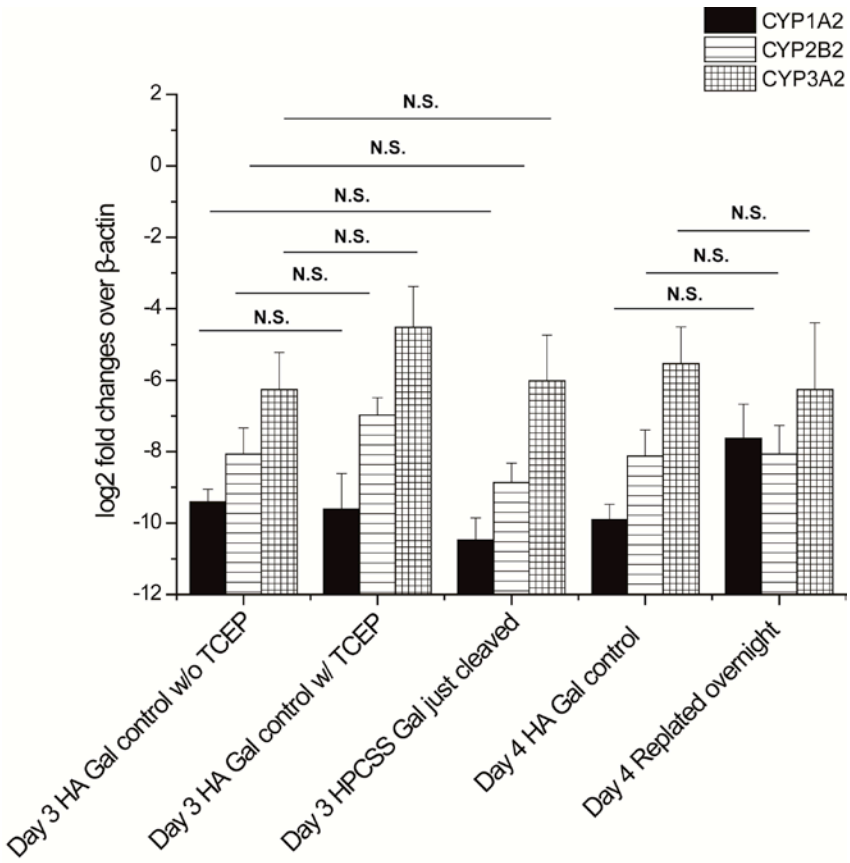

Figure 42. Gene expressions analysis of rat hepatocyte cultured in cleavable HPCSS Gal sponge indicates no significant effect of the incubation of 10 mM TCEP towards CYP450 enzymes. Data are average ± standard error of the mean from 3 independent experiments (N.S.: not significantly different)

Rat hepatocyte spheroids incubation with 10 mM TCEP for 30 minute did not show any significant detrimental effect to the 3 CYP genes (**figure 42**). There was slight drop in the fold expression changes of CYP genes upon cleaving the HPCSS Gal sponge to retrieve the spheroids (~2 fold decrease). However, upon overnight replating these retrieved spheroids on poly-L-lysine coated dish, the spheroids rejuvenated the gene expressions comparable to the spheroids cultured in non-cleavable sponge.

Immunofluorescence staining of F-actin, E-cadherin and MRP2 in the hepatocyte spheroids 72 hours post seeding retrieved from cleavable (HPCSS Gal)

sponges and in non-cleavable (HA Gal) sponge and showed comparable localization of these markers (**figure 43**). As would be expected in non-spreading cells, F-actin staining revealed that the actin cytoskeleton had a predominant cortical localization in the spheroids and an absence of stress fibers. E-cadherin staining, a marker of cell-cell adhesions demonstrated that cells in the hepatocyte spheroids have tight associations between neighbouring cells. MRP2 staining marked the apical domains of the polarized hepatocytes. In MRP2 staining image (**figure 43** rightmost panel), the signals showed a comparable signal as observed in the intact hepatocyte spheroids in the non-cleavable sponge and retrieved spheroids from cleavable sponge.

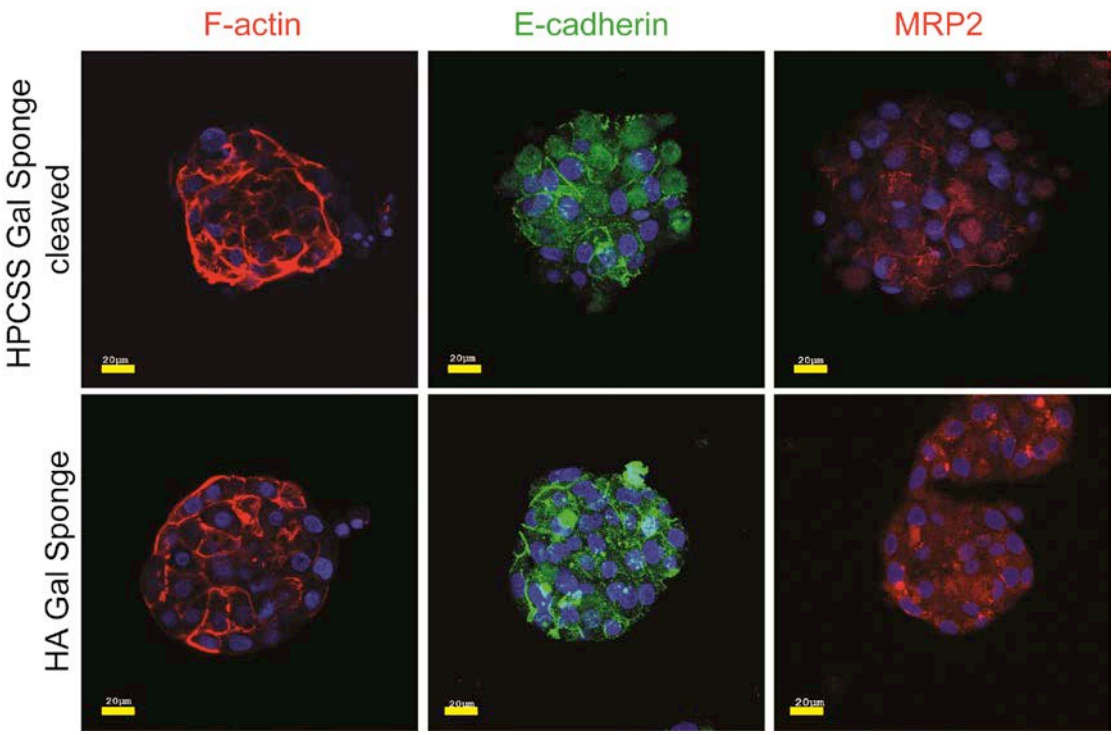

Figure 43. Immunofluorescence staining of polarity markers and cell-cell adhesions of hepatocyte spheroids retrieved from cleavable HPCSS Gal sponge and cultured in non-cleavable HA Gal sponge. The incubation of 10 mM TCEP to cleave the sponge does not show harmful effect to these markers (projected spheroid images, scale bar 20 µm)

Upon confirming the maintenance expression of MRP2 (apical domain marker as well as hepatocyte efflux transporter) in the retrieved spheroids, the excretory

function of these spheroids was studied by incubating the spheroids with fluorescein diacetate (FDA). Viable cells in the spheroids will cleave FDA into fluorosecein dye by intracellular esterases which then be excreted by MRP2 into the bile canaliculi. FDA staining of the retrieved hepatocyte spheroids showed dye accumulation in the bile canaliculi region between the two cells (**figure 44**). This excretion exhibited similarity to what had been observed in the intact hepatocyte spheroids in non-cleavable sponge [80].

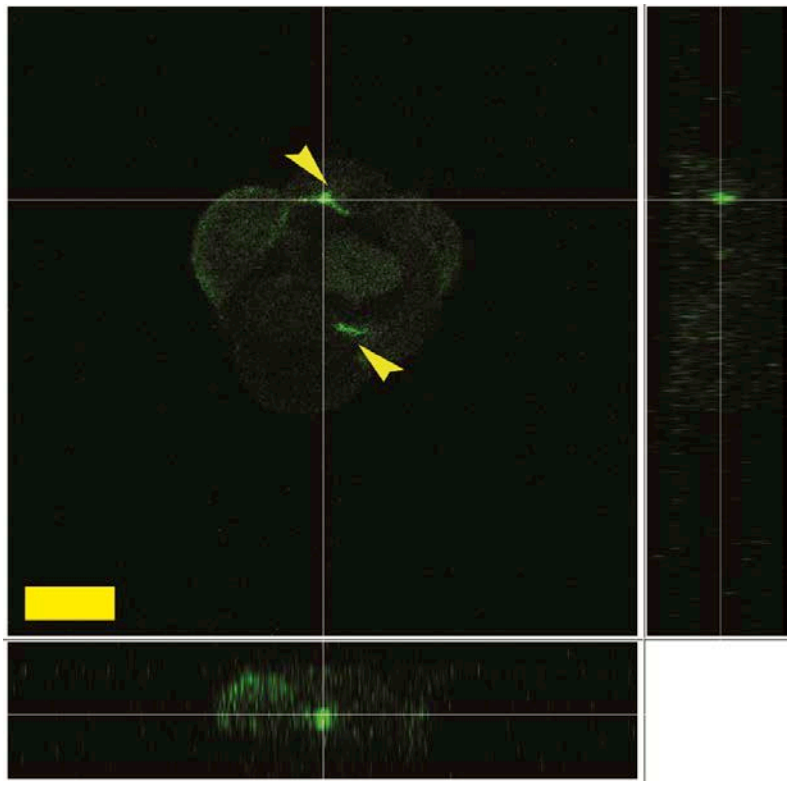

Figure 44. FDA staining of the retrieved rat hepatocyte spheroids from cleavable HPCSS Gal sponge indicates putative accumulation of dye at the bile canaliculi region (projected spheroid images, scale bar 20 μm)

The maintenance of spheroids compact morphology upon retrieving was again confirmed by SEM. The retrieved hepatocyte spheroids still showed surface smoothness and disappearance of the cell-cell boundaries, compared to the spheroids cultured in non cleavable sponge (**figure 45**).

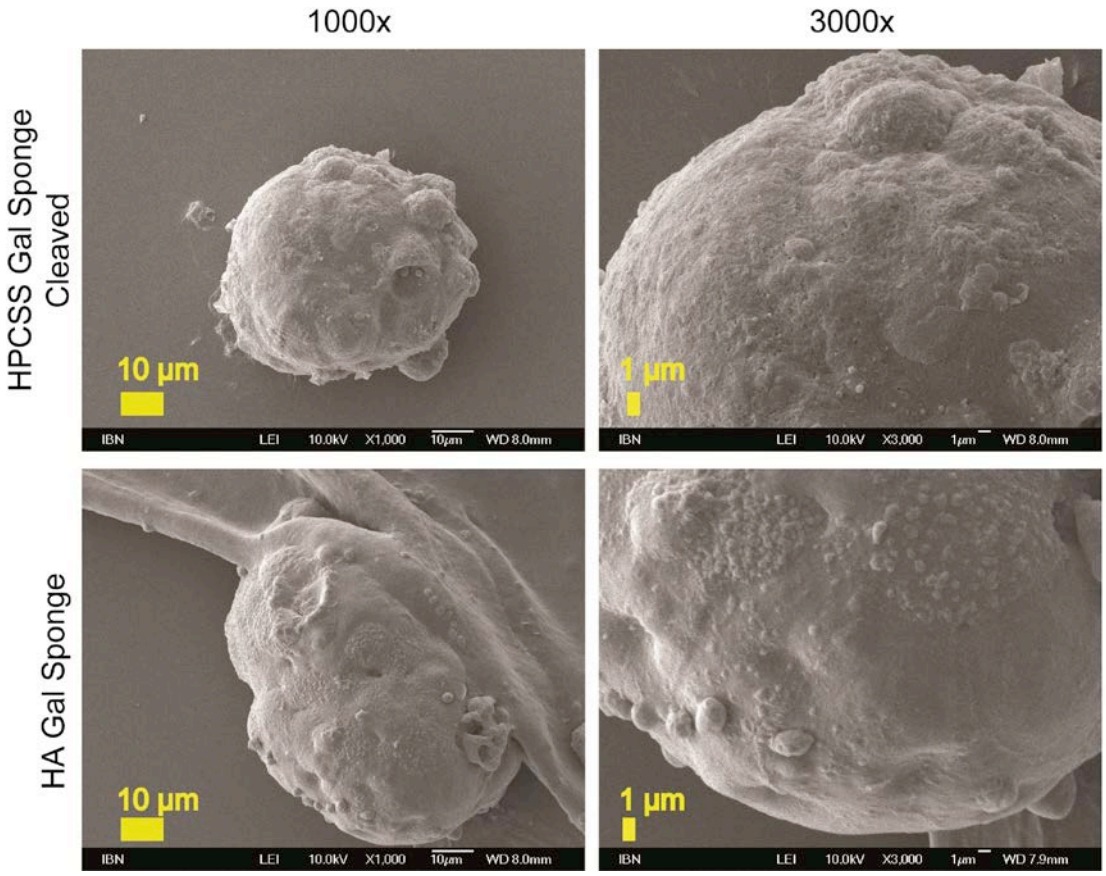

Figure 45. Comparison of rat hepatocyte spheroids SEM images obtained from both cleavable HPCSS Gal sponge and non-cleavable HA Gal sponge indicates no surface morphology difference

5.3.4.3 Retrieved hepatocyte spheroids show replatability and easy manipulation

The applicability of the retrieved spheroids obtained by cleaving the sponge was demonstrated by replating the spheroids on two different kinds of coated dishes; collagen and poly-L-lysine-coated dishes. These two kinds of coated dishes theoretically will either induce spheroids spreading or prevent spheroids spreading, respectively.

Upon spheroids replating on collagen coated dish, the spheroids settled on the bottom of the dish within 1 hour. 4 hours post-replating, the spreading pattern of the spheroids was clearly observed at the spheroids periphery (**figure 46**). And 16 hours later, the spheroids had exhibited an almost complete spreading. Some cells in the

spheroids core did not manage to spread on the collagen gel possibly due to hindrance imposed by cells beneath them. Cells which were spreading out of the spheroids showed the clear bile canaliculi-like structure at the cell-cell boundary, which was normally seen on hepatocyte collagen monolayer culture.

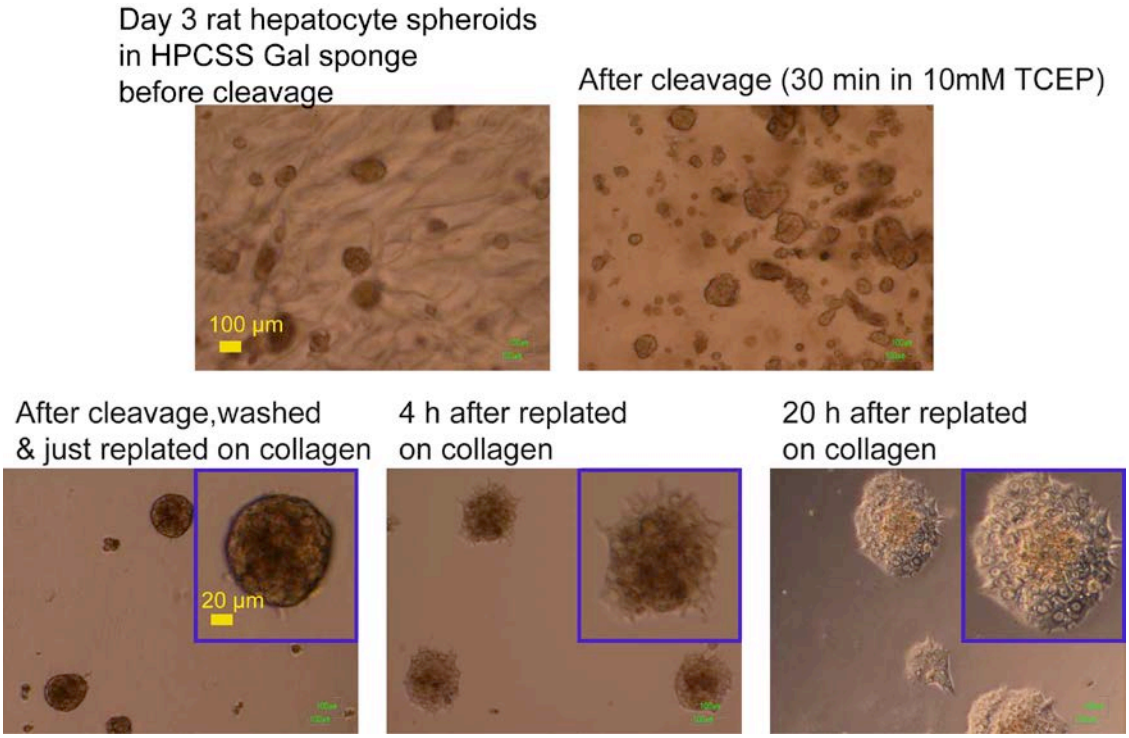

Figure 46. Retrieved rat hepatocyte spheroids replated on collagen dish show the ability to spread (insert image is the zoomed in view of the spheroid)

Instead of allowing the spheroids to spread, the spheroids compact morphology could be maintained for extended period by replating them on poly-L-lysine coated dish. Positively charged polymer such as poly-L-lysine has been known to anchor hepatocyte spheroids but prevent spheroid spreading [248]. When the hepatocyte spheroids were retrieved and replated on poly-L-lysine coated dish, the spheroids settled at the bottom of the dish and remained as intact round spheroids (**figure 47** upper panel). The spheroids also showed good cell viability upon replating (projected spheroid images, **figure 47** lower panel).

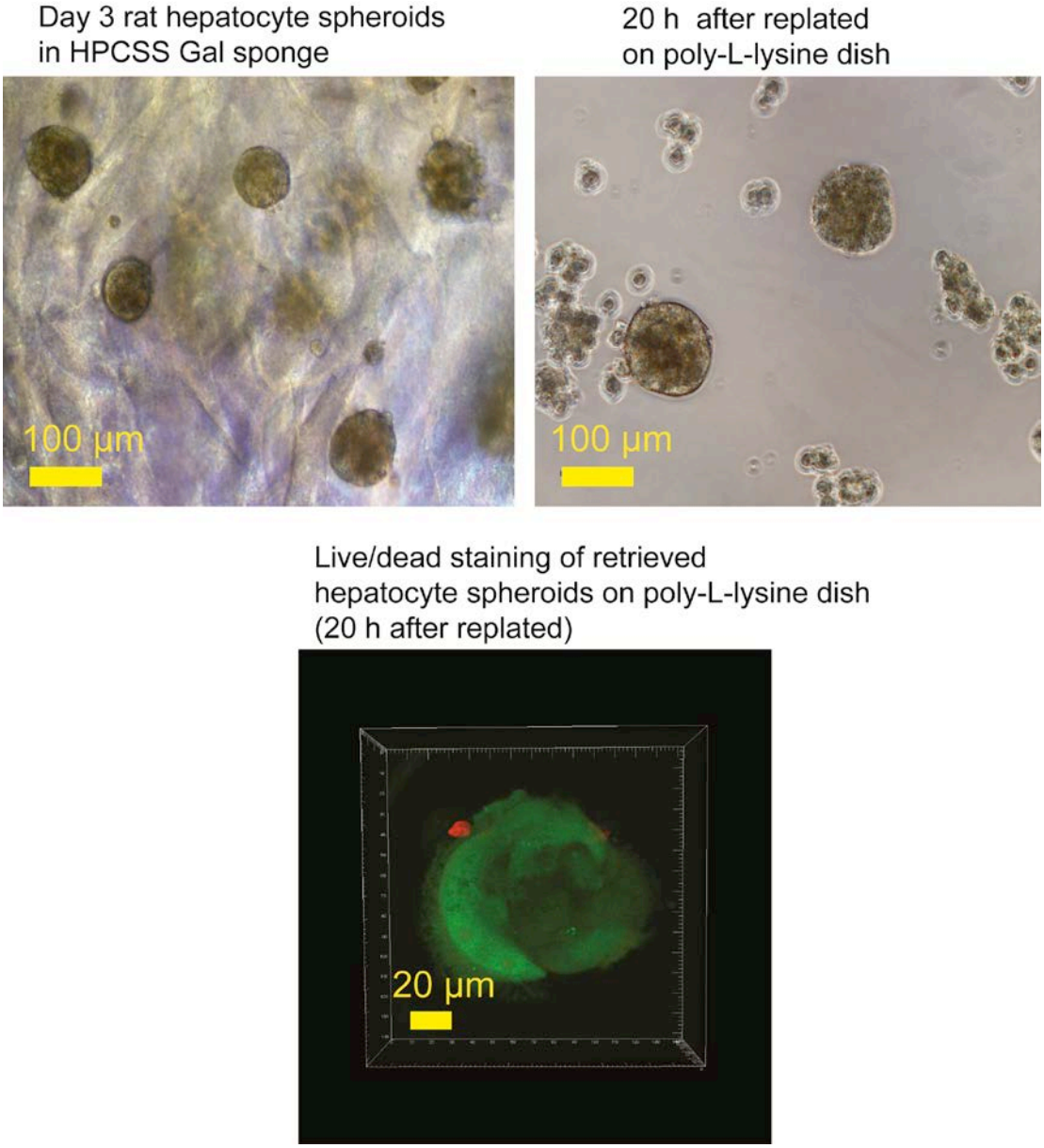

Figure 47. Retrieved hepatocyte spheroids can also be replated on poly-L-lysine dish to prevent spheroids from spreading (lower panel is the projected spheroid images)

5.4 Discussion

We have conjugated disulfide bonds onto side chain group of hydroxypropyl cellulose to create cleavable hydrogel-based sponge. This strategy has shown successful rapid and easy cleavage of cellulosic sponge without hindering the ability of hydroxypropyl cellulose to be crosslinked by γ irradiation and formed macroporous

sponge. The sponge is fabricated without chemical cross-linkers, yet cross-linked through stable chemical bonds [15]. Made of a water soluble precursor, our cleavable cellulosic hydrogel sponges are very hydrophilic thus acting as a non-adhesive matrix and preventing cell spreading, which is important for maintenance of the mature hepatocyte phenotype [181].

The sponge was also easy to be galactosylated for specific hepatocyte culture application. Unlike other hydrogels, the macroporous networks in our cellulosic sponge support the *in situ* formation and maintenance of polarized hepatocyte spheroids [33, 199, 200]. The cellulosic sponge, which acts as a hepatocyte substratum anchor, did not prevent cell aggregation, as would normally happen in cell culture hydrogel with excessive extracellular matrix presentation [201]. The galactose presented chemical cues to the hepatocytes to reorganize into 3D spheroids within 1 day post-seeding, while the macroporous structure constrained them physically. Since the galactose ligand only interacts weakly with ASGPR receptors in the hepatocyte cell membrane [175], it is the combination of the physical and chemical cues in the sponge which is important in establishing stable constrained hepatocyte spheroids.

The cleavable sponge still exhibited soft hydrogel mechanical stiffness characteristic ($E \approx 30$ kPa) with excellent water uptake (> 95%) despite the alteration of side chain chemistry with disulfide bond. Excellent sponge water uptake combined with sponge durable macroporosity had helped in rapid solution exchange when the sponge was incubated with reductant solution, thus induced rapid sponge cleavage. Unlike other disulfide-containing hydrogels which need longer reductant incubation, our cleavable cellulosic sponge showed complete cleavage within 30 minute with

comparable reductant concentration used [240]. We thus ensured short exposure of the cells to reductant solution.

Hepatocytes cultured as 3D spheroids in the cleavable cellulosic sponge were constrained within sponge macroporosity. They exhibited maintenance of cell viability for at least 7 days in culture. When these spheroids were retrieved from the sponge through cleavage, important drug metabolizing enzymes, CYP1A2, CYP2B2 and CYP3A2, were not affected by TCEP used for cleaving the sponge and the enzymes expressed were comparable to the hepatocyte spheroids cultured in the non-cleavable comparator sponge. In addition, polarity marker (cortical F-actin), tight cell-cell adhesions, apical hepatocyte marker (MRP2), biliary excretory function and spheroid compact morphology were not affected by the cleavage process.

Upon retrieval, hepatocyte spheroids showed facile manipulations towards replatable living spheroids either on collagen coated or poly-L-lysine coated dishes. On collagen dish, the spheroids started to settle and spread within 20 hours post-replating, with clear bile canaliculi-like appearance at the cell-cell boundary. While on positively charge surface, poly-L-lysine dish, the spheroids maintained as compact spheroids without visible spheroids spreading. The cell viability was well maintained after overnight replating. Overall, our cleavable cellulosic sponge provided the facile hydrogel-based sponge platform to culture primary rat hepatocytes as 3D spheroids with the ease of spheroids retrieval through non-cytotoxic sponge cleavage.

5.5 Conclusion

We have synthesized and fabricated a cleavable macroporous cellulosic hydrogel sponge conjugated with galactose as a platform to culture primary rat hepatocytes as 3D spheroids with the ability to retrieve the spheroids at physiological condition. Hepatocyte spheroids retrieval is performed through rapid non-cytotoxic sponge cleavage. The soft macroporous structure of cleavable cellulosic sponge conjugated with galactose facilitates the formation of hepatocyte spheroids by presenting both the mechanical cues (via matrix rigidity) and chemical cues for the hepatocytes to reorganise into 3D spheroids within 24 hours post-seeding. The constrained hepatocyte spheroids maintain cell viability for at least a week of culture. Upon spheroids retrieval through sponge cleavage, polarized hepatocyte phenotypes are well maintained; drug metabolizing enzymes (CYP1A2, CYP2B2 and CYP3A2), polarity marker (cortical F-actin), tight cell-cell adhesions, apical hepatocyte domain marker (MRP2), biliary excretory function, spheroid compact morphology and cell viability. The living retrieved spheroids are replatable on both collagen coated and poly-L-lysine coated dishes for further use. As many of tissue engineering-related researches require temporary synthetic scaffold matrix such as stem cell differentiation and *in vitro* organoid and thick tissue culture, this technology offers useful platform to culture cells as 3D spheroid construct with easy, rapid and physiological removal of bulk synthetic sponge.

CHAPTER 6

CONCLUSION AND DIRECTION FOR FUTURE INVESTIGATIONS

6.1 Conclusion

This thesis has covered the development progress of the macroporous cellulosic sponge made of cellulose derivative, hydroxypropyl cellulose, as novel multi-well format 3D hepatocyte culture platform and its applications in drug safety testing and HCV entry study. The last part of this development covers the latest generation of the cellulosic sponge towards cleavable sponge as 3D hepatocyte culture platform with spheroids retrieval capability.

Primary rat hepatocyte reorganized into compact spheroids within 7 hours post-seeding in the galactosylated cellulosic sponge and exhibited excretory function within 16 hours. The spheroids were constrained in the sponge macroporosity over extended culture. These constrained hepatocyte spheroids maintain cell viability, cell polarity markers, and 3D cell morphology. These correlated with enhanced hepatocyte-specific functions and expression of drug metabolic enzymes and drug transporters. Hepatocyte spheroids grown in the sponge also show inducibility of various drug metabolizing enzymes including CYP1A2, CYP2B2 and CYP3A1. The sponge has comparable or lower drug absorbency compared to other cell culture platforms. Importantly, sponge fabrication is amenable for large-scale production and high-throughput screening. Cell seeding into the sponge involves simple steps similar to high-throughput 2D cell cultures.

Similarly, primary human hepatocyte and Huh 7.5 spheroids were formed in the sponge within 24 hours post-seeding and constrained in the sponge macroporosity for prolonged culture. The size of the spheroids was maintained within mass transfer barrier-free range. Spheroids viability was well maintained up to 5 and 2 weeks for human hepatocyte and Huh 7.5, respectively. The compact spheroids morphology was observed at least up to 2 weeks of culture. Compact spheroids morphology correlated well with gene expression showing minimal dedifferentiation of human hepatocyte spheroids and upregulation of mature hepatocyte genes in Huh 7.5 spheroids. Both types of spheroids expressed liver polarity markers and HCV entry markers. When these spheroids were inoculated with HCVpp, an available *in vitro* model to study HCV entry, ~80% of the spheroids were infected with HCVpp distributed throughout whole spheroids region. These spheroids had also shown the ability to be infected at prolonged culture indicating the maintenance of HCV entry markers. By co-incubating both types of spheroids with HCVpp and CD81 antibody, HCVpp entry was inhibited at dose-dependent manner. Together, this spheroids model provides a useful platform to study HCV entry and inhibition *in vitro* and to screen HCV antiviral candidates.

Lastly, we have demonstrated the usefulness of hydroxypropyl cellulose chemical versatility towards functionalization with reducible disulfide bond to design a cleavable cellulosic sponge. We have synthesized and fabricated a cleavable macroporous cellulosic hydrogel sponge conjugated with galactose as a platform to culture primary rat hepatocytes as 3D spheroids with the ability to retrieve the spheroids at physiological condition. Hepatocyte spheroids retrieval was performed through rapid non-cytotoxic sponge cleavage. The soft macroporous structure of

cleavable cellulosic sponge conjugated with galactose facilitated the formation of hepatocyte spheroids by presenting both the mechanical cues (via matrix rigidity) and chemical cues for the hepatocytes to reorganise into 3D spheroids within 24 hours post-seeding. The constrained hepatocyte spheroids maintained cell viability for at least a week of culture. Upon spheroids retrieval through sponge cleavage, polarized hepatocyte phenotypes were well maintained; drug metabolizing enzymes (CYP1A2, CYP2B2 and CYP3A2), polarity marker (cortical F-actin), tight cell-cell adhesions, apical hepatocyte domain marker (MRP2), biliary excretory function, spheroid compact morphology and cell viability. The living retrieved spheroids were replatable on both collagen coated and poly-L-lysine coated dishes for further use. As many of tissue engineering-related researches require temporary synthetic scaffold matrix such as stem cell differentiation and *in vitro* organoid and thick tissue culture, this technology offers useful platform to culture cells as 3D spheroid construct with easy, rapid and physiological removal of bulk synthetic sponge.

Altogether, we have generated a novel class of hydrogel-based macroporous sponge for 3D hepatocyte-based applications in specific and for other soft tissue cultures in general. This sponge provides a relatively easy-to-synthesize, economic and amenable platform to be fabricated in large scale. Cell seeding is rather easy with possible manipulation towards robotic liquid handler-assisted seeding.

6.2 Direction for future investigations

Future directions for further investigations utilizing this sponge as 3D cell culture model will be firstly to further improve the sponge design and cell seeding

technique. The solution to improve current cell loading upon seeding needs to be thought. A possible way is to create leak-proof sponge by coating additional gel on the outer surface of the sponge. A thorough investigation on the effect of sponge thickness to the penetration depth of the seeded cells will be useful, since the current sponge design thickness was not varied. And cell seeding using robotic liquid handler-seeding also can improve the cell seeding variation into large number of sponges for vast multi-well assays and less time consuming experiments.

Secondly for drug safety testing usage of this sponge, since the hepatocyte spheroids could be cultured for prolonged period, it will be interesting to use this model as a chronic liver injury model which is normally challenged by the conventional 2D hepatocyte culture.

Thirdly for HCV infection study, thorough investigation on HCV replication in primary human hepatocyte and Huh 7.5 spheroids in the prolonged culture is necessary. Since these spheroids are able to maintain the differentiated phenotypes for extended period, it will be interesting to observe if HCV could propagate and infect persistently in the spheroids. The persistence HCV infection becomes critical to study HCV transmission from infected cell to naïve cell. This study is currently being performed at Roche Nutley.

Fourthly, the cell source issue also needs to be investigated. The cells used in this thesis were mainly primary cells; however it has been discussed in chapter 2 that primary cells face many limitation and scarceness. Experiments using readily available and commercial cells such as stem cells-derived hepatocytes will be exciting to get more reproducible data.

And lastly the cleavable sponge utility could still bring further extensive investigation towards several other researches such as a) *in vivo* culture of cell-seeded cleavable sponge. Since this sponge is cleavable by reductants, it will be interesting to observe how sponge cleavage occurs in the body naturally (body contains some amounts of natural reductants), b) 3D culture of cancer cells with the retrieval of tumor spheroids as engineered tumor model to study cancer metastasis *in vitro* or *in vivo* and c) sponge mechanical stiffness tunability by its cleavage is useful to study mechanical stiffness influences towards stem cell differentiation lineage. Sponge mechanical stiffness can be simply varied by cleaving the sponge at various degree of completion thus useful as cell culture substratum with a wide range of mechanical stiffness.

References

[1] Gautier A, Carpentier B, Dufresne M, Vu Dinh Q, Paullier P, Legallais C. Impact of alginate type and bead diameter on mass transfers and the metabolic activities of encapsulated C3A cells in bioartificial liver applications. European cells & materials. 2011;21:94-106.
[2] Xia L, Ng S, Han R, Tuo X, Xiao G, Leo HL, et al. Laminar-flow immediate-overlay hepatocyte sandwich perfusion system for drug hepatotoxicity testing. Biomaterials. 2009;30:5927-36.
[3] Ploss A, Khetani SR, Jones CT, Syder AJ, Trehan K, Gaysinskaya VA, et al. Persistent hepatitis C virus infection in microscale primary human hepatocyte cultures. Proceedings of the National Academy of Sciences of the United States of America. 2010;107:3141-5.
[4] Molina-Jimenez F, Benedicto I, Dao Thi VL, Gondar V, Lavillette D, Marin JJ, et al. Matrigel-embedded 3D culture of Huh-7 cells as a hepatocyte-like polarized system to study hepatitis C virus cycle. Virology. 2012;425:31-9.
[5] Pampaloni F, Reynaud EG, Stelzer EH. The third dimension bridges the gap between cell culture and live tissue. Nature reviews Molecular cell biology. 2007;8:839-45.
[6] Liu X, Won Y, Ma PX. Surface modification of interconnected porous scaffolds. Journal of biomedical materials research Part A. 2005;74:84-91.
[7] Gutsche AT, Lo H, Zurlo J, Yager J, Leong KW. Engineering of a sugar-derivatized porous network for hepatocyte culture. Biomaterials. 1996;17:387-93.
[8] Hollister SJ. Porous scaffold design for tissue engineering. Nature materials. 2005;4:518-24.
[9] Chua KN, Tang YN, Quek CH, Ramakrishna S, Leong KW, Mao HQ. A dual-functional fibrous scaffold enhances P450 activity of cultured primary rat hepatocytes. Acta biomaterialia. 2007;3:643-50.
[10] Hurtado A, Moon LD, Maquet V, Blits B, Jerome R, Oudega M. Poly (D,L-lactic acid) macroporous guidance scaffolds seeded with Schwann cells genetically modified to secrete a bi-functional neurotrophin implanted in the completely transected adult rat thoracic spinal cord. Biomaterials. 2006;27:430-42.
[11] Drury JL, Mooney DJ. Hydrogels for tissue engineering: scaffold design variables and applications. Biomaterials. 2003;24:4337-51.
[12] Kevin A. Heitfeld TG, George Yang, Dale W. Schaefer. Temperature responsive hydroxypropyl cellulose for encapsulation. Materials Science and Engineering C. 2008;28:374-9.
[13] Delia Lopez-Velazquez AB, Ernesto Perez. Preparation and Characterisation of Hydrophobically Modified Hydroxypropylcellulose:Side-chain Crystallization. Macromolecular chemistry and physics. 2004;205:1886-92.
[14] Zhibing Hu XL, Jun Gao, Changjie Wang. Polymer Gel Nanoparticle Networks. Advanced Materials. 2000;12:1173-6.
[15] Yue Z, Wen F, Gao S, Ang MY, Pallathadka PK, Liu L, et al. Preparation of three-dimensional interconnected macroporous cellulosic hydrogels for soft tissue engineering. Biomaterials. 2010;31:8141-52.
[16] Fundueanu G, Constantin M, Esposito E, Cortesi R, Nastruzzi C, Menegatti E. Cellulose acetate butyrate microcapsules containing dextran ion-exchange resins as self-propelled drug release system. Biomaterials. 2005;26:4337-47.

[17] Alessandro Sannino CD, Marta Madaghiele. Biodegradable Cellulose-based Hydrogels: Design and Applications. Materials. 2009;2:353-73.
[18] Vueba ML, Batista de Carvalho LA, Veiga F, Sousa JJ, Pina ME. Influence of cellulose ether mixtures on ibuprofen release: MC25, HPC and HPMC K100M. Pharmaceutical development and technology. 2006;11:213-28.
[19] Ostmark E, Lindqvist J, Nystrom D, Malmstrom E. Dendronized hydroxypropyl cellulose: synthesis and characterization of biobased nanoobjects. Biomacromolecules. 2007;8:3815-22.
[20] Muller FA, Muller L, Hofmann I, Greil P, Wenzel MM, Staudenmaier R. Cellulose-based scaffold materials for cartilage tissue engineering. Biomaterials. 2006;27:3955-63.
[21] Miyamoto T, Takahashi S, Ito H, Inagaki H, Noishiki Y. Tissue biocompatibility of cellulose and its derivatives. Journal of biomedical materials research. 1989;23:125-33.
[22] Prause JU. Treatment of keratoconjunctivitis sicca with Lacrisert. Scandinavian journal of rheumatology Supplement. 1986;61:261-3.
[23] Palakuru JR, Wang J, Aquavella JV. Effect of blinking on tear volume after instillation of midviscosity artificial tears. American journal of ophthalmology. 2008;146:920-4.
[24] Chua KN, Lim WS, Zhang P, Lu H, Wen J, Ramakrishna S, et al. Stable immobilization of rat hepatocyte spheroids on galactosylated nanofiber scaffold. Biomaterials. 2005;26:2537-47.
[25] Abu-Absi SF, Friend JR, Hansen LK, Hu WS. Structural polarity and functional bile canaliculi in rat hepatocyte spheroids. Experimental cell research. 2002;274:56-67.
[26] Ong SM, He L, Thuy Linh NT, Tee YH, Arooz T, Tang G, et al. Transient inter-cellular polymeric linker. Biomaterials. 2007;28:3656-67.
[27] Baraniak PR, McDevitt TC. Scaffold-free culture of mesenchymal stem cell spheroids in suspension preserves multilineage potential. Cell and tissue research. 2012;347:701-11.
[28] Fischbach C, Chen R, Matsumoto T, Schmelzle T, Brugge JS, Polverini PJ, et al. Engineering tumors with 3D scaffolds. Nature methods. 2007;4:855-60.
[29] Curcio E, Salerno S, Barbieri G, De Bartolo L, Drioli E, Bader A. Mass transfer and metabolic reactions in hepatocyte spheroids cultured in rotating wall gas-permeable membrane system. Biomaterials. 2007;28:5487-97.
[30] Slaughter BV, Khurshid SS, Fisher OZ, Khademhosseini A, Peppas NA. Hydrogels in regenerative medicine. Adv Mater. 2009;21:3307-29.
[31] Del Duca D, Werbowetski T, Del Maestro RF. Spheroid preparation from hanging drops: characterization of a model of brain tumor invasion. Journal of neuro-oncology. 2004;67:295-303.
[32] Wu FJ, Friend JR, Remmel RP, Cerra FB, Hu WS. Enhanced cytochrome P450 IA1 activity of self-assembled rat hepatocyte spheroids. Cell transplantation. 1999;8:233-46.
[33] Kim M, Lee JY, Jones CN, Revzin A, Tae G. Heparin-based hydrogel as a matrix for encapsulation and cultivation of primary hepatocytes. Biomaterials. 2010;31:3596-603.
[34] Du Y, Han R, Wen F, Ng San San S, Xia L, Wohland T, et al. Synthetic sandwich culture of 3D hepatocyte monolayer. Biomaterials. 2008;29:290-301.

[35] Seymour LW, Ferry DR, Anderson D, Hesslewood S, Julyan PJ, Poyner R, et al. Hepatic drug targeting: phase I evaluation of polymer-bound doxorubicin. Journal of clinical oncology : official journal of the American Society of Clinical Oncology. 2002;20:1668-76.
[36] Liver health. http://www.nutrilligence.com/programs/liver_health1.html
[37] Liver structure (anatomy of the liver and biliary tracts). http://www.healthlln.com/2012/01/liver-structure-anatomy-of-liver-and.html
[38] R. B. Cytochromes P450 as versatile biocatalysts. Journal of Biotechnology. 2006;124:128-45.
[39] Liver cells. http://medical-helpful-info.blogspot.ch/2011/04/liver-cells.html
[40] Gumucio JJ B, C. M., Webster, S. T., Thornton, A. J. Structural and functional organisation of the liver. Liver and Biliary Diseases. 1996:3-19.
[41] Wilkening S, Stahl F, Bader A. Comparison of primary human hepatocytes and hepatoma cell line Hepg2 with regard to their biotransformation properties. Drug metabolism and disposition: the biological fate of chemicals. 2003;31:1035-42.
[42] Yanan D. Identification and stabilization of a novel 3D hepatocyte monolayer for hepatocyte-based applications. Singapore: National University of Singapore; 2008.
[43] Greenwel P RM. The extracellular matrix of the liver. In: In Arias IM BJ, Chisari FV, editor. The Liver: Biology and Pathobiology 4th ed: Philadelphia: Lippincott Williams & Wilkins; 2001.
[44] Anantharaju A, Van Thiel DH. Liver transplantation for alcoholic liver disease. Alcohol research & health : the journal of the National Institute on Alcohol Abuse and Alcoholism. 2003;27:257-68.
[45] Allen JW, Hassanein T, Bhatia SN. Advances in bioartificial liver devices. Hepatology. 2001;34:447-55.
[46] Tan HK. Molecular adsorbent recirculating system (MARS). Annals of the Academy of Medicine, Singapore. 2004;33:329-35.
[47] Hillebrand DJ, Hill KB, Hu KQ, Strutt M, Wilson B, Cottrell A, et al. Formal heparin anticoagulation protocol improves safety of charcoal-based liver-assist treatments. ASAIO J. 2006;52:334-42.
[48] Sechser A, Osorio J, Freise C, Osorio RW. Artificial liver support devices for fulminant liver failure. Clinics in liver disease. 2001;5:415-30.
[49] Sharma NS, Nagrath D, Yarmush ML. Adipocyte-derived basement membrane extract with biological activity: applications in hepatocyte functional augmentation in vitro. FASEB journal : official publication of the Federation of American Societies for Experimental Biology. 2010;24:2364-74.
[50] Dunn JC, Tompkins RG, Yarmush ML. Long-term in vitro function of adult hepatocytes in a collagen sandwich configuration. Biotechnology progress. 1991;7:237-45.
[51] Uyama S, Kaufmann PM, Takeda T, Vacanti JP. Delivery of whole liver-equivalent hepatocyte mass using polymer devices and hepatotrophic stimulation. Transplantation. 1993;55:932-5.
[52] Vosough M, Moslem M, Pournasr B, Baharvand H. Cell-based therapeutics for liver disorders. British medical bulletin. 2011;100:157-72.
[53] Kuppan P, Vasanthan KS, Sundaramurthi D, Krishnan UM, Sethuraman S. Development of poly(3-hydroxybutyrate-co-3-hydroxyvalerate) fibers for skin tissue engineering: effects of topography, mechanical, and chemical stimuli. Biomacromolecules. 2011;12:3156-65.

[54] Liu WF, Chen CS. Cellular and multicellular form and function. Advanced drug delivery reviews. 2007;59:1319-28.
[55] Prokop A. Bioartificial organs in the twenty-first century: nanobiological devices. Annals of the New York Academy of Sciences. 2001;944:472-90.
[56] A G. Liver cell models in in vitro toxicology. Environmental Health Perspectives. 1998;106:511-32.
[57] Khong YM, Zhang J, Zhou S, Cheung C, Doberstein K, Samper V, et al. Novel intra-tissue perfusion system for culturing thick liver tissue. Tissue engineering. 2007;13:2345-56.
[58] Rabkin E, Schoen FJ. Cardiovascular tissue engineering. Cardiovascular pathology : the official journal of the Society for Cardiovascular Pathology. 2002;11:305-17.
[59] Ying L, Yin C, Zhuo RX, Leong KW, Mao HQ, Kang ET, et al. Immobilization of galactose ligands on acrylic acid graft-copolymerized poly(ethylene terephthalate) film and its application to hepatocyte culture. Biomacromolecules. 2003;4:157-65.
[60] Seo SJ, Choi YJ, Akaike T, Higuchi A, Cho CS. Alginate/galactosylated chitosan/heparin scaffold as a new synthetic extracellular matrix for hepatocytes. Tissue engineering. 2006;12:33-44.
[61] Kinasiewicz A, Dudzinski K, Chwojnowski A, Werynski A, Kawiak J. Three-dimensional culture of hepatocytes on spongy polyethersulfone membrane developed for cell transplantation. Transplantation proceedings. 2007;39:2914-6.
[62] Park TG. Perfusion culture of hepatocytes within galactose-derivatized biodegradable poly(lactide-co-glycolide) scaffolds prepared by gas foaming of effervescent salts. Journal of biomedical materials research. 2002;59:127-35.
[63] Park KH, Bae YH. Phenotype of hepatocyte spheroids in Arg-GLY-Asp (RGD) containing a thermo-reversible extracellular matrix. Bioscience, biotechnology, and biochemistry. 2002;66:1473-8.
[64] Wu C, Pan J, Bao Z, Yu Y. Fabrication and characterization of chitosan microcarrier for hepatocyte culture. Journal of materials science Materials in medicine. 2007;18:2211-4.
[65] Wen YA, Liu D, Xiao YY, Luo D, Dong YF, Zhang LP. Enhanced glucose synthesis in three-dimensional hepatocyte collagen matrix. Toxicology in vitro : an international journal published in association with BIBRA. 2009;23:744-7.
[66] Underhill GH, Chen AA, Albrecht DR, Bhatia SN. Assessment of hepatocellular function within PEG hydrogels. Biomaterials. 2007;28:256-70.
[67] Vasanthan KS, Subramanian A, Krishnan UM, Sethuraman S. Role of biomaterials, therapeutic molecules and cells for hepatic tissue engineering. Biotechnology advances. 2012;30:742-52.
[68] Mohammad Morad Farajollahi SH, Ahmad Mehdipour, Ali Samadikuchaksaraei. Recombinant Proteins: Hopes for Tissue Engineering. BioImpacts. 2012;2:123-5.
[69] R. Ian Freshney GNS, Jonathan M. Auerbach. Culture of Human Stem Cells: John Wiley & Sons; 2007.
[70] Mohan N, Nair PD. A synthetic scaffold favoring chondrogenic phenotype over a natural scaffold. Tissue engineering Part A. 2010;16:373-84.
[71] Susan A. Visser RWHaSLC. Biomaterials Science: An Introduction to Materials in Medicine: Elsevier; 1997.
[72] Chen G UT, Tateishi T. Scaffold design for tissue engineering. Macromolecular Bioscience. 2002;2:67-77.

[73] Dixit V, Darvasi R, Arthur M, Brezina M, Lewin K, Gitnick G. Restoration of liver function in Gunn rats without immunosuppression using transplanted microencapsulated hepatocytes. Hepatology. 1990;12:1342-9.
[74] Mitaka T. The current status of primary hepatocyte culture. International journal of experimental pathology. 1998;79:393-409.
[75] Weigel PH, Schmell E, Lee YC, Roseman S. Specific adhesion of rat hepatocytes to beta-galactosides linked to polyacrylamide gels. The Journal of biological chemistry. 1978;253:330-3.
[76] Cho CS, Seo SJ, Park IK, Kim SH, Kim TH, Hoshiba T, et al. Galactose-carrying polymers as extracellular matrices for liver tissue engineering. Biomaterials. 2006;27:576-85.
[77] Lopina ST, Wu G, Merrill EW, Griffith-Cima L. Hepatocyte culture on carbohydrate-modified star polyethylene oxide hydrogels. Biomaterials. 1996;17:559-69.
[78] Kang IK, Lee DW, Lee SK, Akaike T. Grafting of lactose-carrying styrene onto polystyrene dishes using plasma glow discharge and their interaction with hepatocytes. Journal of materials science Materials in medicine. 2003;14:611-6.
[79] Au AY HJ, Frondoza CG. Micropatterned agarose scaffolds covalently modified with collagen for culture of normal and neoplastic hepatocytes. Journal of biomedical materials research Part A. 2012;100:342-52.
[80] Nugraha B, Hong X, Mo X, Tan L, Zhang W, Chan PM, et al. Galactosylated cellulosic sponge for multi-well drug safety testing. Biomaterials. 2011;32:6982-94.
[81] Samuel G. Hirsch RJS. Temperature-dependent property development in hydrogels derived from hydroxypropylcellulose. Polymer. 2002;43:123-9.
[82] Gebhardt R HJ, Müller D, Glöckner R, Buenning P, Laube B, Schmelzer E, Ullrich M, Utesch D, Hewitt N, Ringel M, Hilz BR, Bader A, Langsch A, Koose T, Burger HJ, Maas J, Oesch F. New hepatocyte in vitro systems for drug metabolism: metabolic capacity and recommendations for application in basic research and drug development, standard operation procedures. Drug Metabolism Reviews. 2003;35:145-213.
[83] Business Insights' drug discovery research stream critically analyzes the cutting edge technologies and novel approaches shaping the future of drug discovery. http://www.business-insights.com/drug-discovery
[84] Ananthanarayanan A, Narmada BC, Mo X, McMillian M, Yu H. Purpose-driven biomaterials research in liver-tissue engineering. Trends in biotechnology. 2011;29:110-8.
[85] Seidle T, Robinson S, Holmes T, Creton S, Prieto P, Scheel J, et al. Cross-sector review of drivers and available 3Rs approaches for acute systemic toxicity testing. Toxicological sciences : an official journal of the Society of Toxicology. 2010;116:382-96.
[86] Zhang S, Xia L, Kang CH, Xiao G, Ong SM, Toh YC, et al. Microfabricated silicon nitride membranes for hepatocyte sandwich culture. Biomaterials. 2008;29:3993-4002.
[87] Hewitt NJ, Lechon MJ, Houston JB, Hallifax D, Brown HS, Maurel P, et al. Primary hepatocytes: current understanding of the regulation of metabolic enzymes and transporter proteins, and pharmaceutical practice for the use of hepatocytes in metabolism, enzyme induction, transporter, clearance, and hepatotoxicity studies. Drug Metab Rev. 2007;39:159-234.
[88] B. Naughton et al. Advanced Tissue Sciences Inc. Three dimensional cell and

tissue culture system. US Patent No. 5,510,254
[89] Du Y, Han R, Ng S, Ni J, Sun W, Wohland T, et al. Identification and characterization of a novel prespheroid 3-dimensional hepatocyte monolayer on galactosylated substratum. Tissue engineering. 2007;13:1455-68.
[90] Allen JW, Khetani SR, Bhatia SN. In vitro zonation and toxicity in a hepatocyte bioreactor. Toxicological sciences : an official journal of the Society of Toxicology. 2005;84:110-9.
[91] Toh YC, Zhang C, Zhang J, Khong YM, Chang S, Samper VD, et al. A novel 3D mammalian cell perfusion-culture system in microfluidic channels. Lab on a chip. 2007;7:302-9.
[92] Sivaraman A, Leach JK, Townsend S, Iida T, Hogan BJ, Stolz DB, et al. A microscale in vitro physiological model of the liver: predictive screens for drug metabolism and enzyme induction. Current drug metabolism. 2005;6:569-91.
[93] Chao P, Maguire T, Novik E, Cheng KC, Yarmush ML. Evaluation of a microfluidic based cell culture platform with primary human hepatocytes for the prediction of hepatic clearance in human. Biochemical pharmacology. 2009;78:625-32.
[94] Khetani SR, Bhatia SN. Microscale culture of human liver cells for drug development. Nature biotechnology. 2008;26:120-6.
[95] Wang S, Nagrath D, Chen PC, Berthiaume F, Yarmush ML. Three-dimensional primary hepatocyte culture in synthetic self-assembling peptide hydrogel. Tissue engineering Part A. 2008;14:227-36.
[96] Zhang S. Fabrication of novel biomaterials through molecular self-assembly. Nature biotechnology. 2003;21:1171-8.
[97] Horii A, Wang X, Gelain F, Zhang S. Biological designer self-assembling peptide nanofiber scaffolds significantly enhance osteoblast proliferation, differentiation and 3-D migration. PloS one. 2007;2:e190.
[98] Zhang S. Designer self-assembling Peptide nanofiber scaffolds for study of 3-d cell biology and beyond. Advances in cancer research. 2008;99:335-62.
[99] Schneider A, Garlick JA, Egles C. Self-assembling peptide nanofiber scaffolds accelerate wound healing. PloS one. 2008;3:e1410.
[100] Henriksson HB ST, Jonsson M, Hagman M, Horn M, Lindahl A, Brisby H. Transplantation of human mesenchymal stems cells into intervertebral discs in a xenogeneic porcine model. Spine (Phila Pa 1976). 2009;34:141-8.
[101] Erickson IE HA, Chung C, Li RT, Burdick JA, Mauck RL. Differential maturation and structure-function relationships in mesenchymal stem cell- and chondrocyte-seeded hydrogels. Tissue engineering Part A. 2009;15:1041-52.
[102] Sieminski AL SC, Gong H, Kamm RD. Primary sequence of ionic self-assembling peptide gels affects endothelial cell adhesion and capillary morphogenesis. Journal of biomedical materials research Part A. 2008;87:494-504.
[103] Elkayam T A-SS, Dvir-Ginzberg M, Harel T, Cohen S. Enhancing the drug metabolism activities of C3A--a human hepatocyte cell line--by tissue engineering within alginate scaffolds. Tissue engineering. 2006;12:1357-68.
[104] Glicklis R SL, Agbaria R, Merchuk JC, Cohen S. Hepatocyte behavior within three-dimensional porous alginate scaffolds. Biotechnology and bioengineering. 2000;67:344-53.
[105] Barbetta A BE, Dentini M. Porous Alginate Hydrogels: Synthetic Methods for Tailoring the Porous Texture. Biomacromolecules. 2009;10:2328-37.

[106] Bokhari M, Carnachan RJ, Cameron NR, Przyborski SA. Culture of HepG2 liver cells on three dimensional polystyrene scaffolds enhances cell structure and function during toxicological challenge. J Anat. 2007;211:567-76.
[107] Bokhari M, Carnachan RJ, Cameron NR, Przyborski SA. Novel cell culture device enabling three-dimensional cell growth and improved cell function. Biochemical and biophysical research communications. 2007;354:1095-100.
[108] Lee J, Cuddihy MJ, Cater GM, Kotov NA. Engineering liver tissue spheroids with inverted colloidal crystal scaffolds. Biomaterials. 2009;30:4687-94.
[109] Centers for Disease Control and Prevention. Sexually transmitted diseases treatment guidelines, 2010. Hepatitis C.
http://www.cdc.gov/std/treatment/2010/hepC.htm

[110] Salloum S, Tai AW. Treating hepatitis C infection by targeting the host. Translational research : the journal of laboratory and clinical medicine. 2012;159:421-9.
[111] Wise M, Bialek S, Finelli L, Bell BP, Sorvillo F. Changing trends in hepatitis C-related mortality in the United States, 1995-2004. Hepatology. 2008;47:1128-35.
[112] Simmonds P, Bukh J, Combet C, Deleage G, Enomoto N, Feinstone S, et al. Consensus proposals for a unified system of nomenclature of hepatitis C virus genotypes. Hepatology. 2005;42:962-73.
[113] Schlutter J. Therapeutics: new drugs hit the target. Nature. 2011;474:S5-7.
[114] Yoshida T, Takayama K, Kondoh M, Sakurai F, Tani H, Sakamoto N, et al. Use of human hepatocyte-like cells derived from induced pluripotent stem cells as a model for hepatocytes in hepatitis C virus infection. Biochemical and biophysical research communications. 2011;416:119-24.
[115] Pileri P, Uematsu Y, Campagnoli S, Galli G, Falugi F, Petracca R, et al. Binding of hepatitis C virus to CD81. Science. 1998;282:938-41.
[116] Scarselli E, Ansuini H, Cerino R, Roccasecca RM, Acali S, Filocamo G, et al. The human scavenger receptor class B type I is a novel candidate receptor for the hepatitis C virus. The EMBO journal. 2002;21:5017-25.
[117] Evans MJ, von Hahn T, Tscherne DM, Syder AJ, Panis M, Wolk B, et al. Claudin-1 is a hepatitis C virus co-receptor required for a late step in entry. Nature. 2007;446:801-5.
[118] Ploss A KS, Jones CT, Syder AJ, Trehan K, Gaysinskaya VA, Mu K, Ritola K, Rice CM, Bhatia SN. Persistent hepatitis C virus infection in microscale primary human hepatocyte cultures. Proceedings of the National Academy of Sciences of the United States of America. 2010;107:3141-5.
[119] Bartosch B, Dubuisson J. Recent advances in hepatitis C virus cell entry. Viruses. 2010;2:692-709.
[120] Zeisel MB, Koutsoudakis G, Schnober EK, Haberstroh A, Blum HE, Cosset FL, et al. Scavenger receptor class B type I is a key host factor for hepatitis C virus infection required for an entry step closely linked to CD81. Hepatology. 2007;46:1722-31.
[121] Wilson GK, Stamataki Z. In vitro systems for the study of hepatitis C virus infection. International journal of hepatology. 2012;2012:292591.
[122] Haizhen Zhu JE, Robin Foss, Alan Hemming, Eric Hall, Edward L. LeCluyse, Chen Liu. Primary Human Hepatocyte Culture for HCV Study. Methods Mol Biol. 2008;510:373-82.

[123] Sumpter R, Jr., Loo YM, Foy E, Li K, Yoneyama M, Fujita T, et al. Regulating intracellular antiviral defense and permissiveness to hepatitis C virus RNA replication through a cellular RNA helicase, RIG-I. Journal of virology. 2005;79:2689-99.
[124] Wu X, Robotham JM, Lee E, Dalton S, Kneteman NM, Gilbert DM, et al. Productive hepatitis C virus infection of stem cell-derived hepatocytes reveals a critical transition to viral permissiveness during differentiation. PLoS pathogens. 2012;8:e1002617.
[125] Mee CJ, Grove J, Harris HJ, Hu K, Balfe P, McKeating JA. Effect of cell polarization on hepatitis C virus entry. Journal of virology. 2008;82:461-70.
[126] Harris HJ, Farquhar MJ, Mee CJ, Davis C, Reynolds GM, Jennings A, et al. CD81 and claudin 1 coreceptor association: role in hepatitis C virus entry. Journal of virology. 2008;82:5007-20.
[127] Chen AA, Thomas DK, Ong LL, Schwartz RE, Golub TR, Bhatia SN. Humanized mice with ectopic artificial liver tissues. Proceedings of the National Academy of Sciences of the United States of America. 2011;108:11842-7.
[128] Chong TW, Smith RL, Hughes MG, Camden J, Rudy CK, Evans HL, et al. Primary human hepatocytes in spheroid formation to study hepatitis C infection. The Journal of surgical research. 2006;130:52-7.
[129] Aizaki H, Nagamori S, Matsuda M, Kawakami H, Hashimoto O, Ishiko H, et al. Production and release of infectious hepatitis C virus from human liver cell cultures in the three-dimensional radial-flow bioreactor. Virology. 2003;314:16-25.
[130] Murakami K, Ishii K, Ishihara Y, Yoshizaki S, Tanaka K, Gotoh Y, et al. Production of infectious hepatitis C virus particles in three-dimensional cultures of the cell line carrying the genome-length dicistronic viral RNA of genotype 1b. Virology. 2006;351:381-92.
[131] Lin JH. CYP induction-mediated drug interactions: in vitro assessment and clinical implications. Pharmaceutical research. 2006;23:1089-116.
[132] Gomez-Lechon MJ, Castell JV, Donato MT. An update on metabolism studies using human hepatocytes in primary culture. Expert opinion on drug metabolism & toxicology. 2008;4:837-54.
[133] Obach RS. Predicting drug-drug interactions from in vitro drug metabolism data: challenges and recent advances. Current opinion in drug discovery & development. 2009;12:81-9.
[134] Li AP. The use of the Integrated Discrete Multiple Organ Co-culture (IdMOC) system for the evaluation of multiple organ toxicity. Alternatives to laboratory animals : ATLA. 2009;37:377-85.
[135] McGinnity DF, Soars MG, Urbanowicz RA, Riley RJ. Evaluation of fresh and cryopreserved hepatocytes as in vitro drug metabolism tools for the prediction of metabolic clearance. Drug metabolism and disposition: the biological fate of chemicals. 2004;32:1247-53.
[136] Richert L, Liguori MJ, Abadie C, Heyd B, Mantion G, Halkic N, et al. Gene expression in human hepatocytes in suspension after isolation is similar to the liver of origin, is not affected by hepatocyte cold storage and cryopreservation, but is strongly changed after hepatocyte plating. Drug metabolism and disposition: the biological fate of chemicals. 2006;34:870-9.
[137] Mees C, Nemunaitis J, Senzer N. Transcription factors: their potential as targets for an individualized therapeutic approach to cancer. Cancer gene therapy. 2009;16:103-12.

[138] Shay JW, Wright WE. Senescence and immortalization: role of telomeres and telomerase. Carcinogenesis. 2005;26:867-74.
[139] LeCluyse EL, Witek RP, Andersen ME, Powers MJ. Organotypic liver culture models: meeting current challenges in toxicity testing. Critical reviews in toxicology. 2012;42:501-48.
[140] Harris AJ, Dial SL, Casciano DA. Comparison of basal gene expression profiles and effects of hepatocarcinogens on gene expression in cultured primary human hepatocytes and HepG2 cells. Mutation research. 2004;549:79-99.
[141] Liguori MJ, Blomme EA, Waring JF. Trovafloxacin-induced gene expression changes in liver-derived in vitro systems: comparison of primary human hepatocytes to HepG2 cells. Drug metabolism and disposition: the biological fate of chemicals. 2008;36:223-33.
[142] Olsavsky KM, Page JL, Johnson MC, Zarbl H, Strom SC, Omiecinski CJ. Gene expression profiling and differentiation assessment in primary human hepatocyte cultures, established hepatoma cell lines, and human liver tissues. Toxicology and applied pharmacology. 2007;222:42-56.
[143] Westerink WM, Schoonen WG. Phase II enzyme levels in HepG2 cells and cryopreserved primary human hepatocytes and their induction in HepG2 cells. Toxicology in vitro : an international journal published in association with BIBRA. 2007;21:1592-602.
[144] Vermeir M, Annaert P, Mamidi RN, Roymans D, Meuldermans W, Mannens G. Cell-based models to study hepatic drug metabolism and enzyme induction in humans. Expert opinion on drug metabolism & toxicology. 2005;1:75-90.
[145] Knasmuller S, Parzefall W, Sanyal R, Ecker S, Schwab C, Uhl M, et al. Use of metabolically competent human hepatoma cells for the detection of mutagens and antimutagens. Mutation research. 1998;402:185-202.
[146] Seipp S, Mueller HM, Pfaff E, Stremmel W, Theilmann L, Goeser T. Establishment of persistent hepatitis C virus infection and replication in vitro. The Journal of general virology. 1997;78 (Pt 10):2467-76.
[147] Guillouzo A, Corlu A, Aninat C, Glaise D, Morel F, Guguen-Guillouzo C. The human hepatoma HepaRG cells: a highly differentiated model for studies of liver metabolism and toxicity of xenobiotics. Chemico-biological interactions. 2007;168:66-73.
[148] Kanebratt KP, Andersson TB. HepaRG cells as an in vitro model for evaluation of cytochrome P450 induction in humans. Drug metabolism and disposition: the biological fate of chemicals. 2008;36:137-45.
[149] Turpeinen M, Tolonen A, Chesne C, Guillouzo A, Uusitalo J, Pelkonen O. Functional expression, inhibition and induction of CYP enzymes in HepaRG cells. Toxicology in vitro : an international journal published in association with BIBRA. 2009;23:748-53.
[150] Kanebratt KP, Andersson TB. Evaluation of HepaRG cells as an in vitro model for human drug metabolism studies. Drug metabolism and disposition: the biological fate of chemicals. 2008;36:1444-52.
[151] LeCluyse EL. Human hepatocyte culture systems for the in vitro evaluation of cytochrome P450 expression and regulation. European journal of pharmaceutical sciences : official journal of the European Federation for Pharmaceutical Sciences. 2001;13:343-68.

[152] LeCluyse E, Madan A, Hamilton G, Carroll K, DeHaan R, Parkinson A. Expression and regulation of cytochrome P450 enzymes in primary cultures of human hepatocytes. Journal of biochemical and molecular toxicology. 2000;14:177-88.
[153] Ndongo-Thiam N, Berthillon P, Errazuriz E, Bordes I, De Sequeira S, Trepo C, et al. Long-term propagation of serum hepatitis C virus (HCV) with production of enveloped HCV particles in human HepaRG hepatocytes. Hepatology. 2011;54:406-17.
[154] Shiraki N, Umeda K, Sakashita N, Takeya M, Kume K, Kume S. Differentiation of mouse and human embryonic stem cells into hepatic lineages. Genes to cells : devoted to molecular & cellular mechanisms. 2008;13:731-46.
[155] Matsukage S, Kosugi I, Kawasaski H, Miura K, Kitani H, Tsutsui Y. Mouse embryonic stem cells are not susceptible to cytomegalovirus but acquire susceptibility during differentiation. Birth defects research Part A, Clinical and molecular teratology. 2006;76:115-25.
[156] Ogawa S, Tagawa Y, Kamiyoshi A, Suzuki A, Nakayama J, Hashikura Y, et al. Crucial roles of mesodermal cell lineages in a murine embryonic stem cell-derived in vitro liver organogenesis system. Stem Cells. 2005;23:903-13.
[157] Sullivan GJ, Hay DC, Park IH, Fletcher J, Hannoun Z, Payne CM, et al. Generation of functional human hepatic endoderm from human induced pluripotent stem cells. Hepatology. 2010;51:329-35.
[158] Agarwal S, Holton KL, Lanza R. Efficient differentiation of functional hepatocytes from human embryonic stem cells. Stem Cells. 2008;26:1117-27.
[159] Snykers S, De Kock J, Rogiers V, Vanhaecke T. In vitro differentiation of embryonic and adult stem cells into hepatocytes: state of the art. Stem Cells. 2009;27:577-605.
[160] Strick-Marchand H, Weiss MC. Inducible differentiation and morphogenesis of bipotential liver cell lines from wild-type mouse embryos. Hepatology. 2002;36:794-804.
[161] Yamasaki C, Tateno C, Aratani A, Ohnishi C, Katayama S, Kohashi T, et al. Growth and differentiation of colony-forming human hepatocytes in vitro. Journal of hepatology. 2006;44:749-57.
[162] Guguen-Guillouzo C, Corlu A, Guillouzo A. Stem cell-derived hepatocytes and their use in toxicology. Toxicology. 2010;270:3-9.
[163] Hay DC, Fletcher J, Payne C, Terrace JD, Gallagher RC, Snoeys J, et al. Highly efficient differentiation of hESCs to functional hepatic endoderm requires ActivinA and Wnt3a signaling. Proceedings of the National Academy of Sciences of the United States of America. 2008;105:12301-6.
[164] Basma H, Soto-Gutierrez A, Yannam GR, Liu L, Ito R, Yamamoto T, et al. Differentiation and transplantation of human embryonic stem cell-derived hepatocytes. Gastroenterology. 2009;136:990-9.
[165] Schwartz RE, Trehan K, Andrus L, Sheahan TP, Ploss A, Duncan SA, et al. Modeling hepatitis C virus infection using human induced pluripotent stem cells. Proceedings of the National Academy of Sciences of the United States of America. 2012;109:2544-8.
[166] Gu H, Yue Z, Leong WS, Nugraha B, Tan LP. Control of in vitro neural differentiation of mesenchymal stem cells in 3D macroporous, cellulosic hydrogels. Regenerative medicine. 2010;5:245-53.
[167] Smalley KS, Lioni M, Herlyn M. Life isn't flat: taking cancer biology to the next dimension. In vitro cellular & developmental biology Animal. 2006;42:242-7.

[168] Griffith LG, Swartz MA. Capturing complex 3D tissue physiology in vitro. Nature reviews Molecular cell biology. 2006;7:211-24.
[169] Bartosh TJ, Ylostalo JH, Mohammadipoor A, Bazhanov N, Coble K, Claypool K, et al. Aggregation of human mesenchymal stromal cells (MSCs) into 3D spheroids enhances their antiinflammatory properties. Proceedings of the National Academy of Sciences of the United States of America. 2010;107:13724-9.
[170] Fischbach C, Kong HJ, Hsiong SX, Evangelista MB, Yuen W, Mooney DJ. Cancer cell angiogenic capability is regulated by 3D culture and integrin engagement. Proceedings of the National Academy of Sciences of the United States of America. 2009;106:399-404.
[171] Koide N, Sakaguchi K, Koide Y, Asano K, Kawaguchi M, Matsushima H, et al. Formation of multicellular spheroids composed of adult rat hepatocytes in dishes with positively charged surfaces and under other nonadherent environments. Experimental cell research. 1990;186:227-35.
[172] Yuasa C, Tomita Y, Shono M, Ishimura K, Ichihara A. Importance of cell aggregation for expression of liver functions and regeneration demonstrated with primary cultured hepatocytes. J Cell Physiol. 1993;156:522-30.
[173] Yamada T, Yoshikawa M, Kanda S, Kato Y, Nakajima Y, Ishizaka S, et al. In vitro differentiation of embryonic stem cells into hepatocyte-like cells identified by cellular uptake of indocyanine green. Stem Cells. 2002;20:146-54.
[174] Ivascu A, Kubbies M. Rapid generation of single-tumor spheroids for high-throughput cell function and toxicity analysis. J Biomol Screen. 2006;11:922-32.
[175] Du Y, Chia SM, Han R, Chang S, Tang H, Yu H. 3D hepatocyte monolayer on hybrid RGD/galactose substratum. Biomaterials. 2006;27:5669-80.
[176] Brophy CM, Luebke-Wheeler JL, Amiot BP, Khan H, Remmel RP, Rinaldo P, et al. Rat hepatocyte spheroids formed by rocked technique maintain differentiated hepatocyte gene expression and function. Hepatology. 2009;49:578-86.
[177] Takahashi R, Sonoda H, Tabata Y, Hisada A. Formation of hepatocyte spheroids with structural polarity and functional bile canaliculi using nanopillar sheets. Tissue engineering Part A. 2010;16:1983-95.
[178] Nakazawa K, Izumi Y, Fukuda J, Yasuda T. Hepatocyte spheroid culture on a polydimethylsiloxane chip having microcavities. Journal of biomaterials science Polymer edition. 2006;17:859-73.
[179] Yamashita Y, Shimada M, Tsujita E, Tanaka S, Ijima H, Nakazawa K, et al. Polyurethane foam/spheroid culture system using human hepatoblastoma cell line (Hep G2) as a possible new hybrid artificial liver. Cell transplantation. 2001;10:717-22.
[180] Ijima H, Nakazawa K, Koyama S, Kaneko M, Matsushita T, Gion T, et al. Development of a hybrid artificial liver using a polyurethane foam/hepatocyte-spheroid packed-bed module. Int J Artif Organs. 2000;23:389-97.
[181] Wells RG. The role of matrix stiffness in regulating cell behavior. Hepatology. 2008;47:1394-400.
[182] Seglen PO. Preparation of isolated rat liver cells. Methods Cell Biol. 1976;13:29-83.
[183] Zhang S, Tong W, Zheng B, Susanto TA, Xia L, Zhang C, et al. A robust high-throughput sandwich cell-based drug screening platform. Biomaterials. 2011;32:1229-41.

[184] Tostoes RM, Leite SB, Miranda JP, Sousa M, Wang DI, Carrondo MJ, et al. Perfusion of 3D encapsulated hepatocytes--a synergistic effect enhancing long-term functionality in bioreactors. Biotechnology and bioengineering. 2011;108:41-9.
[185] Chang HK, Park YJ, Koh H, Kim SM, Chung KS, Oh JT, et al. Hepatic fibrosis scan for liver stiffness score measurement: a useful preendoscopic screening test for the detection of varices in postoperative patients with biliary atresia. Journal of pediatric gastroenterology and nutrition. 2009;49:323-8.
[186] Wang MH, Palmeri ML, Guy CD, Yang L, Hedlund LW, Diehl AM, et al. In vivo quantification of liver stiffness in a rat model of hepatic fibrosis with acoustic radiation force. Ultrasound in medicine & biology. 2009;35:1709-21.
[187] Luebke-Wheeler JL, Nedredal G, Yee L, Amiot BP, Nyberg SL. E-cadherin protects primary hepatocyte spheroids from cell death by a caspase-independent mechanism. Cell transplantation. 2009;18:1281-7.
[188] Harada K, Mitaka T, Miyamoto S, Sugimoto S, Ikeda S, Takeda H, et al. Rapid formation of hepatic organoid in collagen sponge by rat small hepatocytes and hepatic nonparenchymal cells. Journal of hepatology. 2003;39:716-23.
[189] Talamini MA, Kappus B, Hubbard A. Repolarization of hepatocytes in culture. Hepatology. 1997;25:167-72.
[190] Larusso NF. Hepatocyte lysosomes in intracellular digestion and biliary secretion. Comprehensive Biology: Wiley; 2011. p. 677–91.
[191] Ng S, Han R, Chang S, Ni J, Hunziker W, Goryachev AB, et al. Improved hepatocyte excretory function by immediate presentation of polarity cues. Tissue engineering. 2006;12:2181-91.
[192] Sidler Pfandler MA, Hochli M, Inderbitzin D, Meier PJ, Stieger B. Small hepatocytes in culture develop polarized transporter expression and differentiation. Journal of cell science. 2004;117:4077-87.
[193] Nussler AK, Wang A, Neuhaus P, Fischer J, Yuan J, Liu L, et al. The suitability of hepatocyte culture models to study various aspects of drug metabolism. ALTEX. 2001;18:91-101.
[194] Sakai Y, Yamagami S, Nakazawa K. Comparative analysis of gene expression in rat liver tissue and monolayer- and spheroid-cultured hepatocytes. Cells Tissues Organs. 2010;191:281-8.
[195] Wolkoff AW, Cohen DE. Bile acid regulation of hepatic physiology: I. Hepatocyte transport of bile acids. Am J Physiol Gastrointest Liver Physiol. 2003;284:G175-9.
[196] Pang KS, Weiss M, Macheras P. Advanced pharmacokinetic models based on organ clearance, circulatory, and fractal concepts. Aaps J. 2007;9:E268-83.
[197] Dunn JC, Tompkins RG, Yarmush ML. Hepatocytes in collagen sandwich: evidence for transcriptional and translational regulation. J Cell Biol. 1992;116:1043-53.
[198] Yin C, Liao K, Mao HQ, Leong KW, Zhuo RX, Chan V. Adhesion contact dynamics of HepG2 cells on galactose-immobilized substrates. Biomaterials. 2003;24:837-50.
[199] Hsiao CC, Wu JR, Wu FJ, Ko WJ, Remmel RP, Hu WS. Receding cytochrome P450 activity in disassembling hepatocyte spheroids. Tissue engineering. 1999;5:207-21.
[200] Ranucci CS, Kumar A, Batra SP, Moghe PV. Control of hepatocyte function on collagen foams: sizing matrix pores toward selective induction of 2-D and 3-D cellular morphogenesis. Biomaterials. 2000;21:783-93.

[201] Green JE, Waters SL, Shakesheff KM, Byrne HM. A mathematical model of liver cell aggregation in vitro. Bull Math Biol. 2009;71:906-30.
[202] Yoon JJ, Nam YS, Kim JH, Park TG. Surface immobilization of galactose onto aliphatic biodegradable polymers for hepatocyte culture. Biotechnology and bioengineering. 2002;78:1-10.
[203] Nyberg SL, Hardin J, Amiot B, Argikar UA, Remmel RP, Rinaldo P. Rapid, large-scale formation of porcine hepatocyte spheroids in a novel spheroid reservoir bioartificial liver. Liver Transpl. 2005;11:901-10.
[204] Feng ZQ, Chu X, Huang NP, Wang T, Wang Y, Shi X, et al. The effect of nanofibrous galactosylated chitosan scaffolds on the formation of rat primary hepatocyte aggregates and the maintenance of liver function. Biomaterials. 2009;30:2753-63.
[205] Tzanakakis ES, Waxman DJ, Hansen LK, Remmel RP, Hu WS. Long-term enhancement of cytochrome P450 2B1/2 expression in rat hepatocyte spheroids through adenovirus-mediated gene transfer. Cell Biol Toxicol. 2002;18:13-27.
[206] Padgham CR, Paine AJ, Phillips IR, Shephard EA. Maintenance of total cytochrome P-450 content in rat hepatocyte culture and the abundance of CYP1A2 and CYP2B1/2 mRNAs. The Biochemical journal. 1992;285 (Pt 3):929-32.
[207] Budinsky RA, LeCluyse EL, Ferguson SS, Rowlands JC, Simon T. Human and rat primary hepatocyte CYP1A1 and 1A2 induction with 2,3,7,8-tetrachlorodibenzo-p-dioxin, 2,3,7,8-tetrachlorodibenzofuran, and 2,3,4,7,8-pentachlorodibenzofuran. Toxicological sciences : an official journal of the Society of Toxicology. 2010;118:224-35.
[208] Sarbah SA, Younossi ZM. Hepatitis C: an update on the silent epidemic. Journal of clinical gastroenterology. 2000;30:125-43.
[209] Genetic Variation and HCV Genotyping.
http://www.hepatitiscentral.com/hcv/genotype/genotyping.html
[210] Cummings R. Ribavirin/Pegylated Interferon Combination Therapy for People with Hepatitis C. 2002.
http://www.hivhepsti.info/documents/ribavirininterferontreatment.pdf
[211] J Shepherd HB, C Cave, N Waugh, A Price and J Gabbay. Pegylated interferon a-2a and -2b in combination with ribavirin in the treatment of chronic hepatitis C: a systematic review and economic evaluation. Health Technology Assessment. 2004;8:1-148.
[212] Bukh J. A critical role for the chimpanzee model in the study of hepatitis C. Hepatology. 2004;39:1469-75.
[213] Aly HH, Watashi K, Hijikata M, Kaneko H, Takada Y, Egawa H, et al. Serum-derived hepatitis C virus infectivity in interferon regulatory factor-7-suppressed human primary hepatocytes. Journal of hepatology. 2007;46:26-36.
[214] Hsu IC, Tokiwa T, Bennett W, Metcalf RA, Welsh JA, Sun T, et al. p53 gene mutation and integrated hepatitis B viral DNA sequences in human liver cancer cell lines. Carcinogenesis. 1993;14:987-92.
[215] Nagao K, Ohyashiki JH, Ohyashiki K, Tabata K, Takai K, Kameyama K, et al. Expression of hTERT mRNA in a mortal liver cell line during S phase without detectable telomerase activity. International journal of molecular medicine. 2005;15:683-8.
[216] Yokoo H, Kondo T, Fujii K, Yamada T, Todo S, Hirohashi S. Proteomic signature corresponding to alpha fetoprotein expression in liver cancer cells. Hepatology. 2004;40:609-17.

[217] Bhatia SN, Balis UJ, Yarmush ML, Toner M. Effect of cell-cell interactions in preservation of cellular phenotype: cocultivation of hepatocytes and nonparenchymal cells. FASEB journal : official publication of the Federation of American Societies for Experimental Biology. 1999;13:1883-900.
[218] Blight KJ, McKeating JA, Rice CM. Highly permissive cell lines for subgenomic and genomic hepatitis C virus RNA replication. Journal of virology. 2002;76:13001-14.
[219] Peshwa MV, Wu FJ, Sharp HL, Cerra FB, Hu WS. Mechanistics of formation and ultrastructural evaluation of hepatocyte spheroids. In vitro cellular & developmental biology Animal. 1996;32:197-203.
[220] Microscopic Anatomy.
http://www.udel.edu/biology/Wags/histopage/histopage.htm
[221] Bartosch B, Cosset FL. Studying HCV cell entry with HCV pseudoparticles (HCVpp). Methods Mol Biol. 2009;510:279-93.
[222] Lindenbach BD, Evans MJ, Syder AJ, Wolk B, Tellinghuisen TL, Liu CC, et al. Complete replication of hepatitis C virus in cell culture. Science. 2005;309:623-6.
[223] Chien HW, Tsai WB, Jiang S. Direct cell encapsulation in biodegradable and functionalizable carboxybetaine hydrogels. Biomaterials. 2012;33:5706-12.
[224] Habib Onsori MRZ, Mostafa Motallebi, Nosratollah Zarghami. Identification of over producer strain of endo-b-1,4-glucanase in Aspergillus Species: Characterization of crude carboxymethyl cellulase. African Journal of Biotechnology 2005;4:26-30.
[225] Zilberman M, Nelson KD, Eberhart RC. Mechanical properties and in vitro degradation of bioresorbable fibers and expandable fiber-based stents. Journal of biomedical materials research Part B, Applied biomaterials. 2005;74:792-9.
[226] Dispinar T, Van Camp W, De Cock LJ, De Geest BG, Du Prez FE. Redox-responsive degradable PEG cryogels as potential cell scaffolds in tissue engineering. Macromol Biosci. 2012;12:383-94.
[227] Kloxin AM, Kasko AM, Salinas CN, Anseth KS. Photodegradable hydrogels for dynamic tuning of physical and chemical properties. Science. 2009;324:59-63.
[228] Meng F, Hennink WE, Zhong Z. Reduction-sensitive polymers and bioconjugates for biomedical applications. Biomaterials. 2009;30:2180-98.
[229] Hamid ZA, Blencowe A, Ozcelik B, Palmer JA, Stevens GW, Abberton KM, et al. Epoxy-amine synthesised hydrogel scaffolds for soft-tissue engineering. Biomaterials. 2010;31:6454-67.
[230] Raines CPaRT. Adjacent cysteine residues as a redox switch. Protein Eng 2001;14:939-42.
[231] Liu Y, Zheng Shu X, Prestwich GD. Biocompatibility and stability of disulfide-crosslinked hyaluronan films. Biomaterials. 2005;26:4737-46.
[232] Hisano N, Morikawa N, Iwata H, Ikada Y. Entrapment of islets into reversible disulfide hydrogels. Journal of biomedical materials research. 1998;40:115-23.
[233] Bromberg L, Temchenko M, Alakhov V, Hatton TA. Kinetics of swelling of polyether-modified poly(acrylic acid) microgels with permanent and degradable cross-links. Langmuir : the ACS journal of surfaces and colloids. 2005;21:1590-8.
[234] Plunkett KN, Berkowski KL, Moore JS. Chymotrypsin responsive hydrogel: application of a disulfide exchange protocol for the preparation of methacrylamide containing peptides. Biomacromolecules. 2005;6:632-7.
[235] Yoshida H, Klinkhammer K, Matsusaki M, Moller M, Klee D, Akashi M. Disulfide-crosslinked electrospun poly(gamma-glutamic acid) nonwovens as reduction-responsive scaffolds. Macromol Biosci. 2009;9:568-74.

[236] Kakizawa Y, Harada A, Kataoka K. Glutathione-sensitive stabilization of block copolymer micelles composed of antisense DNA and thiolated poly(ethylene glycol)-block-poly(L-lysine): a potential carrier for systemic delivery of antisense DNA. Biomacromolecules. 2001;2:491-7.
[237] Lees WJ, and Whitesides, G.M. Equilibrium Constants for Thiol-Disulfide Interchange Reactions. The Journal of organic chemistry. 1993;58:642-7.
[238] Shu XZ, Liu Y, Palumbo F, Prestwich GD. Disulfide-crosslinked hyaluronan-gelatin hydrogel films: a covalent mimic of the extracellular matrix for in vitro cell growth. Biomaterials. 2003;24:3825-34.
[239] John A. Burns JCB, John Moran, and George M. Whitesides. Selective Reduction of Disulfides by Tris(2-carboxyethyl)phosphine The Journal of organic chemistry. 1991;56:2648-50.
[240] Matsusaki M, Yoshida H, Akashi M. The construction of 3D-engineered tissues composed of cells and extracellular matrices by hydrogel template approach. Biomaterials. 2007;28:2729-37.
[241] http://www.qcbio.com/uploaddrivers/233153-000.pdf
[242] Han JC, Han GY. A procedure for quantitative determination of tris(2-carboxyethyl)phosphine, an odorless reducing agent more stable and effective than dithiothreitol. Analytical biochemistry. 1994;220:5-10.
[243] http://www.piercenet.com/instructions/2161434.pdf
[244] Ren XL, Yu Jin; Han, Ho Jae; Kim, In S. Effect of tris-(2-chloroethyl)-phosphate (TCEP) at environmental concentration on the levels of cell cycle regulatory protein expression in primary cultured rabbit renal proximal tubule cells. Chemosphere. 2008;74:84-8.
[245] Zhang J, Skardal A, Prestwich GD. Engineered extracellular matrices with cleavable crosslinkers for cell expansion and easy cell recovery. Biomaterials. 2008;29:4521-31.
[246] TCEP – a reagent of choice in both Proteomics and nucleic acid chemistry. http://www.polyorganix.com/productsubcat.php?category=VENFUCBwcm9kdWN0cw==&catid=17
[247] Shi X, Garcia GE, Neill RJ, Gordon RK. TCEP treatment reduces proteolytic activity of BoNT/B in human neuronal SHSY-5Y cells. Journal of cellular biochemistry. 2009;107:1021-30.
[248] Hamamoto R, Yamada K, Kamihira M, Iijima S. Differentiation and proliferation of primary rat hepatocytes cultured as spheroids. Journal of biochemistry. 1998;124:972-9.

APPENDIX

Institute of Bioengineering and Nanotechnology
A*STAR
Innovations for Tomorrow

CONFIDENTIAL

Technology Disclosure Form

SECTION 1: TECHNOLOGY DISCLOSURE DETAILS

RI Technology Disclosure No	**IBN-310** **Lead Scientist: Prof Hanry Yu**
(1) Title of Technology	**Cleavable Macroporous Cellulosic Sponge for 3D Cell Culture and Spheroids Retrieval**
(2) Keywords relating to your technology (5-10 keywords)	Cleavable, cellulose, sponge, 3D cell culture, retrieval, and hepatocyte
(3) Indicate the category in which your technology falls under	☐ Drug and Gene Delivery ☒ Cell and Tissue Engineering ☐ Biodevices and Diagnostics ☐ Pharmaceuticals Synthesis and Green Chemistry
(4) Brief summary of your technology *Attach also a detailed description of your technology.*	Macroporous hydrogel sponge made of cellulose derivative could entrap cells, induce spheroids formation and maintain these constructs within the macroporous networks over extended culture period. However, the current cellulosic sponge design is physically stable during and after cell culture, thus limiting the retrieval of cells from the sponge for analysis and further use. Addition of trypsin or other dissociating enzymes to retrieve these spheroids is unable to achieve good harvesting yield. By conjugating reducible disulphide bond into hydroxyl groups at the side chain of hydroxypropyl cellulose prior to attaching the double bond for crosslinking, we can tailor the cellulosic sponge to be readily cleavable upon addition of suitable disulphide bond reductant that works best under a range of cell-compatible conditions. The sponge cleavage occurs at physiological conditions (pH 7.4, 37°C, in cell culture medium and or buffer) within 30 minutes without inducing significant cell toxicity, disruption of tight cell-cell junction and primary cell polarity markers. The insertion of disulphide bond at the side chain of hydroxypropyl cellulose also does not interfere with the formation of macroporous network of cellulosic sponge, as well as the crosslinkability of the hydrogel with gamma irradiation. Moreover, this modification does not inhibit the ligand conjugation onto the sponge for subsequent cell culture application. This material provides the capability of culturing various types of cells in three dimensions within the macroporous networks of cellulosic sponge, maintaining the cell culture for extended periods, and retrieving the cells for further downstream applications/assays. The ability of retrieving the cells from the sponge could ease the downstream functional analysis, which is normally challenged by the physical stability of other existing materials.

(5) Key technical features (excluding advantages such as cost, efficiency).	A platform to culture cells in three dimensional macroporous networks, as well as to safely retrieve the cell constructs formed therein.

SECTION 2: INTELLECTUAL PROPERTY ASSESSMENT

	Date & Details
(1) Conception of Invention	March 1, 2012 (Notebook series 1504Bramasta02 page 58)
(2) Public Disclosure	August 5, 2012

	RI Ref No:	**Patent / Appl. Title**
(3) Related RI's Patents/Applications/ TDs	IBN-149	Forming Porous Scaffold from Cellulose Derivatives U.S. Provisional Application No. 61/006,090, filed Dec. 18, 2007

(4) Prior Art *Provide references to what you consider to be the closest published work (inc. your own).* *Provide the details in separate sheets if necessary.*	1) J. Zhang, *et al.* Engineered extracellular matrices with cleavable crosslinkers for cell expansion and easy cell recovery. Biomaterials, 29 (2008) 4521-4531 2) M. Matsusaki, *et al.* The construction of 3D-engineered tissues composed of cells and extracellular matrices by hydrogel template approach. Biomaterials, 28 (2007) 2729-2737
(5) Novelty / Non-obviousness *Highlight the novelty and non-obviousness of your technology disclosure in view of prior art in which you have cited. Provide the details in separate sheets if necessary.*	Comparing our disulfide-containing cellulosic sponge to the other disulfide-containing hydrogel systems, our technology shows the importance of having macroporous networks with mechanically and chemically tunable properties in the sponge for 3D cell culture within diffusible construct rather than cell encapsulated in hydrogel system. Our disulfide-containing sponge also shows faster cleavage rate at the addition of comparable reductants concentration than other disulfide-containing hydrogels (which cannot form spheroids as in our sponge possibly due to blockage of cell-cell interactions by hydrogels), i.e. spheroids can be easily retrieved from our sponge in as fast as 30 minutes. Compared with the prior art of cellulosic sponge (U.S. provisional application No. 61/006,090, filed Dec. 18, 2007), this cleavable disulfide-containing material has been designed and synthesized with novel chemistry. The reduction conditions that are important for cell compatibility and speed in applications have experimentally optimized.

(6) Does this technology arise out of an	No

external collaboration? If yes, list the collaborators and provide details	

SECTION 3: COMMERCIAL ASSESSMENT

(1) List the top 5 organizations that may be interested in this invention or working in the similar field. Please also provide contacts if any.	1) Bio-byblos Biomedical Co. Ld., Taiwan 2) Invitrogen 3) Glycosan 4) Becton Dickinson 5) 3D Biomatrix
(2) Does the technology possess disadvantages or limitations? Can they be overcome and how?	The reductant used to cleave the sponge is unstable for long-term storage in physiological buffer/medium. Freshly prepared reductant has to be prepared before cleaving the sponge. The sponge must also be stored dry in desiccators at room temperature for stability.
(3) How can the technology be traced? Please elaborate.	The chemical construct of the cleavable sponge can be traced by nuclear magnetic resonance (NMR) and Fourier transform infrared (FTIR) spectroscopy. The cleavage mechanism of the sponge can be confirmed by incubating the sponge with various chemical reductants e.g. 10 mM dithiothreitol (DTT), 25 mM glutathione (GSH) and 10 mM tris 2-carboxyethyl phosphine (TCEP) in cell medium or buffer.
(4) How can the technology be worked around?	One can theoretically develop a different material that has the similar macroporosity, mechanical and chemical tenability, cell biocompatibility, and sensitive/rapid reductant cleavability (with different types of biocompatible reductants), e.g. enzymes to cleave peptide that is sensitive to matrix-metaloproteases (Lutolf MP, et al. PNAS 100 (2003) 5413-5418) or UV-cleavable hydrogels (A.M. Kloxin, et al. Science 324 (2009) 59-63). However, the combination of all these characteristics required for the intended 3D cell culture with strong cell-cell interactions in epithelial tissues for in vitro and in vivo applications of tissue-engineered constructs are very unlikely to be achieved in any other ways.
(5) Indicate the level of development.	☐ No data ☐ Simulation results available ☒ Experimental results available ☐ Animal models created ☒ Prototype built ☐ Others, Please Highlight:

SECTION 4: INVENTORS' DETAILS AND CONTRIBUTIONS

I/We hereby declare that we are the inventors for the technology.

(Note: An inventor means the actual deviser of the invention. A person is NOT an inventor if he/she

- *Only helps to implement the invention*
- *Only financially contribute or sponsor the work*
- *Employs or manages the actual deviser/devisers of the invention)*

1. Family name: Nugraha Given name: Bramasta Country of Permanent Residency: Citizenship: Indonesian Resident of Singapore during Invention: Yes Email: bram@ibn.a-star.edu.sg Tel: 6824 7378 Employer: Institute of Bioengineering and Nanotechnology State aspect and percentage of contribution: Conceptualization of invention and establish the proof of concept, (50%). Signature: 29 JUN 2012	2. Family name: Yu Given name: Hanry Country of Permanent Residency: Citizenship: Singaporean Resident of Singapore during Invention: Yes Email: hanry_yu@nuhs.ed.sg Tel: 6824 7103 Employer: Institute of Bioengineering and Nanotechnology State aspect and percentage of contribution: Conceptualization of invention and establish the proof of concept, (50%). Signature:

SECTION 5: ENDORSEMENT

Endorsed by:

2/7/12

Prof. Jackie Y. Ying / Date
Executive Director
Institute of Bioengineering and Nanotechnology

Please attach any additional sections.

Copyright Clearance Center

1 PAYMENT 2 REVIEW 3 CONFIRMATION

Step 3: Order Confirmation

Thank you for your order! A confirmation for your order will be sent to your account email address. If you have questions about your order, you can call us at 978-646-2600, M-F between 8:00 AM and 6:00 PM (Eastern), or write to us at info@copyright.com.

Confirmation Number: 11066528
Order Date: 02/01/2013

If you pay by credit card, your order will be finalized and your card will be charged within 24 hours. If you pay by invoice, you can change or cancel your order until the invoice is generated.

Payment Information

Bramasta Nugraha
brammies2002@gmail.com
+41 788472117
Payment Method: CC ending in 3078

Special order invoices will be sent to:

Erlenstrasse 24
Basel, Not available 4058
CH

Order Details

Pearson Education Australia custom book

Order detail ID:	63415476
ISBN:	978-1-74009-635-5
Publication Type:	Book
Publisher:	Pearson Education Australia
Rightsholder:	CAL, COPYRIGHT AGENCY LIMITED

Permission Status:	**Granted**
Permission type:	Photocopy for general business or academic use
Type of use:	Photocopy for internal/external business use
Per Page Fee:	$ 0.60
Total number of pages:	1
Number of copies:	1

$ 4.10

Biotechnology advances

Order detail ID:	63415480
Order License Id:	3080161046390
Article Title:	Role of biomaterials, therapeutic molecules and cells for hepatic tissue engineering
Author(s):	Vasanthan, Kirthanashri Srinivasan ; et al
DOI:	10.1016/J.BIOTECHADV.2012.01.004
Date:	Jan 01, 2012
ISSN:	1873-1899
Publication Type:	e-Journal
Volume:	30
Issue:	3
Start page:	742
Publisher:	ELSEVIER INC.

Permission Status:	**Granted**
Permission type:	Republish or display content
Type of use:	reuse in a thesis/dissertation
Number of pages	11
Portion	figures/tables/illustrations
Number of figures/tables/illustrations	2
Format	both print and electronic
Are you the author of this Elsevier article?	No
Will you be translating?	No
Order reference number	

Title of your thesis/dissertation	Macroporous cellulosic sponge for 3D hepatocyte-based applications
Expected completion date	Jun 2013
Estimated size (number of pages)	180
Elsevier VAT number	GB 494 6272 12
Permissions price	0.00 EUR
VAT/Local Sales Tax	0.00 USD / 0.00 GBP

Note: This item will be invoiced or charged separately through CCC's **RightsLink** service. More info **$ 0.00**

Biomaterials

Order detail ID:	63415483
Order License Id:	3080161048227
Article Title:	Galactosylated cellulosic sponge for multi-well drug safety testing
Author(s):	Nugraha, Bramasta ; et al
DOI:	10.1016/J.BIOMATERIALS.2011.05.087
Date:	Okt 01, 2011
ISSN:	0142-9612
Publication Type:	Journal
Volume:	32
Issue:	29
Start page:	6982
Publisher:	PERGAMON
Author/Editor:	Biological Engineering Society

Permission Status:	**Granted**
Permission type:	Republish or display content
Type of use:	reuse in a thesis/dissertation
Number of pages	13
Portion	figures/tables/illustrations
Number of figures/tables/illustrations	6
Format	both print and electronic
Are you the author of this Elsevier article?	Yes
Will you be translating?	No
Order reference number	
Title of your thesis/dissertation	Macroporous cellulosic sponge for 3D hepatocyte-based applications
Expected completion date	Jun 2013
Estimated size (number of pages)	180
Elsevier VAT number	GB 494 6272 12
Permissions price	0.00 EUR
VAT/Local Sales Tax	0.00 USD / 0.00 GBP

Note: This item will be invoiced or charged separately through CCC's **RightsLink** service. More info **$ 0.00**

Translational research : the journal of laboratory and clinical medicine

Order detail ID:	63415487
Order License Id:	3080161050013
Article Title:	Treating hepatitis C infection by targeting the host
Author(s):	Salloum, Shadi ; Tai, Andrew W.
DOI:	10.1016/J.TRSL.2011.12.007
ISSN:	1931-5244
Publication Type:	Journal
Volume:	
Issue:	
Start page:	
Publisher:	MOSBY INC
Author/Editor:	Central Society for Clinical Research (U.S.)

Permission Status:	**Granted**
Permission type:	Republish or display content
Type of use:	reuse in a thesis/dissertation
Number of pages	9
Portion	figures/tables/illustrations
Number of figures/tables/illustrations	1
Format	both print and electronic
Are you the author of this Elsevier article?	No
Will you be translating?	No
Order reference number	
Title of your thesis/dissertation	Macroporous cellulosic sponge for 3D hepatocyte-based applications
Expected completion date	Jun 2013
Estimated size (number of pages)	180
Elsevier VAT number	GB 494 6272 12
Permissions price	0.00 EUR
VAT/Local Sales Tax	0.00 USD / 0.00 GBP

Note: This item will be invoiced or charged separately through CCC's **RightsLink** service. More info **$ 0.00**

Trends in biotechnology

Order detail ID:	63415490
Order License Id:	3080161051761
Article Title:	Purpose-driven biomaterials research in liver-tissue engineering
Author(s):	Ananthanarayanan, Abhishek ; et al
DOI:	10.1016/J.TIBTECH.2010.10.006
Date:	Jan 01, 2011
ISSN:	0167-7799
Publication Type:	Journal
Volume:	29
Issue:	3
Start page:	110
Publisher:	ELSEVIER LTD.

Permission Status:	**Granted**
Permission type:	Republish or display content
Type of use:	reuse in a thesis/dissertation
Number of pages	9
Portion	figures/tables/illustrations
Number of figures/tables/illustrations	1
Format	both print and electronic
Are you the author of this Elsevier article?	No

Will you be translating?	No
Order reference number	
Title of your thesis/dissertation	Macroporous cellulosic sponge for 3D hepatocyte-based applications
Expected completion date	Jun 2013
Estimated size (number of pages)	180
Elsevier VAT number	GB 494 6272 12
Permissions price	0.00 EUR
VAT/Local Sales Tax	0.00 USD / 0.00 GBP

Note: This item will be invoiced or charged separately through CCC's **RightsLink** service. More info **$ 0.00**

Special Orders

WILEY CATALOG

Order detail ID: 63415497
CCC System ID: 122879644
Publication Type: Other
Publisher: JOHN WILEY & SONS INC (B)
Rightsholder: JOHN WILEY & SONS - BOOKS

Permission Status: **Special Order**
Special Order Update: Forwarded to rightsholder

Permission type: Photocopy for general business or academic use
Total number of pages: 1
Number of copies: 1

$TBD

Total order items: 6

Order Total: € 3.01 (USD$ 4.10)
(Excludes $TBD items)

Note: $ 4.10 of your total will be charged to your credit card immediately. Your card will be charged for Special Order items later.

Confirmation Number: 11066528

Special Rightsholder Terms & Conditions

The following terms & conditions apply to the specific publication under which they are listed

Pearson Education Australia custom book
Permission type: Photocopy for general business or academic use
Type of use: Photocopy for internal/external business use

Terms and Conditions for Permission Categories: "Deliver via ILL or Document Delivery" and "Photocopy for General Business or Academic Use"

1. Scope of Authorization.

You may reproduce chapters and articles from the publications included in CCC's pay-per-use service by reporting those copies and paying the rightsholders' fees through CCC. Reproduction by photocopy machine is covered by this pay-per-use system of authorizations, as is the facsimile transmission of copies ("faxing", "telecopying" or equivalent technology).

2. Limitations on Use.

Authorizations are limited (a) to the use of the person or entity reporting to CCC and (b) to the use of a specific customer of the person or entity reporting to CCC unless otherwise indicated in the permissions policy statement printed in the publication. Other limitations may be imposed by individual publications, as described in their own masthead or permission policy statements.

3. Uses expressly excluded:

- electronic storage of any reproduction (whether in plain-text, PDF, or any other format) other than on a transitory basis
- the input of works into computerized databases
- reproduction of an entire publication (cover-to-cover)
- reproduction for resale to anyone other than a specific customer
- republication in a different form

Please obtain authorizations for these uses through other CCC services or directly from the rightsholder.

All rights not expressly granted are reserved; any license granted is further limited as set forth in any restrictions included in the Order Confirmation and/or in these terms and conditions.

4. Copyright Rights.

All Works and all rights therein, including copyright rights, remain the sole and exclusive property of the Rightsholder. The license created by the exchange of an Order Confirmation (and/or any invoice) and payment by User of the full amount set forth on that document includes only those rights expressly set forth in the Order Confirmation and in these terms and conditions, and conveys no other rights in the Work(s) to User.

5. Payment and Term.

While User may exercise the rights licensed immediately upon issuance of the Order Confirmation, the license is automatically revoked and is null and void, as if it had never been issued, if complete payment for the license is not received on a timely basis either from User directly or through a payment agent, such as a credit card company. In the event that the material for which an electronic reproduction license is sought includes third party materials (such as photographs, illustrations, graphs and similar materials) which are identified as included in a Work by permission, such third party materials may not be reproduced except in the context of the Work. Unless otherwise provided in the Order Confirmation, any grant of rights to User (i) is "one-time", (ii) is non-exclusive and non-transferable, and (iii) is limited to one year all as measured from the "republication date" as identified in the Order Confirmation, if any, and otherwise from the date of the Order Confirmation. Upon completion of the licensed use, or at the end of the period identified in the previous sentence (if earlier), User shall immediately cease any new use of the Work(s) and shall destroy any further copies of the Work (except for copies printed on paper in accordance with this license and still in User's stock at the end of such period).

6. Limitations on Use.

User may not make or permit any alterations to the Work, unless expressly set forth in the Order Confirmation (after request by User and approval by Rightsholder). No Work may be used in any way that is defamatory, violates the rights of third parties (including such third parties' rights of copyright, privacy, publicity, or other tangible or intangible property), or is otherwise illegal, sexually explicit or obscene. In addition, User may not conjoin a Work with any other material that may result in damage to the reputation of the Rightsholder.

7. Duty to Inform.

User agrees to inform CCC if it becomes aware of any infringement of any rights in a Work and to cooperate with any reasonable request of CCC or the Rightsholder in connection therewith.

8. Indemnification.

User hereby indemnifies and agrees to defend the Rightsholder and CCC, and their respective employees and directors, against all claims, liability, damages, costs and expenses, including legal fees and expenses, arising out of any use of a Work beyond the scope of the rights granted herein, or any use of a Work which has been altered in any way by User, including claims of defamation or infringement of rights of copyright, publicity, privacy or other tangible or intangible property.

Biotechnology advances
Permission type: Republish or display content
Type of use: reuse in a thesis/dissertation

Central Storage: This license does not include permission for a scanned version of the material to be stored in a central repository such as that provided by Heron/XanEdu.

17. Author website for journals with the following additional clauses:
All content posted to the web site must maintain the copyright information line on the bottom of each image, and the permission granted is limited to the personal version of your paper. You are not allowed to download and post the published electronic version of your article (whether PDF or HTML, proof or final version), nor may you scan the printed edition to create an electronic version. A hyper-text must be included to the Homepage of the journal from which you are licensing at http://www.sciencedirect.com/science/journal/xxxxx . As part of our normal production process, you will receive an e-mail notice when your article appears on Elsevier's online service ScienceDirect (www.sciencedirect.com). That e-mail will include the article's Digital Object Identifier (DOI). This number provides the electronic link to the published article and should be included in the posting of your personal version. We ask that you wait until you receive this e-mail and have the DOI to do any posting.
Central Storage: This license does not include permission for a scanned version of the material to be stored in a central repository such as that provided by Heron/XanEdu.

18. Author website for books with the following additional clauses:
Authors are permitted to place a brief summary of their work online only.
A hyper-text must be included to the Elsevier homepage at http://www.elsevier.com . All content posted to the web site must maintain the copyright information line on the bottom of each image. You are not allowed to download and post the published electronic version of your chapter, nor may you scan the printed edition to create an electronic version.
Central Storage: This license does not include permission for a scanned version of the material to be stored in a central repository such as that provided by Heron/XanEdu.

19. Website (regular and for author): A hyper-text must be included to the Homepage of the journal from which you are licensing at http://www.sciencedirect.com/science/journal/xxxxx. or for books to the Elsevier homepage at http://www.elsevier.com

20. Thesis/Dissertation: If your license is for use in a thesis/dissertation your thesis may be submitted to your institution in either print or electronic form. Should your thesis be published commercially, please reapply for permission. These requirements include permission for the Library and Archives of Canada to supply single copies, on demand, of the complete thesis and include permission for UMI to supply single copies, on demand, of the complete thesis. Should your thesis be published commercially, please reapply for permission.

21. Other Conditions:

v1.6

Biomaterials
Permission type: Republish or display content
Type of use: reuse in a thesis/dissertation

INTRODUCTION

1. The publisher for this copyrighted material is Elsevier. By clicking "accept"; in connection with completing this licensing transaction, you agree that the following terms and conditions apply to this transaction (along with the Billing and Payment terms and conditions established by Copyright Clearance Center, Inc. ("CCC"), at the time that you opened your Rightslink account and that are available at any time at http://myaccount.copyright.com).

GENERAL TERMS

2. Elsevier hereby grants you permission to reproduce the aforementioned material subject to the terms and conditions indicated.

3. Acknowledgement: If any part of the material to be used (for example, figures) has appeared in our publication with credit or acknowledgement to another source, permission must also be sought from that source. If such permission is not obtained then that material may not be included in your publication/copies. Suitable acknowledgement to the source must be made, either as a footnote or in a reference list at the end of your publication, as follows: "Reprinted from Publication title, Vol /edition number, Author(s), Title of article / title of chapter, Pages No., Copyright (Year), with permission from Elsevier [OR APPLICABLE SOCIETY COPYRIGHT OWNER]." Also Lancet special credit - "Reprinted from The Lancet, Vol. number, Author(s), Title of article, Pages No., Copyright (Year), with permission from Elsevier."

4. Reproduction of this material is confined to the purpose and/or media for which permission is hereby given.

5. Altering/Modifying Material: Not Permitted. However figures and illustrations may be altered/adapted minimally to serve your work. Any other abbreviations, additions, deletions and/or any other alterations shall be made only with prior written authorization of Elsevier Ltd. (Please contact Elsevier at permissions@elsevier.com)

6. If the permission fee for the requested use of our material is waived in this instance, please be advised that your future requests for Elsevier materials may attract a fee.

7. Reservation of Rights: Publisher reserves all rights not specifically granted in the combination of (i) the license details provided by you and accepted in the course of this licensing transaction, (ii) these terms and conditions and (iii) CCC's Billing and Payment terms and conditions.

8. License Contingent Upon Payment: While you may exercise the rights licensed immediately upon issuance of the license at the end of the licensing process for the transaction, provided that you have disclosed complete and accurate details of your proposed use, no license is finally effective unless and until full payment is received from you (either by

publisher or by CCC) as provided in CCC's Billing and Payment terms and conditions. If full payment is not received on a timely basis, then any license preliminarily granted shall be deemed automatically revoked and shall be void as if never granted. Further, in the event that you breach any of these terms and conditions or any of CCC's Billing and Payment terms and conditions, the license is automatically revoked and shall be void as if never granted. Use of materials as described in a revoked license, as well as any use of the materials beyond the scope of an unrevoked license, may constitute copyright infringement and publisher reserves the right to take any and all action to protect its copyright in the materials.

9. Warranties: Publisher makes no representations or warranties with respect to the licensed material.

10. Indemnity: You hereby indemnify and agree to hold harmless publisher and CCC, and their respective officers, directors, employees and agents, from and against any and all claims arising out of your use of the licensed material other than as specifically authorized pursuant to this license.

11. No Transfer of License: This license is personal to you and may not be sublicensed, assigned, or transferred by you to any other person without publisher's written permission.

12. No Amendment Except in Writing: This license may not be amended except in a writing signed by both parties (or, in the case of publisher, by CCC on publisher's behalf).

13. Objection to Contrary Terms: Publisher hereby objects to any terms contained in any purchase order, acknowledgment, check endorsement or other writing prepared by you, which terms are inconsistent with these terms and conditions or CCC's Billing and Payment terms and conditions. These terms and conditions, together with CCC's Billing and Payment terms and conditions (which are incorporated herein), comprise the entire agreement between you and publisher (and CCC) concerning this licensing transaction. In the event of any conflict between your obligations established by these terms and conditions and those established by CCC's Billing and Payment terms and conditions, these terms and conditions shall control.

14. Revocation: Elsevier or Copyright Clearance Center may deny the permissions described in this License at their sole discretion, for any reason or no reason, with a full refund payable to you. Notice of such denial will be made using the contact information provided by you. Failure to receive such notice will not alter or invalidate the denial. In no event will Elsevier or Copyright Clearance Center be responsible or liable for any costs, expenses or damage incurred by you as a result of a denial of your permission request, other than a refund of the amount(s) paid by you to Elsevier and/or Copyright Clearance Center for denied permissions.

LIMITED LICENSE

The following terms and conditions apply only to specific license types:

15. Translation: This permission is granted for non-exclusive world English rights only unless your license was granted for translation rights. If you licensed translation rights you may only translate this content into the languages you requested. A professional translator must perform all translations and reproduce the content word for word preserving the integrity of the article. If this license is to re-use 1 or 2 figures then permission is granted for non-exclusive world rights in all languages.

16. Website: The following terms and conditions apply to electronic reserve and author websites:
Electronic reserve: If licensed material is to be posted to website, the web site is to be password-protected and made available only to bona fide students registered on a relevant course if:
This license was made in connection with a course,
This permission is granted for 1 year only. You may obtain a license for future website posting,
All content posted to the web site must maintain the copyright information line on the bottom of each image,
A hyper-text must be included to the Homepage of the journal from which you are licensing at http://www.sciencedirect.com/science/journal/xxxxx or the Elsevier homepage for books at http://www.elsevier.com, and
Central Storage: This license does not include permission for a scanned version of the material to be stored in a central repository such as that provided by Heron/XanEdu.

17. Author website for journals with the following additional clauses:
All content posted to the web site must maintain the copyright information line on the bottom of each image, and the permission granted is limited to the personal version of your paper. You are not allowed to download and post the published electronic version of your article (whether PDF or HTML, proof or final version), nor may you scan the printed edition to create an electronic version. A hyper-text must be included to the Homepage of the journal from which you are licensing at http://www.sciencedirect.com/science/journal/xxxxx . As part of our normal production process, you will receive an e-mail notice when your article appears on Elsevier's online service ScienceDirect (www.sciencedirect.com). That e-mail will include the article's Digital Object Identifier (DOI). This number provides the electronic link to the published article and should be included in the posting of your personal version. We ask that you wait until you receive this e-mail and have the DOI to do any posting.
Central Storage: This license does not include permission for a scanned version of the material to be stored in a central repository such as that provided by Heron/XanEdu.

18. Author website for books with the following additional clauses:
Authors are permitted to place a brief summary of their work online only.
A hyper-text must be included to the Elsevier homepage at http://www.elsevier.com . All content posted to the web site must maintain the copyright information line on the bottom of each image. You are not allowed to download and post the published electronic version of your chapter, nor may you scan the printed edition to create an electronic version.
Central Storage: This license does not include permission for a scanned version of the material to be stored in a central repository such as that provided by Heron/XanEdu.

19. Website (regular and for author): A hyper-text must be included to the Homepage of the journal from which you are licensing at http://www.sciencedirect.com/science/journal/xxxxx. or for books to the Elsevier homepage at http://www.elsevier.com

20. Thesis/Dissertation: If your license is for use in a thesis/dissertation your thesis may be submitted to your institution in either print or electronic form. Should your thesis be published commercially, please reapply for permission. These requirements include permission for the Library and Archives of Canada to supply single copies, on demand, of the complete thesis and include permission for UMI to supply single copies, on demand, of the complete thesis. Should your

thesis be published commercially, please reapply for permission.

21. Other Conditions:

v1.6

Translational research : the journal of laboratory and clinical medicine
Permission type: Republish or display content
Type of use: reuse in a thesis/dissertation

INTRODUCTION

1. The publisher for this copyrighted material is Elsevier. By clicking "accept"; in connection with completing this licensing transaction, you agree that the following terms and conditions apply to this transaction (along with the Billing and Payment terms and conditions established by Copyright Clearance Center, Inc. ("CCC"), at the time that you opened your Rightslink account and that are available at any time at http://myaccount.copyright.com).

GENERAL TERMS

2. Elsevier hereby grants you permission to reproduce the aforementioned material subject to the terms and conditions indicated.

3. Acknowledgement: If any part of the material to be used (for example, figures) has appeared in our publication with credit or acknowledgement to another source, permission must also be sought from that source. If such permission is not obtained then that material may not be included in your publication/copies. Suitable acknowledgement to the source must be made, either as a footnote or in a reference list at the end of your publication, as follows: "Reprinted from Publication title, Vol /edition number, Author(s), Title of article / title of chapter, Pages No., Copyright (Year), with permission from Elsevier [OR APPLICABLE SOCIETY COPYRIGHT OWNER]." Also Lancet special credit - "Reprinted from The Lancet, Vol. number, Author(s), Title of article, Pages No., Copyright (Year), with permission from Elsevier."

4. Reproduction of this material is confined to the purpose and/or media for which permission is hereby given.

5. Altering/Modifying Material: Not Permitted. However figures and illustrations may be altered/adapted minimally to serve your work. Any other abbreviations, additions, deletions and/or any other alterations shall be made only with prior written authorization of Elsevier Ltd. (Please contact Elsevier at permissions@elsevier.com)

6. If the permission fee for the requested use of our material is waived in this instance, please be advised that your future requests for Elsevier materials may attract a fee.

7. Reservation of Rights: Publisher reserves all rights not specifically granted in the combination of (i) the license details provided by you and accepted in the course of this licensing transaction, (ii) these terms and conditions and (iii) CCC's Billing and Payment terms and conditions.

8. License Contingent Upon Payment: While you may exercise the rights licensed immediately upon issuance of the license at the end of the licensing process for the transaction, provided that you have disclosed complete and accurate details of your proposed use, no license is finally effective unless and until full payment is received from you (either by publisher or by CCC) as provided in CCC's Billing and Payment terms and conditions. If full payment is not received on a timely basis, then any license preliminarily granted shall be deemed automatically revoked and shall be void as if never granted. Further, in the event that you breach any of these terms and conditions or any of CCC's Billing and Payment terms and conditions, the license is automatically revoked and shall be void as if never granted. Use of materials as described in a revoked license, as well as any use of the materials beyond the scope of an unrevoked license, may constitute copyright infringement and publisher reserves the right to take any and all action to protect its copyright in the materials.

9. Warranties: Publisher makes no representations or warranties with respect to the licensed material.

10. Indemnity: You hereby indemnify and agree to hold harmless publisher and CCC, and their respective officers, directors, employees and agents, from and against any and all claims arising out of your use of the licensed material other than as specifically authorized pursuant to this license.

11. No Transfer of License: This license is personal to you and may not be sublicensed, assigned, or transferred by you to any other person without publisher's written permission.

12. No Amendment Except in Writing: This license may not be amended except in a writing signed by both parties (or, in the case of publisher, by CCC on publisher's behalf).

13. Objection to Contrary Terms: Publisher hereby objects to any terms contained in any purchase order, acknowledgment, check endorsement or other writing prepared by you, which terms are inconsistent with these terms and conditions or CCC's Billing and Payment terms and conditions. These terms and conditions, together with CCC's Billing and Payment terms and conditions (which are incorporated herein), comprise the entire agreement between you and publisher (and CCC) concerning this licensing transaction. In the event of any conflict between your obligations established by these terms and conditions and those established by CCC's Billing and Payment terms and conditions, these terms and conditions shall control.

14. Revocation: Elsevier or Copyright Clearance Center may deny the permissions described in this License at their sole discretion, for any reason or no reason, with a full refund payable to you. Notice of such denial will be made using the contact information provided by you. Failure to receive such notice will not alter or invalidate the denial. In no event will Elsevier or Copyright Clearance Center be responsible or liable for any costs, expenses or damage incurred by you as a

result of a denial of your permission request, other than a refund of the amount(s) paid by you to Elsevier and/or Copyright Clearance Center for denied permissions.

LIMITED LICENSE

The following terms and conditions apply only to specific license types:

15. Translation: This permission is granted for non-exclusive world English rights only unless your license was granted for translation rights. If you licensed translation rights you may only translate this content into the languages you requested. A professional translator must perform all translations and reproduce the content word for word preserving the integrity of the article. If this license is to re-use 1 or 2 figures then permission is granted for non-exclusive world rights in all languages.

16. Website: The following terms and conditions apply to electronic reserve and author websites:
Electronic reserve: If licensed material is to be posted to website, the web site is to be password-protected and made available only to bona fide students registered on a relevant course if:
This license was made in connection with a course,
This permission is granted for 1 year only. You may obtain a license for future website posting,
All content posted to the web site must maintain the copyright information line on the bottom of each image,
A hyper-text must be included to the Homepage of the journal from which you are licensing at http://www.sciencedirect.com/science/journal/xxxxx or the Elsevier homepage for books at http://www.elsevier.com, and
Central Storage: This license does not include permission for a scanned version of the material to be stored in a central repository such as that provided by Heron/XanEdu.

17. Author website for journals with the following additional clauses:
All content posted to the web site must maintain the copyright information line on the bottom of each image, and the permission granted is limited to the personal version of your paper. You are not allowed to download and post the published electronic version of your article (whether PDF or HTML, proof or final version), nor may you scan the printed edition to create an electronic version. A hyper-text must be included to the Homepage of the journal from which you are licensing at http://www.sciencedirect.com/science/journal/xxxxx . As part of our normal production process, you will receive an e-mail notice when your article appears on Elsevier's online service ScienceDirect (www.sciencedirect.com). That e-mail will include the article's Digital Object Identifier (DOI). This number provides the electronic link to the published article and should be included in the posting of your personal version. We ask that you wait until you receive this e-mail and have the DOI to do any posting.
Central Storage: This license does not include permission for a scanned version of the material to be stored in a central repository such as that provided by Heron/XanEdu.

18. Author website for books with the following additional clauses:
Authors are permitted to place a brief summary of their work online only.
A hyper-text must be included to the Elsevier homepage at http://www.elsevier.com . All content posted to the web site must maintain the copyright information line on the bottom of each image. You are not allowed to download and post the published electronic version of your chapter, nor may you scan the printed edition to create an electronic version.
Central Storage: This license does not include permission for a scanned version of the material to be stored in a central repository such as that provided by Heron/XanEdu.

19. Website (regular and for author): A hyper-text must be included to the Homepage of the journal from which you are licensing at http://www.sciencedirect.com/science/journal/xxxxx. or for books to the Elsevier homepage at http://www.elsevier.com

20. Thesis/Dissertation: If your license is for use in a thesis/dissertation your thesis may be submitted to your institution in either print or electronic form. Should your thesis be published commercially, please reapply for permission. These requirements include permission for the Library and Archives of Canada to supply single copies, on demand, of the complete thesis and include permission for UMI to supply single copies, on demand, of the complete thesis. Should your thesis be published commercially, please reapply for permission.

21. Other Conditions:

v1.6

Trends in biotechnology
Permission type: Republish or display content
Type of use: reuse in a thesis/dissertation

INTRODUCTION

1. The publisher for this copyrighted material is Elsevier. By clicking "accept"; in connection with completing this licensing transaction, you agree that the following terms and conditions apply to this transaction (along with the Billing and Payment terms and conditions established by Copyright Clearance Center, Inc. ("CCC"), at the time that you opened your Rightslink account and that are available at any time at http://myaccount.copyright.com).

GENERAL TERMS

2. Elsevier hereby grants you permission to reproduce the aforementioned material subject to the terms and conditions indicated.

3. Acknowledgement: If any part of the material to be used (for example, figures) has appeared in our publication with credit or acknowledgement to another source, permission must also be sought from that source. If such permission is not obtained then that material may not be included in your publication/copies. Suitable acknowledgement to the source

must be made, either as a footnote or in a reference list at the end of your publication, as follows: "Reprinted from Publication title, Vol /edition number, Author(s), Title of article / title of chapter, Pages No., Copyright (Year), with permission from Elsevier [OR APPLICABLE SOCIETY COPYRIGHT OWNER]." Also Lancet special credit - "Reprinted from The Lancet, Vol. number, Author(s), Title of article, Pages No., Copyright (Year), with permission from Elsevier."

4. Reproduction of this material is confined to the purpose and/or media for which permission is hereby given.

5. Altering/Modifying Material: Not Permitted. However figures and illustrations may be altered/adapted minimally to serve your work. Any other abbreviations, additions, deletions and/or any other alterations shall be made only with prior written authorization of Elsevier Ltd. (Please contact Elsevier at permissions@elsevier.com)

6. If the permission fee for the requested use of our material is waived in this instance, please be advised that your future requests for Elsevier materials may attract a fee.

7. Reservation of Rights: Publisher reserves all rights not specifically granted in the combination of (i) the license details provided by you and accepted in the course of this licensing transaction, (ii) these terms and conditions and (iii) CCC's Billing and Payment terms and conditions.

8. License Contingent Upon Payment: While you may exercise the rights licensed immediately upon issuance of the license at the end of the licensing process for the transaction, provided that you have disclosed complete and accurate details of your proposed use, no license is finally effective unless and until full payment is received from you (either by publisher or by CCC) as provided in CCC's Billing and Payment terms and conditions. If full payment is not received on a timely basis, then any license preliminarily granted shall be deemed automatically revoked and shall be void as if never granted. Further, in the event that you breach any of these terms and conditions or any of CCC's Billing and Payment terms and conditions, the license is automatically revoked and shall be void as if never granted. Use of materials as described in a revoked license, as well as any use of the materials beyond the scope of an unrevoked license, may constitute copyright infringement and publisher reserves the right to take any and all action to protect its copyright in the materials.

9. Warranties: Publisher makes no representations or warranties with respect to the licensed material.

10. Indemnity: You hereby indemnify and agree to hold harmless publisher and CCC, and their respective officers, directors, employees and agents, from and against any and all claims arising out of your use of the licensed material other than as specifically authorized pursuant to this license.

11. No Transfer of License: This license is personal to you and may not be sublicensed, assigned, or transferred by you to any other person without publisher's written permission.

12. No Amendment Except in Writing: This license may not be amended except in a writing signed by both parties (or, in the case of publisher, by CCC on publisher's behalf).

13. Objection to Contrary Terms: Publisher hereby objects to any terms contained in any purchase order, acknowledgment, check endorsement or other writing prepared by you, which terms are inconsistent with these terms and conditions or CCC's Billing and Payment terms and conditions. These terms and conditions, together with CCC's Billing and Payment terms and conditions (which are incorporated herein), comprise the entire agreement between you and publisher (and CCC) concerning this licensing transaction. In the event of any conflict between your obligations established by these terms and conditions and those established by CCC's Billing and Payment terms and conditions, these terms and conditions shall control.

14. Revocation: Elsevier or Copyright Clearance Center may deny the permissions described in this License at their sole discretion, for any reason or no reason, with a full refund payable to you. Notice of such denial will be made using the contact information provided by you. Failure to receive such notice will not alter or invalidate the denial. In no event will Elsevier or Copyright Clearance Center be responsible or liable for any costs, expenses or damage incurred by you as a result of a denial of your permission request, other than a refund of the amount(s) paid by you to Elsevier and/or Copyright Clearance Center for denied permissions.

LIMITED LICENSE

The following terms and conditions apply only to specific license types:

15. Translation: This permission is granted for non-exclusive world English rights only unless your license was granted for translation rights. If you licensed translation rights you may only translate this content into the languages you requested. A professional translator must perform all translations and reproduce the content word for word preserving the integrity of the article. If this license is to re-use 1 or 2 figures then permission is granted for non-exclusive world rights in all languages.

16. Website: The following terms and conditions apply to electronic reserve and author websites:
Electronic reserve: If licensed material is to be posted to website, the web site is to be password-protected and made available only to bona fide students registered on a relevant course if:
This license was made in connection with a course,
This permission is granted for 1 year only. You may obtain a license for future website posting,
All content posted to the web site must maintain the copyright information line on the bottom of each image,
A hyper-text must be included to the Homepage of the journal from which you are licensing at http://www.sciencedirect.com/science/journal/xxxxx or the Elsevier homepage for books at http://www.elsevier.com, and
Central Storage: This license does not include permission for a scanned version of the material to be stored in a central repository such as that provided by Heron/XanEdu.

17. Author website for journals with the following additional clauses:
All content posted to the web site must maintain the copyright information line on the bottom of each image, and the permission granted is limited to the personal version of your paper. You are not allowed to download and post the published electronic version of your article (whether PDF or HTML, proof or final version), nor may you scan the printed edition to create an electronic version. A hyper-text must be included to the Homepage of the journal from which you are licensing at http://www.sciencedirect.com/science/journal/xxxxx . As part of our normal production process, you will receive an e-mail notice when your article appears on Elsevier's online service ScienceDirect (www.sciencedirect.com). That e-mail will include the article's Digital Object Identifier (DOI). This number provides the electronic link to the

published article and should be included in the posting of your personal version. We ask that you wait until you receive this e-mail and have the DOI to do any posting.
Central Storage: This license does not include permission for a scanned version of the material to be stored in a central repository such as that provided by Heron/XanEdu.

18. Author website for books with the following additional clauses:
Authors are permitted to place a brief summary of their work online only.
A hyper-text must be included to the Elsevier homepage at http://www.elsevier.com . All content posted to the web site must maintain the copyright information line on the bottom of each image. You are not allowed to download and post the published electronic version of your chapter, nor may you scan the printed edition to create an electronic version.
Central Storage: This license does not include permission for a scanned version of the material to be stored in a central repository such as that provided by Heron/XanEdu.

19. Website (regular and for author): A hyper-text must be included to the Homepage of the journal from which you are licensing at http://www.sciencedirect.com/science/journal/xxxxx. or for books to the Elsevier homepage at http://www.elsevier.com

20. Thesis/Dissertation: If your license is for use in a thesis/dissertation your thesis may be submitted to your institution in either print or electronic form. Should your thesis be published commercially, please reapply for permission. These requirements include permission for the Library and Archives of Canada to supply single copies, on demand, of the complete thesis and include permission for UMI to supply single copies, on demand, of the complete thesis. Should your thesis be published commercially, please reapply for permission.

21. Other Conditions:

v1.6

WILEY CATALOG
Permission type: Photocopy for general business or academic use
Type of use:

Terms and Conditions for Permission Categories: "Deliver via ILL or Document Delivery" and "Photocopy for General Business or Academic Use"

1. Scope of Authorization.

You may reproduce chapters and articles from the publications included in CCC's pay-per-use service by reporting those copies and paying the rightsholders' fees through CCC. Reproduction by photocopy machine is covered by this pay-per-use system of authorizations, as is the facsimile transmission of copies ("faxing", "telecopying" or equivalent technology).

2. Limitations on Use.

Authorizations are limited (a) to the use of the person or entity reporting to CCC and (b) to the use of a specific customer of the person or entity reporting to CCC unless otherwise indicated in the permissions policy statement printed in the publication. Other limitations may be imposed by individual publications, as described in their own masthead or permission policy statements.

3. Uses expressly excluded:

- electronic storage of any reproduction (whether in plain-text, PDF, or any other format) other than on a transitory basis
- the input of works into computerized databases
- reproduction of an entire publication (cover-to-cover)
- reproduction for resale to anyone other than a specific customer
- republication in a different form

Please obtain authorizations for these uses through other CCC services or directly from the rightsholder.

All rights not expressly granted are reserved; any license granted is further limited as set forth in any restrictions included in the Order Confirmation and/or in these terms and conditions.

4. Copyright Rights.

All Works and all rights therein, including copyright rights, remain the sole and exclusive property of the Rightsholder. The license created by the exchange of an Order Confirmation (and/or any invoice) and payment by User of the full amount set forth on that document includes only those rights expressly set forth in the Order Confirmation and in these terms and conditions, and conveys no other rights in the Work(s) to User.

5. Payment and Term.

While User may exercise the rights licensed immediately upon issuance of the Order Confirmation, the license is automatically revoked and is null and void, as if it had never been issued, if complete payment for the license is not received on a timely basis either from User directly or through a payment agent, such as a credit card company. In the event that the material for which an electronic reproduction license is sought includes third party materials (such as photographs, illustrations, graphs and similar materials) which are identified as included in a Work by permission, such third party materials may not be reproduced except in the context of the Work. Unless otherwise provided in the Order Confirmation, any grant of rights to User (i) is "one-time", (ii) is non-exclusive and non-transferable, and (iii) is limited to one year all as measured from the "republication date" as identified in the Order Confirmation, if any, and otherwise from the date of the Order Confirmation. Upon completion of the licensed use, or at the end of the period identified in the

previous sentence (if earlier), User shall immediately cease any new use of the Work(s) and shall destroy any further copies of the Work (except for copies printed on paper in accordance with this license and still in User's stock at the end of such period).

6. Limitations on Use.

User may not make or permit any alterations to the Work, unless expressly set forth in the Order Confirmation (after request by User and approval by Rightsholder). No Work may be used in any way that is defamatory, violates the rights of third parties (including such third parties' rights of copyright, privacy, publicity, or other tangible or intangible property), or is otherwise illegal, sexually explicit or obscene. In addition, User may not conjoin a Work with any other material that may result in damage to the reputation of the Rightsholder.

7. Duty to Inform.

User agrees to inform CCC if it becomes aware of any infringement of any rights in a Work and to cooperate with any reasonable request of CCC or the Rightsholder in connection therewith.

8. Indemnification.

User hereby indemnifies and agrees to defend the Rightsholder and CCC, and their respective employees and directors, against all claims, liability, damages, costs and expenses, including legal fees and expenses, arising out of any use of a Work beyond the scope of the rights granted herein, or any use of a Work which has been altered in any way by User, including claims of defamation or infringement of rights of copyright, publicity, privacy or other tangible or intangible property.

9. LIMITATION OF LIABILITY.

(a) UNDER NO CIRCUMSTANCES WILL CCC OR THE RIGHTSHOLDER BE LIABLE FOR ANY DIRECT, INDIRECT, CONSEQUENTIAL OR INCIDENTAL DAMAGES (INCLUDING WITHOUT LIMITATION DAMAGES FOR LOSS OF BUSINESS PROFITS OR INFORMATION, OR FOR BUSINESS INTERRUPTION) ARISING OUT OF THE USE OR INABILITY TO USE A WORK, EVEN IF ONE OF THEM HAS BEEN ADVISED OF THE POSSIBILITY OF SUCH DAMAGES.

(b) IN ANY EVENT, THE TOTAL LIABILITY OF THE RIGHTSHOLDER AND CCC (INCLUDING THEIR RESPECTIVE EMPLOYEES AND DIRECTORS) SHALL NOT EXCEED THE TOTAL AMOUNT ACTUALLY PAID BY USER FOR THIS LICENSE. USER ASSUMES FULL LIABILITY FOR THE ACTIONS AND OMISSIONS OF ITS PRINCIPALS, EMPLOYEES, AGENTS, AFFILIATES, SUCCESSORS AND ASSIGNS.

10. WARRANTIES; DISCLAIMERS.

(a) THE WORK(S) AND RIGHT(S) ARE PROVIDED "AS IS". THE RIGHTSHOLDER(S) HAS GRANTED CCC THE RIGHT TO GRANT PERMISSION UNDER THESE PAY-PER-USE SERVICES, AND HAS WARRANTED THAT IT HAS ALL RIGHTS NECESSARY TO AUTHORIZE CCC TO ACT ON ITS BEHALF. CCC AND THE RIGHTSHOLDER DISCLAIM ALL OTHER WARRANTIES RELATING TO THE WORK(S) AND RIGHT(S), EITHER EXPRESS OR IMPLIED, INCLUDING WITHOUT LIMITATION IMPLIED WARRANTIES OF MERCHANTABILITY OR FITNESS FOR A PARTICULAR PURPOSE. ADDITIONAL RIGHTS MAY BE REQUIRED TO USE PORTIONS OF THE WORK (AS OPPOSED TO THE ENTIRE WORK) IN A MANNER CONTEMPLATED BY USER; USER UNDERSTANDS AND AGREES THAT NEITHER CCC NOR THE RIGHTSHOLDER MAY HAVE SUCH ADDITIONAL RIGHTS TO GRANT.

(b) USER ACKNOWLEDGES THAT THE RIGHTS GRANTED HEREUNDER OR UNDER ANY ORDER CONFIRMATION DO NOT INCLUDE ANY MODEL, PROPERTY OR OTHER RELEASES WHICH MAY BE NECESSARY FOR CERTAIN USES OF WORKS CONSISTING OF OR CONTAINING PHOTOGRAPHS, OTHER STILL IMAGES OR AUDIOVISUAL CONTENT. USER ACKNOWLEDGES THAT ADDITIONAL RIGHTS OR RELEASES MAY BE NECESSARY FOR CERTAIN USES OF MATERIALS WHICH INCLUDE DEPICTIONS OF PERSONS, PROPERTY OR TRADEMARKS AND THAT USER (AND NOT CCC OR ANY RIGHTSHOLDER) IS SOLELY RESPONSIBLE FOR OBTAINING ANY SUCH REQUIRED RIGHT OR RELEASE.

11. Miscellaneous

11.1: Assignment or Transfer: The licensing transaction described in the Order Confirmation is personal to User. Therefore, User may not assign or transfer to any other person (whether a natural person or an organization of any kind) the license created by the Order Confirmation and these terms and conditions or any rights granted hereunder, subject to the following exception. The exception: in cases where a person is specifically engaged by a second person to provide reproductions of Works to (and/or to obtain licenses on behalf of) the second person and EITHER (i) the first person expressly notifies the second person of its obligation not to redistribute or otherwise use the material without authorization, OR (ii) the second person is identified in the Order Confirmation as the publisher of the material to include the Work licensed under this service, then the license may be transferred to the second person and both the first person and the second person shall be jointly deemed to be the "User" under the Order Confirmation and these terms and conditions for that transaction. An organizational User and its principals, employees, agents and affiliates are jointly and severally liable for the performance of all payments and other obligations hereunder.

11.2: Amendment or Waiver, Objection to Contrary Terms. No amendment or waiver of any terms is binding unless set forth in a writing other than a standard User or CCC form and signed by the parties. The Rightsholder and CCC hereby object to any terms contained in any writing prepared by the User or its principals, employees, agents or affiliates and purporting to govern or otherwise relate to the licensing transaction described in the Order Confirmation, which terms are in any way inconsistent with any terms set forth in the Order Confirmation and/or in these terms and conditions or CCC's standard operating procedures, whether such writing is prepared prior to, simultaneously with or subsequent to the Order Confirmation, and whether such writing appears on a copy of the Order Confirmation or in a separate instrument.

11.3: Effect of Breach. Any failure by User to pay any amount when due, or any use by User of a Work beyond the scope of the license set forth in the Order Confirmation and/or these terms and conditions, shall be a material breach of the license created by the Order Confirmation and these terms and conditions. Any breach not cured within 10 days of notice thereof shall result in immediate termination of such license without further notice. Invoices are due and payable upon receipt. Any unauthorized (but licensable) use of a Work that is terminated immediately upon notice thereof may be liquidated by payment of the Rightsholder's ordinary license price therefore; any unauthorized (and unlicensable) use that is not terminated immediately for any reason (including, for example, because materials containing the Work cannot reasonably be recalled) will be subject to all remedies available at law or in equity, but in no event to a payment of less than three times the Rightsholder's ordinary license price for the most closely analogous licensable use plus Rightsholder's and/or CCC's costs and expenses incurred in collecting such payment.

Close

Confirmation Number: 11066528

Citation Information

Order Detail ID: 63415476

Pearson Education Australia custom book by Gudergan, Siegfried P. Reproduced with permission of CAL, COPYRIGHT AGENCY LIMITED in the format Photocopy for internal/external business use via Copyright Clearance Center.

Order Detail ID: 63415480

Biotechnology advances by ELSEVIER INC.. Reproduced with permission of ELSEVIER INC. in the format reuse in a thesis/dissertation via Copyright Clearance Center.

Order Detail ID: 63415483

Biomaterials by Biological Engineering Society Reproduced with permission of PERGAMON in the format reuse in a thesis/dissertation via Copyright Clearance Center.

Order Detail ID: 63415487

Translational research : the journal of laboratory and clinical medicine by Central Society for Clinical Research (U.S.) Reproduced with permission of MOSBY INC in the format reuse in a thesis/dissertation via Copyright Clearance Center.

Order Detail ID: 63415490

Trends in biotechnology by ELSEVIER LTD.. Reproduced with permission of ELSEVIER LTD. in the format reuse in a thesis/dissertation via Copyright Clearance Center.

Order Detail ID: 63415497

WILEY CATALOG by JOHN WILEY & SONS - BOOKS. Reproduced with permission of JOHN WILEY & SONS - BOOKS

Close